ORNL-2947
UC-81 - Reactors-Power

HOMOGENEOUS REACTOR PROGRAM
QUARTERLY PROGRESS REPORT
FOR PERIOD ENDING APRIL 30, 1960

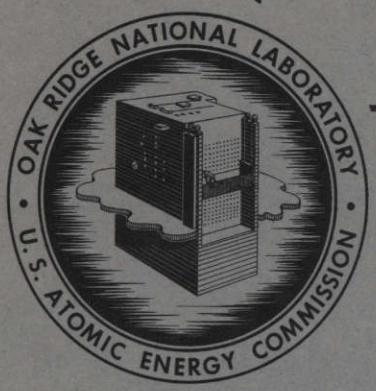

OAK RIDGE NATIONAL LABORATORY
operated by
UNION CARBIDE CORPORATION
for the
U.S. ATOMIC ENERGY COMMISSION

Printed in USA. Price $2.75 . Available from the
Office of Technical Services
Department of Commerce
Washington 25, D.C.

ORNL-2947
Reactors-Power
TID-4500 (15th ed.)

Contract No. W-7405-eng-26

HOMOGENEOUS REACTOR PROGRAM

QUARTERLY PROGRESS REPORT

for Period Ending April 30, 1960

Program Director - R. B. Briggs

Homogeneous Reactor Test - S. E. Beall
Reactor Analysis and Engineering Development - R. N. Lyon
Reactor Materials Research - E. G. Bohlmann
Chemical Engineering Development - D. E. Ferguson
Supporting Chemical Research - H. F. McDuffie
Analytical Chemistry - M. T. Kelley

DATE ISSUED

AUG 9 1960

OAK RIDGE NATIONAL LABORATORY
Oak Ridge, Tennessee
operated by
UNION CARBIDE CORPORATION
for the
U.S. ATOMIC ENERGY COMMISSION

SUMMARY

PART I. HOMOGENEOUS REACTOR TEST

1. HRT Remote Operations, Maintenance, and Testing

A program of major reactor alterations and repairs was initiated after run 21, which was concluded when a second hole formed in the Zircaloy core vessel. The program is now approximately 60% complete. So far, the upper five core diffuser screens have been removed from the core, plastic impressions of the core holes have been made to aid in patching them, and several major pieces of reactor equipment have been replaced or altered.

Tools were prepared for cutting a sample of the core wall from around the second hole, for taper-reaming the circular opening left by the sample, for cleaning the core wall, and for plugging the two holes.

Helium leak detection was used to locate a crack that occurred in the purge line of the core circulating pump during run 21 shutdown.

Reactor containment-shield penetrations are being leak tested to ensure that the integrity of the shield is maintained.

2. HRT Processing Plant

A revised multiple-hydroclone system was designed and is being fabricated for installation prior to the next run. The efficiency has been improved by using more hydroclones (18 instead of 13) and by using a smaller, more efficient size; by utilizing the full head of the circulating pump (for increased pressure drop); and by recycling overflow from the cell-C collecting hydroclone to prevent loss of solids from that unit.

A gamma survey of reactor cell piping 80 days after shutdown indicates that about 85% of the insoluble fission-product activity remained in the high-pressure system. The highest reading found exceeded 6000 r/hr and was at the multiclone feed chamber. Piping in the high-pressure system read from 800 to 3900 r/hr. The dirt trap in the suction line to the fuel feed pump, which read 1100 r/hr following run 13, was only 120 r/hr at this survey.

3. HRT Component Development

The ignition of a titanium wear ring while operating in a pump circulating high-pressure oxygen caused a burn-through of the stainless steel discharge pipe. Such fires can be avoided by the use of adequate wear-ring clearance, and particularly by stopping the pump upon a low-power signal caused by the presence of gas.

A stress analysis of the HRT core indicated that operation of the core and blanket at widely differing temperatures will not cause excessive stresses in the core tank.

Flow tests, coupled with computations of nuclear heating, indicated that the HRT in reverse flow will operate with a maximum core wall temperature of 300°C, if no scale is deposited. The maximum interior temperature is expected to be 305°C.

4. HRT Reactor Analysis

A study was made of the critical concentration in the HRT at 260°C, with various blanket fuel concentrations; harmonics-method results and two-group and multigroup results were in good agreement. With blanket-to-core fuel-concentration ratios of zero and 0.4, the clean-core critical concentration was 6.9 and 4.7 g of U^{235} per liter, respectively. Addition of poisons presently within the system increased the fuel concentration about 2%. Changing the fuel from U^{235} to U^{233} with no fuel in the blanket decreased the critical concentration from 6.9 to 5.5 g of uranium per liter.

PART II. REACTOR ANALYSIS AND ENGINEERING DEVELOPMENT

5. Reactor Analysis

Estimates were made of the core critical concentration in small, cylindrical reactors; the core region contained UO_2SO_4-D_2O, while the blanket region consisted of three discrete thoria-pellet regions containing 5300 g of Th per liter, separated by D_2O regions. With a core diameter of 18 in. and a length of 48 in., and with 7.5 in. of D_2O separating the core from the first thoria-pellet region, the fuel concentration at 280°C for a clean core was 17.4 g of U^{233} per liter. Keeping other thicknesses constant, decreasing the thickness of the first D_2O gap from 7.5 to 4 in. increased the core critical fuel concentration by 40%. Increasing the core length from 48 to 72 in. decreased the critical fuel concentration about 17%, while increasing the core diameter from 18 to 21 in. decreased the core concentration by about 35%.

6. Development of Reactor Components and Systems

A cylindrical core model 2 ft in diameter and 6 ft long was operated. The first set of entry vanes tested promoted bypassing of about half the fluid from inlet to outlet, so that new vanes were designed and fabricated for test.

An evaluation was made of two-region thoria breeders which indicated that blankets containing stationary thoria pellets are quite promising. Detail design was begun of an experimental model simulating the blanket of a 40-Mw(th) reactor. Lead shot were circulated in a simple model, illustrating the arrangement proposed for handling blanket thoria.

The 200Z pump, containing alumina bearings, continued to operate satisfactorily. A test stator appeared to remain in a useful condition after an irradiation dose of 5.43×10^9 rads, indicating acceptable radiation resistance.

The three-stage oxygen compressor was further instrumented in an attempt to determine the cause of persistent diaphragm failures. Increased-capacity solution feed pumps continued to perform satisfactorily.

The 300-SM system was charged with slurry, following completion of numerous modifications. Charging was performed easily, and improved valves increased the reliability of the system as a whole.

A slurry of 1600°C-fired thoria circulating in the 200B loop appeared to be forming a scale on the heat transfer surface. Its yield stress at elevated temperatures appeared to be unexpectedly low. A correlation derived for slurry nonuniformity in the 200A loop suggested that dilute slurries are less uniform than high-concentration slurries. In the 50A loop, a 3.65-μ thoria slurry retained moderately dilatant properties after circulation.

7. Instrument and Valve Development

After 5540 hr of service in a 30-gpm slurry loop, the Zircaloy-2 plug and seat of a flushed-bellows Hammel-Dahl valve was found to have suffered considerable damage. The damage, however, was not catastrophic.

Life-testing of 12 titanium stem-sealing bellows was completed. Average life of the 12 units tested was 24,139 cycles. Tests were performed in uranyl sulfate solution at 280°C, with 2300-psig pressure applied externally to the bellows.

PART III. SOLUTION FUELS

8. Reactions in Aqueous Solutions

Measurements of the rate of peroxide decomposition in 0.034 M uranyl nitrate solution were made to establish whether the decomposition was sufficiently rapid to permit consideration of uranyl nitrate solution as a potential reactor fuel. Tests were made over the temperature range 40 to 100°C with several levels of excess acidity. The effects of known catalysts and corrosion-product materials were established.

The results were quite similar to those previously obtained with sulfate and perchlorate systems. The temperature dependence of the decomposition rate was essentially the same as indicated by the calculated activation energy of 25,000 cal/mole. The rate was inversely related to the excess-acid concentration. Iron salts were extremely effective catalysts for the decomposition, and copper salts promoted this activity substantially. Extrapolation of these results to higher temperatures suggests that the rates of peroxide decomposition should prove adequate under anticipated reactor conditions.

9. Heterogeneous Equilibria in Aqueous Systems

The determinations of the compositions of light- and heavy-liquid phases in the system UO_3-SO_3-H_2O and its D_2O counterpart at 300, 325, and 350°C were extended to include light-liquid phases less than 0.1 m in SO_3 and heavy-liquid phases which contained small excesses of UO_3. Further information was obtained on the equilibrium distribution of CuO and/or NiO between the heavy- and light-liquid phases at 325 and 350°C.

Solid-liquid equilibria in the system UO_3-CuO-SO_3-H_2O at 325 and 350°C are under investigation. Preliminary values for the simultaneous solubilities of $CuO \cdot 3UO_3$ and $3CuO \cdot SO_3 \cdot 2H_2O$ in sulfate solutions indicate little change from values at 300°C.

10. Radiation Corrosion

A rocking-autoclave experiment was performed in which a D_2O solution of uranyl nitrate (0.032 m) with $Cu(NO_3)_2$ and excess DNO_3 was exposed in Zircaloy-2. Low-power, low-temperature exposures of short duration were made in order to obtain pressure data from which G_{D_2} and K_{Cu} (225°C) values could be estimated. Exposure at 280°C to the full reactor power was made in five periods, the total irradiation time being 134 hr. The pressure and temperature were followed closely both during and between irradiation periods. Analyses were made of the irradiated solution, the autclave rinse, the large amount of precipitate, and the specimen surfaces.

K_{Cu} (225°C) was estimated to be 1600 to 1700 liters/mole-hr, about three times as large as out-of-pile values found by others. G_{D_2} was estimated to be 1.3 to 1.4. The various pertinent pressure and analytical data were not completely interconsistent but allow an estimated range of Zircaloy-2 corrosion rates of 6 to 12 mpy during most of the exposure. The corrosion rate appeared to increase during the last 30 hr of exposure, and the final rate was probably 30 mpy or more. From various features of the pressure data, estimates of G_{N_2} of 2×10^{-3} to 2.5×10^{-2} were made, which are 7 to 70 times larger than reported values from fission-fragment irradiations of $Ca(NO_3)_2$ solution. Recombination of nitrogen and oxygen was indicated, the apparent rate corresponding to a vapor-phase recombination with a $G_{NO_3^-}$ value of 1 to 3, which is within the range of values for vapor-phase fixation previously reported by others.

PART IV. SLURRY FUELS

11. Engineering and Physical Properties

Previous studies of the minimum velocity required to transport flocculated suspensions in horizontal pipes have shown two regions of flow, depending on the concentration. The critical concentration for the transition from one type of flow to the other has been shown to be a function of degree of flocculation and tube diameter. It has also been shown that the critical concentration can be determined from a systematic study of the hindered-settling rate as a function of container diameter and suspension concentration.

An analysis of the minimum-transport condition for particles sufficiently small to settle according to Stokes' law and with diameters smaller than the thickness of the laminar sublayer has shown that at least two forces act on the particle causing it to be transported. The first condition results from the particle settling through a fluid having a velocity gradient. The difference in stream velocity between the top and bottom of the particle results in a pressure difference between the top and bottom of the particle. The net force at the minimum-transport condition was found to be just equal to the gravitational force on the particle. The other condition results from application of the penetration theory in which turbulent eddies are postulated as penetrating through the laminar sublayer to the pipe wall. It was found that at the minimum-transport condition the magnitude of the fluctuations one particle diameter from the wall is just equal to the settling rate of the particle.

Tests have shown that Li_2SO_4 is an effective dispersant of thoria suspensions even at temperatures as great as 250°C. Therefore, a run was made

in a high-temperature loop to determine whether the presence of Li_2SO_4 would prevent cake deposition when ThO_2 spheres, known to be cake formers, were circulated. The test was more favorable than any previous tests with different electrolytes and indicated that selection of the proper concentration of Li_2SO_4 might result in a marked decrease in caking tendency.

Addition of 50 wt % noncaking oxide to a known caking oxide decreased but did not prevent the formation of deposits in the loop.

Coprecipitation of 0.05 to 0.25 mole fraction Zr, Al, and Pb with thorium followed by calcination at 800°C increased particle integrity greatly over that observed with oxides prepared in a similar manner except that metal oxide additives were not present.

12. Thorium Oxide Irradiations

Two series of thorium oxide powders that had been fired at 650, 800, 900, 1100, and 1500°C and then irradiated 16 and 22 months in an LITR lattice position were recovered for examination. The 650, 800, and 900°C-fired samples in both series were red and had sintered into hard agglomerates; the 1100°C-fired samples were off-white powders; and the 1500°C-fired samples were blue powders. Radiochemical analyses of the 16-month irradiated oxides and flux monitors indicated the neutron flux to have ranged from 1.7 to 2.5 x 10^{13}. The irradiation produced a marked decrease in surface area for the lower-fired materials, but no change in surface area was observed for the 1500°C-fired material. The estimated maximum temperature of all oxides while being irradiated was <300°C. Thus the observed effect of irradiation was a sintering action comparable to about a 1500°C calcination.

A heavy-water slurry of >25-μ 1000°C-fired thoria spheres containing 0.5% natural uranium that had been irradiated 52 days in the C-43 facility in the LITR at temperatures from 180 to 280°C was recovered. A dried plug, composed of more than half the original solids, was found at the top of the irradiation autoclave, apparently deposited by the reflux conditions introduced by the method used for temperature control during irradiation.

Irradiation of a settled bed of 0.2-in.-dia thoria pellets in heavy water was initiated, and hot-cell techniques for evaluation of irradiation effects are under development.

13. Development of Gas-Recombination Catalysts

The sol method of preparing the palladium catalyst for use in the catalytic recombination of hydrogen and oxygen in thoria and thoria-urania slurries gave reproducible activities and the highest specific activities yet obtained. The specific activity appeared also to be independent of the type and concentration of slurry solids.

Under excess oxygen, the catalyst performance index (CPI) per millimole of palladium concentration at 280°C and 100 psi hydrogen partial pressure varied from 9 to 22 w/ml. Under excess hydrogen, the CPI was increased by several orders of magnitude. Data obtained in-pile with a slurry of a thorium - 8% uranium oxide containing palladium indicated a CPI about four times higher than that obtained out-of-pile in a similar system. Laboratory tests on a slurry sample containing palladium obtained from a loop gas-recombination experiment confirmed qualitatively the drop-off in activity with pumping time observed in the loop run but did not explain the order-of-magnitude-lower specific activities in the loop experiment.

14. Slurry Corrosion and Blanket Materials Tests

Procedures have been developed for evaluating the relative durability of experimental preparations of thoria pellets which might be suitable for use in a proposed pebble-bed blanket of a TBR. Experimental preparations calcined from 1000 to 1750°C, including 0.2-in.-dia spheres and right cylinders and cylinders with hemispherical ends, approximately 0.2 in. in diameter and 0.2 in. in length, were compared in accelerated (1- to 2-hr) tests at room temperature using spouted beds to determine general particle integrity and attrition rates. Static autoclave tests and 300-hr exposures of packed pellet beds in flowing D_2O at 260°C in 100A pump loops were made to evaluate high-temperature durability and potential leach-out of additives (0.5 to 5% CaO and/or Al_2O_3) from the pellets.

During the examination of 50 different pellet preparations, weight losses during exposure in D_2O (12 to 200 hr) in static autoclaves at 260°C using ambient atmosphere ranged from 0.001 to 0.2%/hr. Materials which displayed losses greater than 0.0003%/hr failed due to spalling, leach-out of additives or partial disintegration. Sixty-seven per cent of the preparations showed losses below 0.0003%/hr.

Pellets which showed weight losses of less than 0.0003%/hr in static autoclaves displayed weight losses during 1-hr exposures in spouted-bed tests (10 pellets, 0.24 fps superficial velocity, 24 fps jet velocity) at room temperature of 0.3 to 30%/hr. Twenty per cent of the materials showed low rates, $\leq$0.6%/hr.

Two preparations exposed in horizontal packed beds at approximately 2 fps superficial velocity in 100A loop tests at 260°C using D_2O with inert-gas atmosphere displayed attrition rates of 0.006 and 0.008%/hr respectively during 300-hr exposures. Over 50% of the attrition products were retained as fines in the packed beds. Six per cent of the calcium was leached from one of the preparations which contained 0.5 wt % CaO as additive.

In-pile Zircaloy-2 autoclave slurry corrosion experiment L5Z-152S was operated satisfactorily at 280°C under oxygen atmosphere at a fission power density of 20 w/ml for a short period, with satisfactory recombination catalysis and no pronounced corrosion effects. Some tendency of the thoria - 8% enriched-urania slurry to form deposits was indicated during both out-of-pile (673 hr) and in-pile (65 hr) operation, but no notable deposits were found in postrun examination. The experiment was terminated when a plug developed in the 20-mil-ID capillary tubing leading to the pressure cell.

Zircaloy-2 specimens from various in-pile autoclave experiments were examined. A pickup of 20 to 110 ppm hydrogen was noted, but appeared to be associated with water corrosion rather than with atmosphere or irradiation effects.

A new coiled-pipe core was installed in the 5-gpm in-pile slurry loop which minimized plug-inducing geometries as well as permitting a satisfactory disposition of corrosion specimens. In the prototype loop the installation of a similarly designed core eliminated the problem of slurry deposition previously observed with the annular-flow core.

Satisfactory operation of the prototype loop for more than 1500 hr with a slurry of the thoria - 1/2% enriched urania proposed for in-pile use indicated that the present loop design is satisfactory for in-pile operation.

Only mild degradation in particle size occurred for this period, and corrosion rates were also low.

Measurements of recombination kinetics and stability of the palladium catalyst in the prototype loop with three slurry preparations were made at various catalyst levels. The thoria - 1/2% enriched-urania preparation to be used in-pile gave the longest retention of catalyst activity, with half the activity remaining after four weeks. The catalyst-slurry combination appears to be adequate for the proposed in-pile experiment without unduly frequent additions of catalyst. A sampling system designed to remove slurry samples from the loop while operating in-pile was satisfactorily tested on the prototype loop.

The first loop package scheduled for in-pile operation has been constructed and is under test.

PART V. FUEL MANUFACTURE

15. Thorium Oxide Preparation

Three 3-kg batches of spheroidal thoria pellets of ~0.2 in. diameter, 9.6 to 9.7 g/cc density, and having good resistance to attrition in a spouting bed test were prepared for feasibility studies for the pebble-bed blanket. The best results were obtained from oxalate powder which had been prepared by precipitation under oxalate-deficient conditions and had then been fired to 800°C for 1 hr. It was pressed to a green density of 4.5 g/cc with aluminum stearate binder and then fired to 1750°C in air.

Four kilograms of 1450°C-fired Davison pellets of low density, strength, and attrition resistance were densified, strengthened, and hardened to a satisfactory degree by soaking in diban (dibasic aluminum nitrate solution) and then firing to 1750°C.

The average size of thoria microspheres prepared by the flame denitration of methanol solutions of thorium nitrate tetrahydrate was not changed by increasing the size of the droplets fed to the combustion zone or by substituting water for methanol and nitrogen for propane-oxygen for atomizing the feed solution. Decreasing the reflector temperature in the combustion zone from 1600 to 900°C doubled the average particle size, increasing it from 1 μ to 2 μ.

PART VI. METALLURGY

16. Metallurgy

Resistance measurements were made on Zircaloy-2 as a function of temperature from 100 to 1050°C, at heating and cooling rates from 2 to 70°C per minute. The alpha/alpha-plus-beta temperature is shifted slightly upward to above 827°C at the highest heating rates; on cooling, it is depressed to 785°C for rates of 2 and 5°C per minute, 781°C for 10°C per minute, and 760°C for 70°C per minute. Two "bumps" appear in the resistance-temperature curve that cannot be explained through the present knowledge of the physical metallurgy of Zircaloy-2. One, about 2% in magnitude, occurs between 250 and 450°C, and the second occurs in

the alpha-plus-beta two-phase field. Both are affected by heating and cooling rate and, to some extent, by prior thermal history. Hydrogen content is not the cause.

Transformation kinetics studies were started on the Zr-15Nb-1Cu ternary alloy and the Zr-Cu and Zr-Mo binary alloys. Both isothermal and beta-quench and reheat transformations are being studied. The ternary alloy behaves similarly to the parent binary alloy except that, in the beta-quench and reheat transformation, greater amounts of omega phase seem to be formed during the heating to aging temperature. The isothermal transformation product is nodular and grows grain by grain. Metallographic etchants have been developed for the revelation of the microstructures of the isothermally transformed Zr-Cu specimens but not for the Zr-Mo specimens. The isothermal transformation product for the Zr-Cu system is nodular and grows from the grain boundary into the grain.

Twenty-four sets of pellets were fabricated with varying compositions and fabrication techniques for abrasion testing to determine optimum manufacturing combinations. Techniques adequate for making flat-ended, cylindrical pellets were found to result in pressure laminations when used in making spherical-ended pellets.

The underwater constricted-arc cutting process utilizing special torches was applied successfully in cutting the diffuser screens into strips for removal from the HRT core vessel.

PART VII. ANALYTICAL CHEMISTRY

17. Analytical Chemistry

Flame-photometric methods were devised for the determination of calcium and also rare-earth elements in ThO_2. In the determination of calcium, an additive to the ThO_2 for the purpose of increasing its density, an $HClO_4$ solution of the sample is aspirated into the flame, and standard solutions of calcium containing thorium in a concentration approximately that of the sample are used for calibration purposes. In the application of flame photometry for the estimation of rare-earth elements in ThO_2, the sample is dissolved in a nitrate medium. The thorium is then removed by an extraction procedure to prevent its interference. After destruction of ammonium acetate in the raffinate, the rare-earth elements are extracted and subsequently determined flame-photometrically in the organic phase.

A direct coulometric titration method was applied to the estimation of U(IV) in slurries of $ThO_2 \cdot UO_x$. For samples containing 1 to 10 mg of U(IV) the coefficient of variation was 1%.

Conductometric titrimetry was used to determine free H_2SO_4 in radioactive uranyl sulfate fuel solutions. For 0.05 $\underline{M}$ H_2SO_4 solutions, the relative standard deviation was less than 1%.

CONTENTS

Part I

HOMOGENEOUS REACTOR TEST

1. HRT REMOTE OPERATIONS, MAINTENANCE, AND TESTING

S. E. Beall, P. N. Haubenreich, J. W. Hill, Jr.
I. Spiewak, W. R. Gall, F. N. Peebles, M. I. Lundin

H. F. Bauman
R. Blumberg
N. C. Bradley
J. R. Buchanan
S. R. Buxton
B. D. Draper[1]
D. F. Frech
R. H. Guymon
R. J. Harvey
E. C. Hise
P. P. Holz
J. E. Jones
J. O. Kolb
H. R. Payne
H. B. Piper
J. L. Redford
H. C. Roller
R. C. Robertson
W. Terry
P. Vignet[2]

In run 21, which occupied the major portion of the previous report period,[3] the reactor operated continuously for 105 days at power levels up to 5 Mw. The run was ended on January 22, after the rate of mixing of fuel between the core and blanket regions suddenly doubled. An inspection of the core revealed a second hole in the Zircaloy vessel. A program of maintenance and major repairs, which had been planned after the first hole occurred, was begun in order to remove the five uppermost diffuser screens, repair the core-vessel holes, reverse the direction of flow through the core, and replace several pieces of equipment. Approximately 60% of this program has now been completed.

1.1 CORE PROBLEMS AND REPAIR

After the formation of the first core-vessel hole[4] and recognition of the fuel-instability problem,[5] studies were initiated to find methods of improving the core hydrodynamics and vessel cooling. These studies indicated that to improve the performance of the existing core vessel it would be necessary to remove the upper five diffuser screens and reverse the core flow;[6] and in order to restore the reactor to a two-region machine, it would be necessary, of course, to repair the core hole. Tools for modifying and repairing the core were designed and fabricated and were tested in the maintenance mockup.[7,8]

Concurrent with the core studies and tool development, the reactor was operated as a single-region machine (fuel in both core and blanket regions) to advance the understanding of the fuel-instability problem. In order to delineate regions of instability, it was necessary to operate on the boundaries of these regions. Since the core was essentially unaltered since the time that the first hole developed, the potential for the formation of a second hole was high.

Upon completion of run 21, techniques for modifying and repairing the core were in an advanced state, and the effects of the variables of acid level and system pressure on the reactor stability were fairly well defined.[3] Consequently, the program of reactor alterations was initiated.

1.1.1 Second Core Hole

On February 3, the second hole was found in the Zircaloy core vessel with the aid of a 7/8-in. optical periscope. The hole, shown in Fig. 1.1, was located 1-1/2 in. below the equator of the core. Since the metal immediately around the hole appeared weakened, a tool (shown in operation in Fig. 1.2) was used to chip away the unsound material, enlarging the hole from approximately 1 x 3/8 in. to 1-1/2 x 3/4 in.

1.1.2 Core-Vessel Appearance

The spherical and conical sections of the core vessel down to the elevation of the first core hole were inspected with the optical periscope. The portion of the vessel above the equator was essentially free of blemishes or pits. It did appear to have more scale deposit than the lower portion of the vessel. The scale, however, appeared to be very thin. Below the equator there

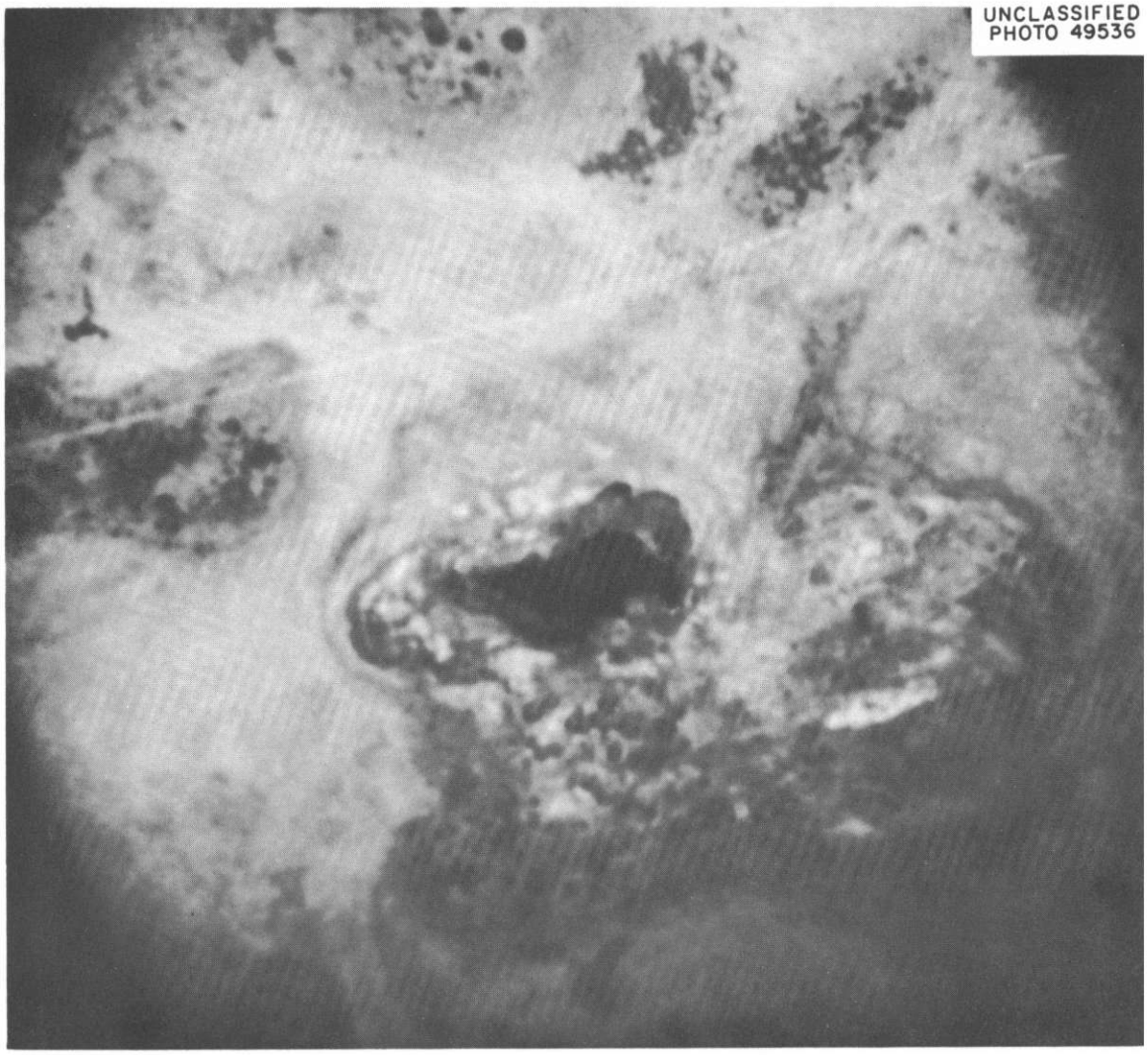

Fig. 1.1. Second Hole in HRT Core Vessel.

Fig. 1.2. Chipping Tool ($\frac{1}{4}$-in. Diameter) in Second Core.

were brownish areas that contained many small pits and interspersed globules having the appearance of molten-weld splatter. In the diffuser-screen area, nubbins were visible where the upper five screens were once attached.

The shape and size of the first core hole appeared unchanged since being previously observed. The vessel wall around the hole and for a few inches above it had a bright etched, metallic appearance.

1.1.3 Reaming of Core Access Flange

The core access flange was reamed with a remotely operated tool,[8] removing excessive weld metal from the opening. This enlargement permits use of the full 2-1/8-in.-dia opening.

1.1.4 Cutting of Diffuser Screens into Strips

The upper five screens were cut into 1-1/2-in.-wide strips with an underwater cutting torch and manipulator.[8,9] The top two screens, already separated from the wall by corrosion, were cut first, and the strips were removed. The third screen from the top was broken loose with a hook, and cut next. Then the fourth and fifth screens (also loosened by corrosion) were picked up and cut into strips. Only 24 hr were spent in cutting all five screens.

1.1.5 Removal of Screen Strips and Loose Objects from Core

Ninety-two pieces of screen were removed from the core with hooks mounted at the end of long rods[10] while the operator viewed the operation with an external-light-source telescope.[11]

Fifty-three pieces, including several corrosion pins, were removed, using various combinations of tools[12] while viewing through a 7/8-in.-dia optical periscope. A simple grapple operated with a speedometer cable encased in a flexible metallic sheath was used extensively to approach out-of-the-way objects. The removal of the 145 pieces of screen was accomplished in approximately 10 days.

1.1.6 Plastic Impressions of Core Holes

After removing the screens, impressions of the two holes were made to obtain the accurate dimensional descriptions needed to patch them. Satisfactory impressions were made after several attempts. The impressions were made with remotely controlled thermoplastic plugs,[8,13] a separate tool being required for each of the two holes. This operation required four days.

The impression of the lower hole was replicated in a "hot" hood by making successive castings with rubber and epoxy resin until the activity level was reduced to below 2 mr/hr. Replication of the second impression is in progress.

1.1.7 Containment of Activity During Core Alteration

With a core radiation level of 10^5 to 10^6 r/hr (ref 7) after shutdown and tools contaminated so that they indicated as high as 100 r/hr at contact when withdrawn from the core, radiation and contamination control was a first-priority consideration in all the reactor alterations work. That the control has been effective is attested to by the fact that personnel exposures have been well below permissible levels.

Disposal of contaminated tools has become routine. Tools are pulled into a disposable plastic containment sheath that extends below, and thus prevents contamination of, the personnel shield through which the core work is done. The entire assembly is lifted into a plastic bag, which is sealed remotely to prevent dusting of activity into the personnel area (see Fig. 1.3). The bagged assembly is then conveyed from the area for burial or decontamination.

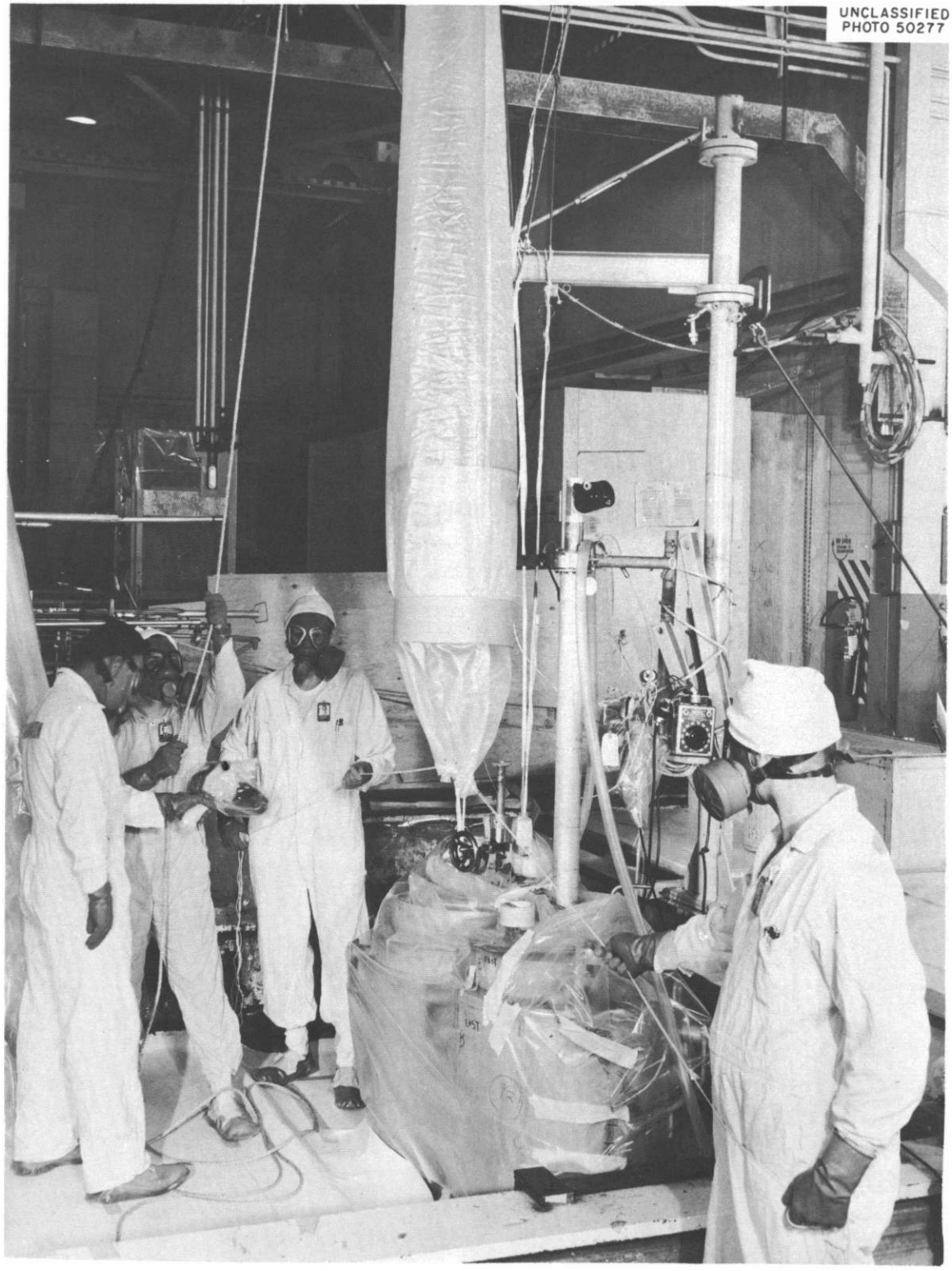

Fig. 1.3. Removal of Contaminated Tool from HRT Core Vessel.

1.2 PREPARATIONS FOR COMPLETION OF THE CORE REPAIR

The future core-repair program includes the following sequence of operations:

1. A sample of the core wall (for metallographic examination) will be cut from around the second hole, creating a round hole.
2. The round hole will be reamed to provide a seating surface for a conically tapered plug.
3. The core vessel will be cleaned with a wire brush to remove scale.
4. The lower hole will be patched and leak-tested.
5. The upper hole will be patched and leak-tested.
6. The system will be flushed with water.

The tools described below have been designed and tested to perform these tasks.

1.2.1 Core-Hole Sample Cutter

A tool to cut, retain, and recover a sample of the core wall (at the edge of the second hole) for metallographic examination was designed, and sub-assemblies were tested successfully. This tool (Fig. 1.4) utilizes a hole saw that is fed into the wall by a double-acting hydraulic cylinder and is rotated from above by means of a 3/8-in.-dia flexible shaft.

1.2.2 Core-Hole Reamer

A reamer assembly was designed to cut a 60° tapered seating surface into the circle left by the sample cutter, and testing was begun. The drive mechanism is the same as that used in the cutter.

1.2.3 Core-Wall Cleaning Tool

Preliminary tests were made of steam-cleaning, grit-blasting, argon-arc-blasting and wire-brushing as methods of removing zirconia-urania scales. Steam-cleaning alone was ineffective, although with the addition of grit it was the best method tried. However, disposal of steam and grit in the HRT would be difficult and time-consuming. A blast of argon ions from a modified weld torch removed heavy oxide effectively, but it had a tendency to melt a thin surface layer of the Zircaloy wall. The wire-brush technique was chosen as the simplest and best method.

A high-speed, air-motor-driven wire-brush assembly was designed for cleaning scale from the inside wall of the core. This tool (Fig. 1.5) can brush both the spherical and conical surfaces of the core wall.

1.2.4 Patching of the Holes

The tool for patching the lower hole was described previously.[7] A similar tool will be used for patching the second hole.

UNCLASSIFIED
ORNL-LR-DWG 49256

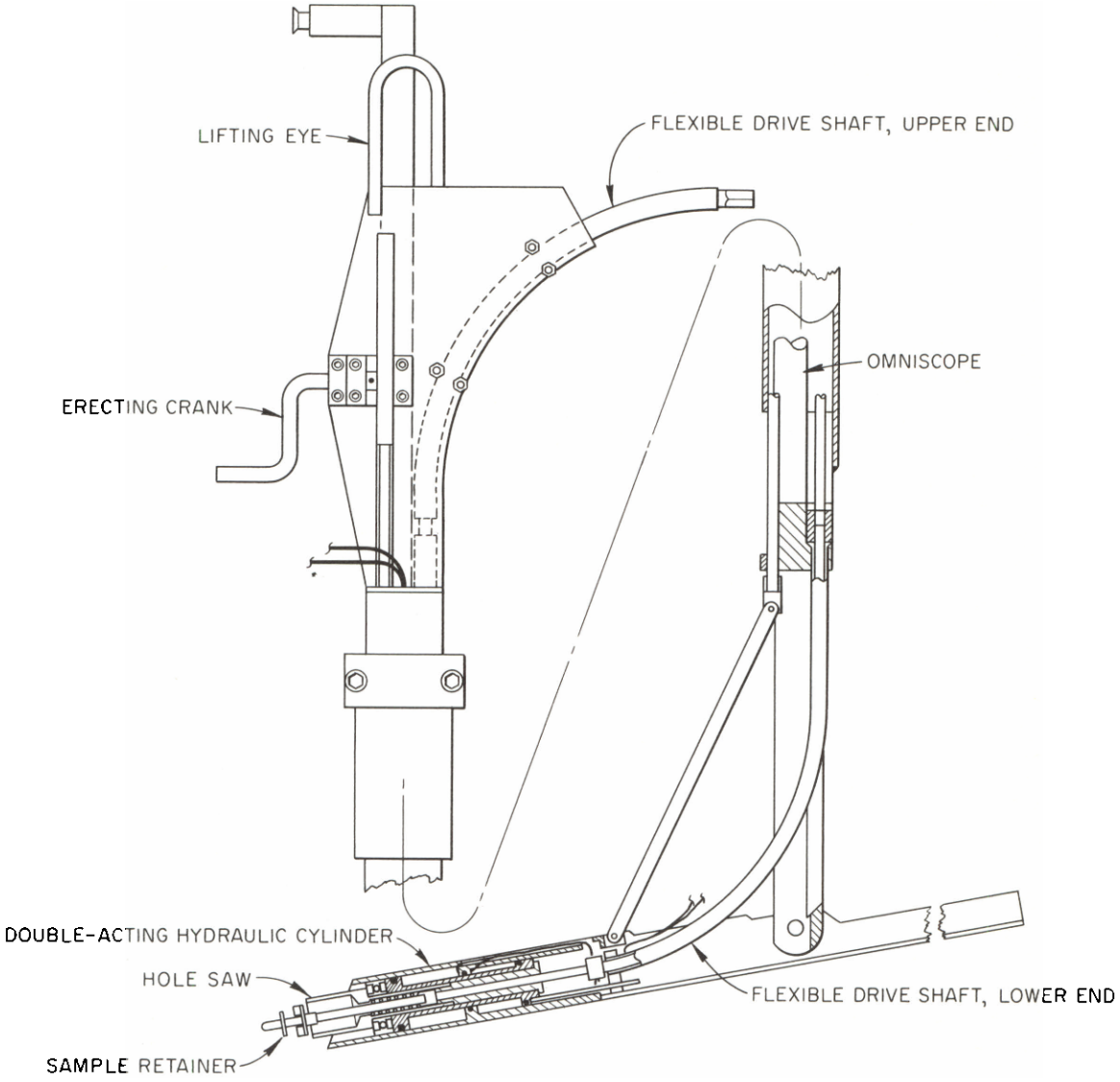

Fig. 1.4. Core-Hole Sample Cutter.

Whereas the first hole is in a region of direct impingement by the jet when the fluid flow is from the top of the core downward, the second hole is in a region where uranium-bearing solids might collect in the wake of projections above the surface of the core vessel.[14] Therefore it is desired to mount a flush patch which will create a minimum of flow disturbance. A flush Zircaloy plug, having a 60° included-angle taper, will be placed into the hole and fastened by means of a Zircaloy toggle bolt. The Zircaloy bolt will have a flush, countersunk head with a carbon-steel hexagon glued on with Eastman 910 adhesive. After the bolt has been properly torqued, the glued bond will be softened by hot water, and the hexagon will be removed, leaving a flush bolt and patch assembly. A mockup of this type of patch was tested and found to leak less than 500 cc/min at a 15 psi differential with a 1/4-in. bolt torqued to 35 in-lb.

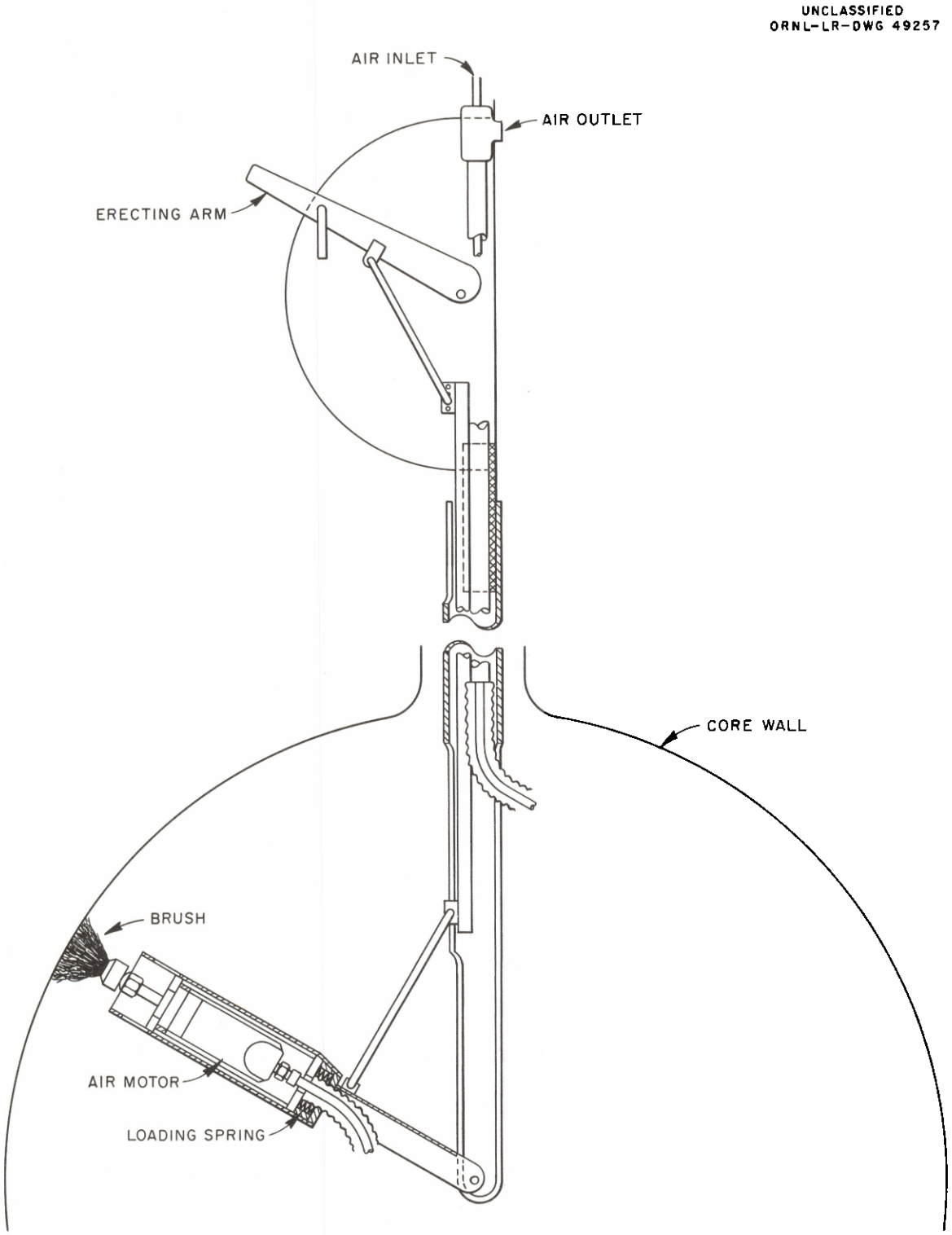

Fig. 1.5. Core-Wall Brush.

1.3 MAINTENANCE AND SYSTEM ALTERATIONS

Concurrent with the core repair work, maintenance and alterations of other major pieces of reactor equipment have been in progress. The reactor shield was flooded and underwater procedures were followed. Sufficient light-water condensate was added to the reactor to establish ice plugs and prevent gross entry of flooding water into the piping and equipment during replacement operations.

1.3.1 Installation of Dual Personnel Shields and Standpipes

Modifications were made to the two existing personnel shields (lead) to permit them to be aligned over the respective core and blanket inlet holes simultaneously. Standpipes were then mounted above the core and blanket access flanges to permit dry operations to be carried out in the core and blanket regions while the cell is flooded with shield water. An off-gas system was attached to the standpipes to prevent spread of radioactive gas from the reactor vessel to the high-bay area.

1.3.2 Alterations to Permit Core Backflushing

Cutting of the core diffuser screens produced about 1/2 liter of metal droplets.[7] In order to remove this and other loose debris, the core circulating pump was raised and temporary crossover pipes were installed so that the debris can be back-flushed from the core. The suction pipe contains a basket-type strainer to collect the solids.

The core dump valve was removed temporarily, and a hand-valve assembly was installed with a strainer to prevent debris from entering the dump tanks.

1.3.3 Equipment Replacements

(a) Valves.--The inlet valves (HCV-136 and -236) to both high-pressure samplers were replaced, because of excess leakage through their seats.

One of the block valves (HCV-936) between the low-pressure systems was replaced, because the valve stem occasionally stuck, necessitating higher than normal air loadings in order to operate the valve.

The three valves had been in use since the reactor was built.

(b) Pumps.--Two diaphragm pump heads were replaced. One was a fuel-feed head in which the diaphragm had failed early in run 21. The head, which had seen only about 450 hr of service at the time of failure, will be cut open to determine the cause for the failure. The second head replaced, from the fuel-pressurizer purge pump, was used throughout run 21, but the check valves leaked excessively during the latter part of the run.[3] The head had operated for a total of 9264 hr.

(c) Multiclone.--As an initial step in the reversal of the core-circulating-pump flow path (see Sec. 1.3.2), the multiple-hydroclone assembly was removed and transferred to the equipment storage pool in a shielded carrier. One spot on the assembly surveyed as high as 6000 r/hr at contact. A multiclone of revised design will be installed (see Sec. 2.1).

1.3.4 Sampler Mechanism Repair

The core sampler assembly was removed for repair of a pinned connection on the stem of the low-pressure isolation-chamber valve. After the assembly was reinstalled, the sampler connections were made leak-tight, as indicated by helium detection methods.

1.3.5 Condensate-Transfer Jumper-Line Installation

During operation of the reactor with fuel in the blanket, fuel has been able to accumulate in the blanket dump tanks through sampling or valve leakage. This has necessitated emptying the dump tanks in batches every few days. A new line[15] was installed so that condensate which is transferred from the core system will flow into the blanket dump tanks. This will enable the blanket feed pump to pump continuously from the dump tanks. In order to install the line it was necessary to replace the blanket transfer valve (HCV-434), although it had no defects. This valve was used in another replacement [see Sec. 1.3.3(a)].

1.3.6 Radiation Containment Experience

Personnel exposures were well below permissible levels during all phases of the work performed on equipment replacement or alteration. The highest single exposure in a 24-hr period was 220 mr. Working backgrounds have usually been 10 to 60 mr/hr.

The reactor shield has been filled with water (~200,000 gal) for approximately 85% of the report period. Only one of the underwater maintenance operations added any large amount of activity to the water. This occurred when about 70 curies of predominantly (>80%) beta emitters drained from the core circulating pump while it was being repositioned for the backflushing operation. When the pump was unbolted from its flanges, a scavenging jet was used to pull light-water condensate from the pump to the waste system, but it was not wholly effective. The rest of the underwater maintenance activities added only 10 curies of activity to the water. Since activity in the water did not add appreciably to the working background and since visibility has been good, there has been no need to dispose of and renew the shielding water so far during the maintenance period.

1.3.7 Future Alterations

Replacement jobs still remaining are:

1. primary and secondary fuel recombiners,
2. core circulating pump,
3. the fuel condensate-tank block valve, and
4. a core pressurizer-heater element.

1.4 REACTOR CONTAINMENT TESTS

1.4.1 Location of D_2O Leak

During the cool-down following run 21, a leak developed in the piping of the fuel system and allowed about 400 lb of D_2O condensate to escape to the containment-shield sumps. Before the initiation of the reactor alterations program, helium leak-detection methods located the leak at a crack which had

developed between two welds made close together in the purge line to the core circulating pump (see Fig. 1.6). The line will be removed with the circulating pump, which is to be replaced.

1.4.2 Shield-Penetration Leak Tests

All reactor containment-shield penetrations are being leak-tested. These tests are repeated routinely to ensure that the integrity of the secondary containment is maintained.

1.5 METHODS OF OPERATION FOLLOWING CORE REPAIR

Studies of reactor operating methods following core repair were completed. The reactor will be operated with the core and blanket pressurizers interconnected if possible. If the leakage through the core patches is too great to permit interconnecting the pressurizers, the following methods will be investigated: (1) operation with the pressurizers separated by an orifice and rupture disc, and (2) operation with the pressurizers separated by rupture discs and with the blanket pressurizer filled with liquid.

To improve core wall cooling, the blanket operating temperature will be kept below the core temperature.

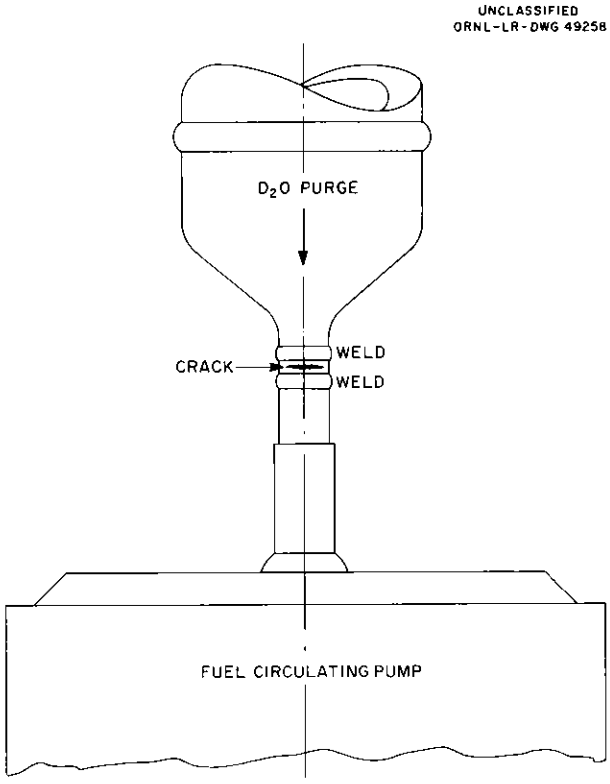

Fig. 1.6. Location of Crack in Purge Line.

REFERENCES

1. On loan from TVA to AEC.

2. On loan from the French Atomic Energy Commission.

3. S. E. Beall et al., HRP Quar. Prog. Rep. Jan. 31, 1960, ORNL-2920, p 3-8.

4. S. E. Beall et al., HRP Prog. Rep. July 31, 1958, ORNL-2561, p 6.

5. S. E. Beall et al., HRP Quar. Prog. Rep. Oct. 31, 1958, ORNL-2654, p 3-7.

6. C. G. Lawson, Proposed Modifications to HRE-2 Core, ORNL-CF-60-1-20 (Jan. 12, 1960).

7. I. Spiewak and F. N. Peebles, HRP Quar. Prog. Rep. Apr. 30, 1959, ORNL-2743, p 13-30.

8. I. Spiewak and F. N. Peebles, HRP Prog. Rep. Oct. 31, 1959, ORNL-2879, p 17-28.

9. P. P. Holz, Underwater Electric Arc Cutting Manipulator for HRT Screen Removal, ORNL-CF-59-11-130 (November 26, 1959).

10. P. P. Holz, Some Miscellaneous Maintenance Tools Used to Manipulate Loose Objects in the HRT Core, ORNL-CF-59-11-123 (Nov. 17, 1959).

11. W. R. Gall, HRP Quar. Prog. Rep. Jan. 31, 1959, ORNL-2696, pp 23, 25.

12. I. Spiewak, HRP Quar. Prog. Rep. Apr. 30, 1959, ORNL-2743, pp 16, 18.

13. B. D. Draper and E. C. Hise, Remote Maintenance Procedure Report, ORNL-CF-59-11-128 (November 26, 1959).

14. C. G. Lawson and F. N. Peebles, Effect of Uranium-Bearing Scale Deposits on HRE-2 Core Wall Temperature, Heat Flux and Patch Temperature, ORNL-CF-60-3-124 (Mar. 17, 1960).

15. W. R. Gall et al., HRP Quar. Prog. Rep. Jan. 31, 1960, ORNL-2920, p 17.

2. HRT PROCESSING PLANT

W. D. Burch O. O. Yarbro

2.1 IMPROVED SOLIDS-SEPARATION SYSTEM

After the early runs in which solids removal rates with the original single-hydroclone system were found to be considerably less than production rates from corrosion, the system was modified by installation in the reactor cell of a unit containing 13 hydroclones.[1,2] Solids concentrated in this unit were then collected by the original system and dissolved in the normal manner. Collection rates were increased, approximately to the production rate in run 20, when corrosion rates were very low. Further improvements, however, are necessary to prevent a continual increase in solids inventory in the reactor. A revised multiclone has been designed and is being fabricated for replacement of the original unit during the present maintenance period. The efficiency of the system has been improved by:

1. Reducing the size of the hydroclones from 0.6 in. to 0.4 in., but retaining approximately the same flow rate by adding five hydroclones, for a total of eighteen. The efficiency for particles in the range of 0.5 to 1 μ is 50 to 100% higher for the smaller hydroclones.

2. Increasing the available head across the multiclone from 48 ft to nearly 94 ft, the full head of the circulating pump. The revised system feed and return lines originate on the legs of the replacement circulating pump instead of at the flanges across the heat exchanger. Hydroclone efficiencies for 1-μ particles are 50% at 90 ft of head, but only 30% for 48 ft.

3. Recycling the cell-C hydroclone overflow stream to the multiclone underflow receiver. Thus all solids collected by the multiclone should eventually be transferred to the processing cell, independent of the efficiency of the cell-C hydroclone.

4. Removing the multiclone underflow receiver to overflow stream bypass, which prevented a continued accumulation of solids in the multiclone underflow pot. With this arrangement, the cell-C collection system need be operated for only a short interval after a convenient-sized batch of solids has been collected in the multiclone underflow pot.

The piping layout is shown in Fig. 2.1.

2.2 LOCATION OF SOLIDS IN THE REACTOR PIPING SYSTEM BY GAMMA SURVEY

An extensive gamma survey of piping in the reactor system has been in progress during the core maintenance period following run 21. Since the piping system was rinsed thoroughly, it is assumed that essentially all the activity is associated with insoluble fission products, and past experience has shown that these insoluble fission products are rather uniformly dispersed with

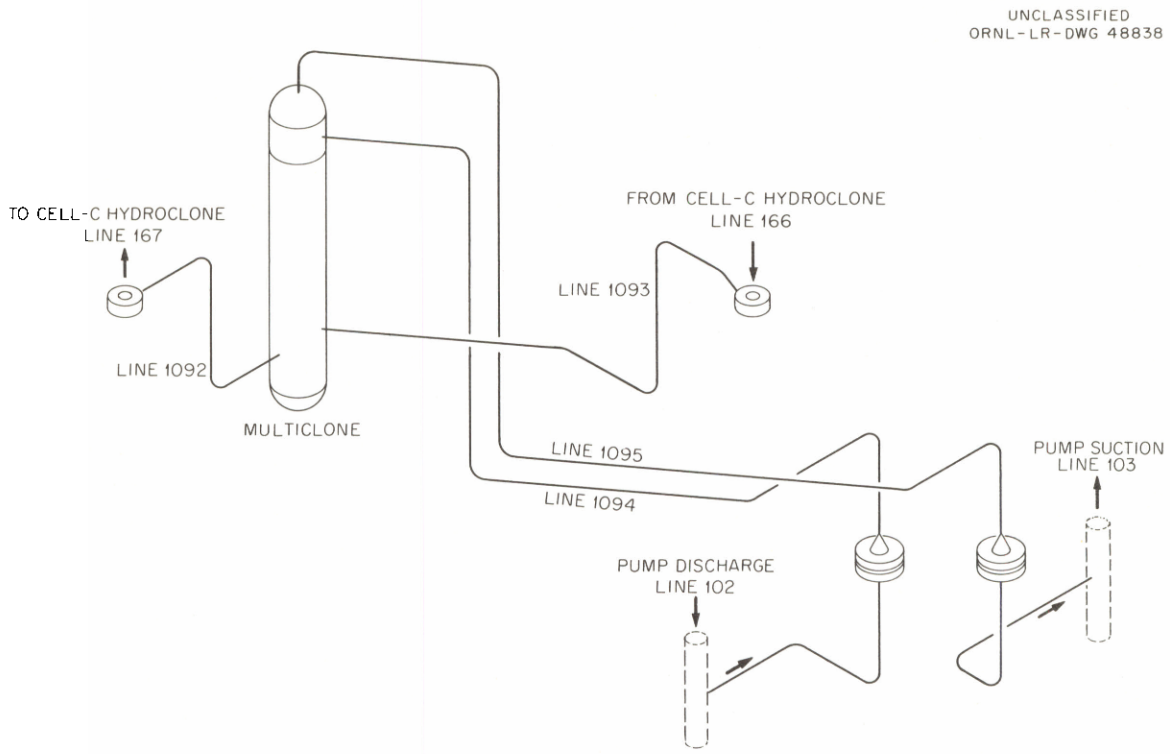

Fig. 2.1. Multiclone Installation for Reverse Pump Flow.

the insoluble corrosion products. In the period 80 to 100 days after shutdown, when the readings were taken, the activity was predominantly from Zr^{95}, Nb^{95}, and $Ru^{103,106}$.

Significant gamma readings obtained to date are listed in Table 2.1. The main circulating-system piping above the core will be surveyed at a later date.

A preliminary material balance indicates that about 70% of the total insoluble fission-product activity is in the heat exchangers, 15% is in the rest of the high-pressure system, and about 15% is in the low-pressure system. While it may be inferred that the corrosion-product material balance is approximately the same, the possibility exists that there are accumulations of old, decayed solids in the low-pressure system which would not be detected by this survey. One interesting fact was noted in connection with interpreting scale thicknesses on corrosion specimens inserted in the system. The activity level in line 101 (where the corrosion-specimen assembly was installed just upstream of the heat exchanger) was a factor of 6 less than the average readings in the fuel circulating loop. The scale on the specimens and piping at this point is obviously considerably less than on the majority of the piping.

A gamma survey of the iodine bed revealed significant activity at the bottom of the bed as expected, but, in addition, over twice as much activity at a point about 4 to 6 in. below the top of the bed. The majority of this activity is I^{131}, since readings seven days after the initial reading were only about 60% as high as the first reading.

The hottest reading obtained in the cell (>6000 r/hr) was at the feed chamber of the multiclone. Calculations show that about 100 g of solids are

Table 2.1. Gamma Activities in the Reactor System

Location	Activity (r/hr)
Fuel-system piping upstream of heat exchanger	900 - 1740
Fuel-system piping downstream of heat exchanger	840 - 1440
Blanket system, line 200, in vicinity of fuel circ. pump	2400 - 3900
Fuel-circ.-pump discharge line 18 in. past and under thermal shield	2400
Blanket dump tank (bottom)	180 - 3000
Fuel dump tank (bottom)	120 - 240
Dirt trap in fuel-feed-pump suction line	120
Multiclone at feed chamber	>6000
East head, fuel feed pump	2400
Fuel feed line downstream of feed pumps	Up to 2100
Letdown heat exchanger, hot end	1800 - 3200
Letdown heat exchanger, cold end	6 - 600
Iodine bed (due to 8-day I^{131} as verified by readings one week apart)	360
Fuel storage tanks; fuel charge contained therein	600

required to give such a reading. In a previous survey, following run 13,[3] the dirt trap in the feed-pump line read 1100 r/hr, a factor of 30 to 50 above most of the high-pressure system piping. It was clear that a large accumulation of solids existed in the dirt trap at that time, but the present survey showed the trap to be essentially free of activity.

REFERENCES

1. W. D. Burch et al., HRP Quar. Prog. Rep. Apr. 30, 1959, ORNL-2743, p. 10.

2. W. D. Burch et al., HRP Prog. Rep. Oct. 31, 1959, ORNL-2879, p. 9.

3. S. E. Beall et al., HRP Prog. Rep. July 31, 1958, ORNL-2561, p. 5.

3. HRT COMPONENT DEVELOPMENT

I. Spiewak
F. N. Peebles

C. H. Gabbard
J. C. Moyers
C. G. Lawson
M. Richardson

3.1 CIRCULATING-PUMP TESTS UNDER ADVERSE FLOW CONDITIONS

As the result of two titanium impeller fires several months ago in the HRT, a series of tests was conducted to determine how to avoid such incidents in the future when using titanium or zirconium impellers. The test of a zirconium impeller was reported previously, as well as the start of the test of a stainless steel impeller containing titanium wear rings.[1]

During the cool-down from steam-oxygen circulation at 250°C and 1250 psi, the titanium wear rings ignited at nominal loop conditions of 101°C and 875 psia oxygen pressure. The resultant fire burned a large portion of the stainless steel impeller and scroll liner. A section of the stainless steel discharge line was also ignited at a tube fitting approximately 6 in. from the pump casing and burned through the pipe wall as shown in Fig. 3.1.

The tests indicated that titanium or Zircaloy probably will not ignite unless the surfaces are relatively dry. On pumps using titanium or Zircaloy hydraulic parts, the wear-ring clearances should be increased to avoid rubbing contact, and the pumps should not be run under cavitating or dry conditions. A complete report of the tests is being written.

Fig. 3.1. Pipe-Wall Burn-Through of Pump Torture Loop.

3.2 HRT-CORE STRESS ANALYSIS

An analysis of the stresses that would exist in the HRT core with various blanket temperatures down to 100°C was completed.[2] Stresses considered were those due to axial differential expansion between the core and the pressure vessel, radial temperature gradients in the core wall, and a differential pressure of 100 psi between the core and blanket fluids. The maximum calculated stress, which occurs at the sphere-to-cone transition, is 7760 psi. This compares with a 14,000-psi yield strength at 600°F obtained from the original core material.[3] Since the calculated stress is a combination of thermal and pressure stresses and can, therefore, exceed the allowable design stress value to a certain extent without serious consequences, the lower limit of the blanket operating temperature is not set by core-vessel stresses.

3.3 REVERSE FLOW IN THE HRT CORE

Calculations were made to estimate the temperature distribution that would exist in the HRT with the flow reversed and the screens removed from the 90° cone.[4] These calculations were based on observations with dye of the flow distribution in the low-pressure HRT core model and on measurements of the dilution of a salt stream added to the core. In addition, transport lags of fluid recirculated from the outlet back into the entry jet were calculated.[5] The conclusion from these calculations and tests are (1) that the core wall may be kept to 300°C (or lower) at 5 Mw if the blanket is at 250°C (or less) and no uranium-bearing scale is present on the wall and (2) that the maximum fluid temperature in the core at the above conditions will be about 305°C. Figure 3.2 shows a temperature map of the core.

The effects of uranium-bearing deposits were considered along with cooling of the core-wall patches.[6] The temperature of the core wall is shown in Fig. 3.3 as a function of scale deposit where the scale contains 10 wt % uranium. These calculations assume that the zirconium oxide remains where the corrosion occurred. The three curves shown are for the following cases: The upper curve is computed on the assumption that both the blanket and the core are pressurized so that boiling does not occur. The middle curve is obtained on the assumption that the blanket is pressurized and the core is at 1500 psi. The lowest curve is for both the core and the blanket at 1500 psi.

Measurements of velocity distribution were made at five locations near the wall of the HRT model in support of temperature computations. The results are summarized in Table 3.1. In all cases the flow was found to have a tangential and a meridional component. The minimum peak velocity is 1.53 fps and is just above the equator.

A radial velocity estimated at 1/3 fps or greater exists in the region between the central jet and the wall jet.

Axial velocity distribution in the central jet indicates that the incoming stream of 450 gpm entrains 172 gpm in its first 7.75 in. of travel, and 670 gpm in the next 9.75 in. Velocity measurements in the lower part of the core show that the jet is somewhat unsymmetrical.

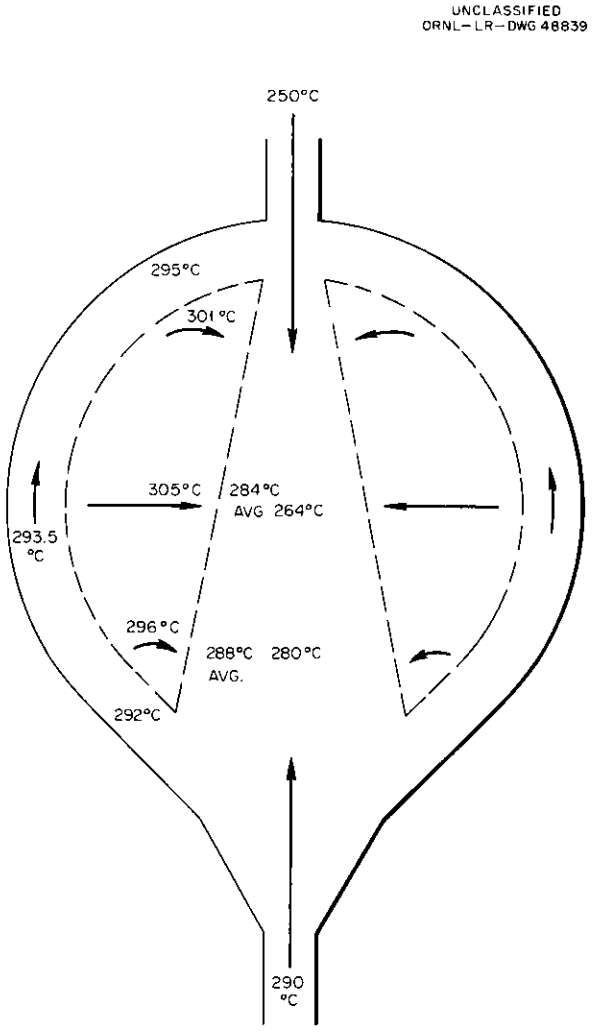

Fig. 3.2. Steady-State Temperature Distribution for Revised HRT at 5-Mw Core Power.

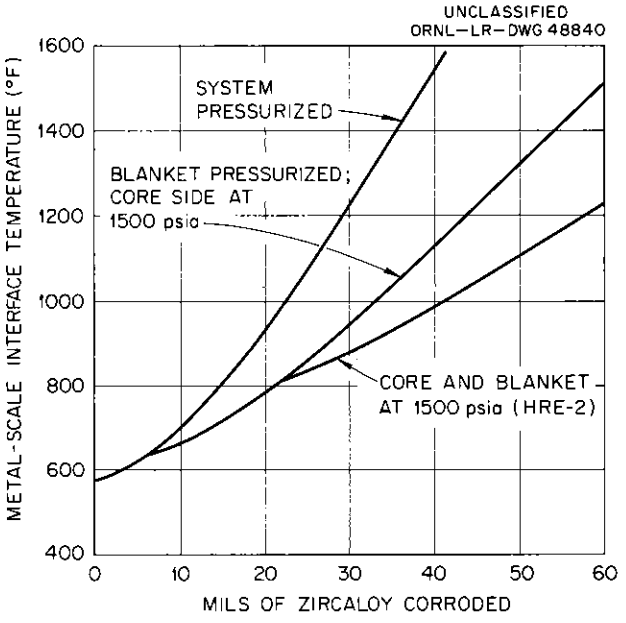

Fig. 3.3. Metal-Scale Interface Temperature vs Mils of Zircaloy Corroded. Uranium concentration, 0.1 g of U per g of Zr.

Table 3.1. Wall Velocity Measurements in 32-in. HRT Core Model; Flow Rate, 450 gpm

Position*	Peak Velocity (fps)	Meridional Velocity Component (fps)	Distance from Wall to Peak Velocity (in.)	Distance from Wall to Zero Meridional Component (in.)
22°	4.24	3.0	0.25	1.3125
52°	3.3	2.33	0.375	1.8125
90°	1.88	1.33	0.5	1.6875
133°	1.53	1.08	0.125	1.25
165°	2.64	1.87	0.125	

*See the sketch below for identification of probe positions:

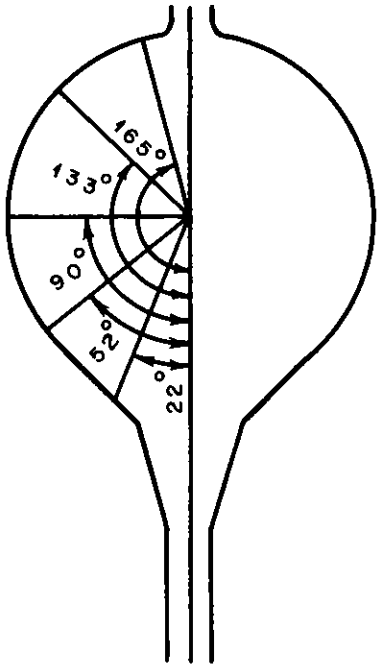

REFERENCES

1. I. Spiewak, HRP Quar. Prog. Rep. Jan. 31, 1960, ORNL-2920, p 11.
2. J. C. Moyers, Investigation of Stresses in HRT Core Vessel as Influenced by Blanket Operating Temperature, ORNL CF-60-4-112 (Apr. 22, 1960).
3. Auburn Research Foundation, Final Report, Tests of Special Materials, (Mar. 20, 1957).
4. C. G. Lawson, Proposed Modifications to HRT Core, ORNL CF-60-1-20 (Jan. 12, 1960).
5. C. G. Lawson, Fuel Transport Lag Time and Temperature Distribution for Reversed Flow HRE-2 Core, HRP-60-41 (Apr. 4, 1960).
6. C. G. Lawson and F. N. Peebles, Effect of Uranium-Bearing Scale on HRE-2 Core Wall Temperature, Heat Flux and Patch Temperatures, ORNL CF-60-3-124 (Mar. 17, 1960).

4. HRT REACTOR ANALYSIS

P. R. Kasten

M. L. Tobias D. R. Vondy

4.1 ESTIMATES OF THE CRITICAL CONCENTRATION IN THE HRT AT 260°C

A number of calculations by various methods were used to obtain the HRT critical concentration at 260°C as a function of blanket-to-core fuel ratio, poison level, and D_2O concentration. Figure 4.1 shows the critical concentrations as a function of blanket-to-core fuel ratio as computed by the harmonics method,[1] the multigroup code GNU,[2] and WANDA,[3] using two-group constants obtained from GNU.

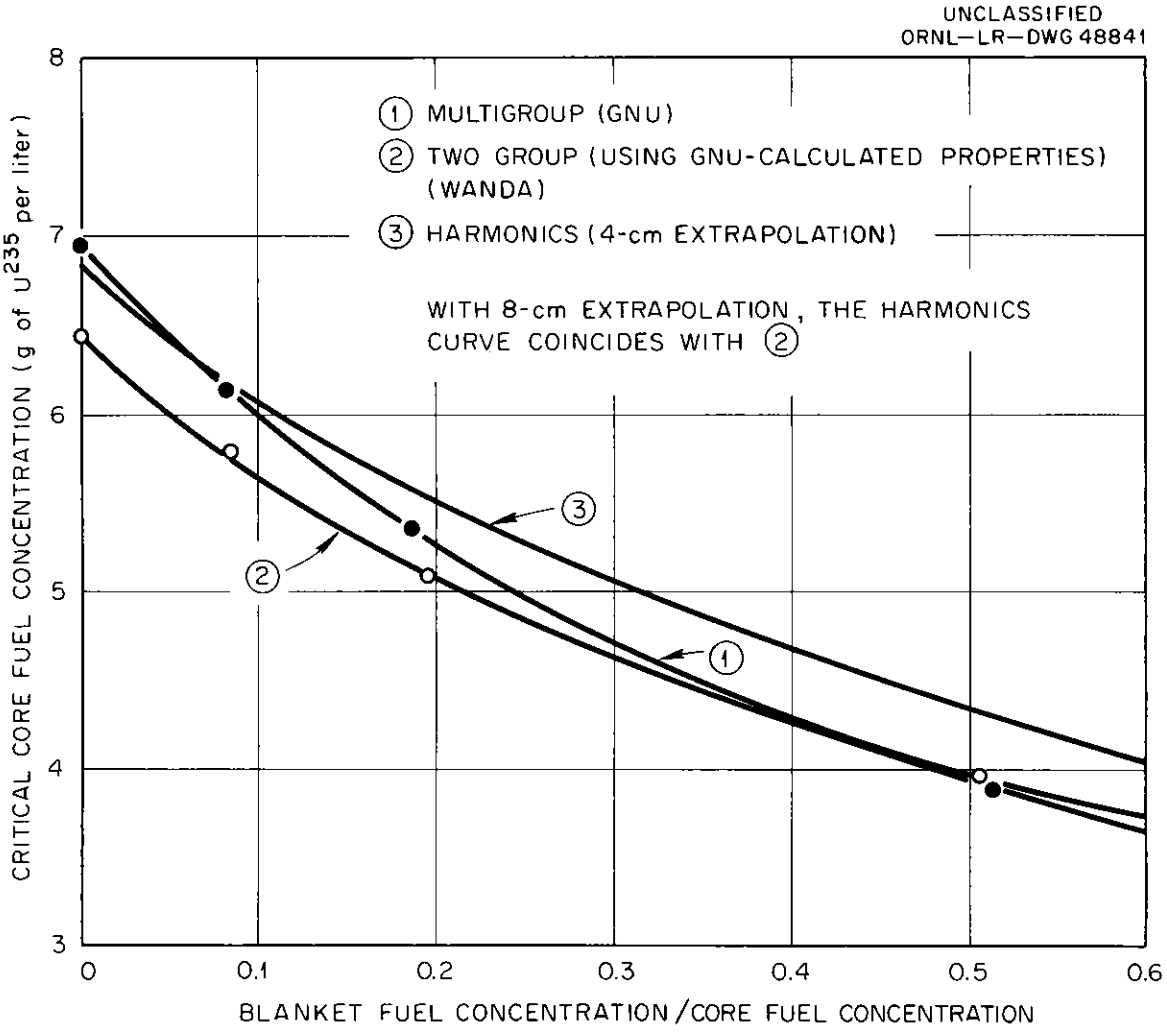

Fig. 4.1. Critical Core Fuel Concentration as a Function of Blanket-to-Core Fuel Ratio in the HRT at 260°C.

The results obtained by the various methods are in good agreement. Figure 4.2 shows the effect of core poison level upon the critical concentration as computed by the harmonics method. Also shown are the effects of ±20% changes in the concentrations of nickel, sulfur, and copper at a poison fraction of 8.5×10^{-3}; this latter value represents an estimate of the present poison level in the fuel solution.

Harmonics-method calculations were performed to determine the reduction in the critical concentration associated with the use of U^{233} in place of U^{235}. The results are given in Fig. 4.3, with the U^{235} curve showing harmonics-method results obtained by Edlund and Wood.[4] With U^{233} fuel, a single point at 280°C was obtained with the GNU-multigroup method, and it was in good agreement with the harmonics-method results.

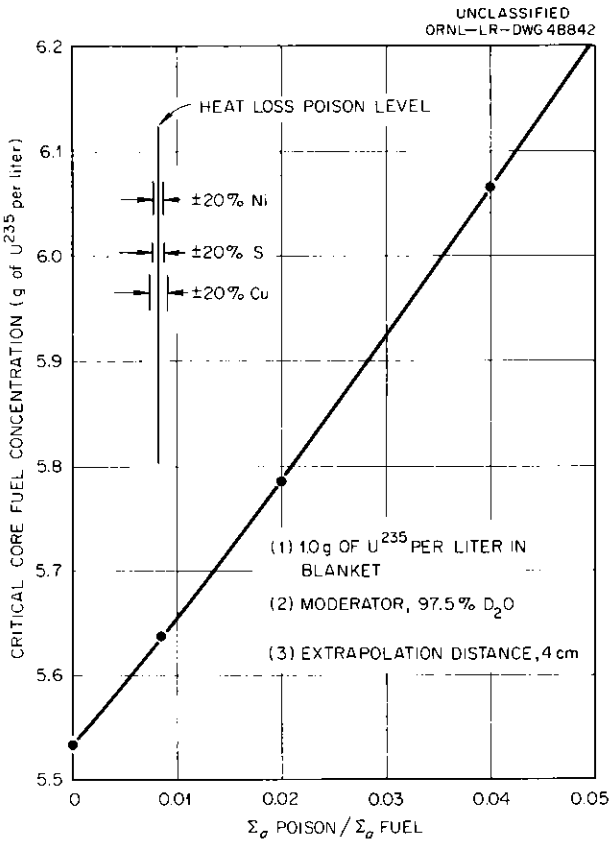

Fig. 4.2. Effect of Poison Level on Critical Fuel Concentration in the HRT at 260°C (Harmonics Method).

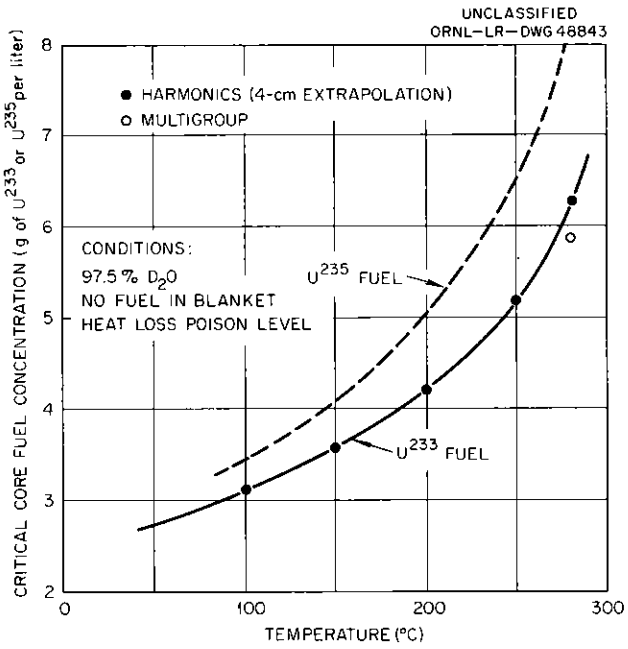

Fig. 4.3. Critical Concentration in the HRT as a Function of Temperature, with U^{233} or U^{235} as the Fuel.

REFERENCES

1. R. Chalkley et al., An IBM-704 Code for a Harmonics Method Applied to Two-Region Spherical Reactors, ORNL-2809 (Mar. 1, 1960).

2. C. L. Davis et al., GNU-II - A Multigroup One-Dimension-Diffusion Program, GMR-101 (Nov. 12, 1957).

3. O. J. Marlowe, WANDA - A One-Dimensional Few Group Diffusion Equation Code for the IBM-704, WAPD-TM-28, Addendum 2 (July 1959).

4. M. C. Edlund and P. M. Wood, Physics of the Homogeneous Reactor Test; Statics, ORNL-1780 (Aug. 27, 1954).

Part II

REACTOR ANALYSIS AND ENGINEERING DEVELOPMENT

5. REACTOR ANALYSIS

P. R. Kasten

M. L. Tobias D. R. Vondy

5.1 THORIUM-PELLET-BLANKET REACTOR STUDIES

Estimates were made of the critical fuel concentration in certain small, cylindrical reactors containing fertile material in the blanket region. The reactor cores consisted of U^{233}-D_2O solutions contained in a $\frac{1}{2}$-in.-thick Zircaloy tank. The core was surrounded by a layer of D_2O followed by three pebble-blanket regions separated from one another by heavy-water layers; the pebble-blanket regions contained 5300 g of Th per liter. The core fuel concentration was obtained as a function of core length, diameter, and the thickness of the water layer between the core and the first thorium region. The core region was assumed to contain no poisons, and the blanket region contained no fuel. The dimensions of the various regions are given in Table 5.1. The reactor temperature was 280°C in all cases.

Table 5.1. Dimensions of Pebble-Blanket Reactor Regions

Core diameter		15 - 24 in.
Core length		48 - 72 in.
Thickness of:	1st heavy-water layer	0 - 9 in.
	core tank	1/2 in.
	1st pebble blanket	3 in.
	2d water layer	3 in.
	2d and 3d blankets	2 in.
	3d water layer	2 in.
	4th water layer	$1\frac{1}{2}$ in.
	pressure vessel	4 in.
Extrapolation distance		1 cm

Figure 5.1 shows the variation of critical concentration with the parameters cited plotted on a relative basis. Most of the calculations were performed using two groups of neutrons. As a check, a multigroup calculation was performed for a core 4 ft long and 18 in. in diameter, and the concentration obtained was 17.4 g of U^{233} per liter; using two groups, the estimate was 12.3 g/liter. The discrepancy is due to differences in the slowing-down model as well as to differences in the estimate of blanket resonance captures.

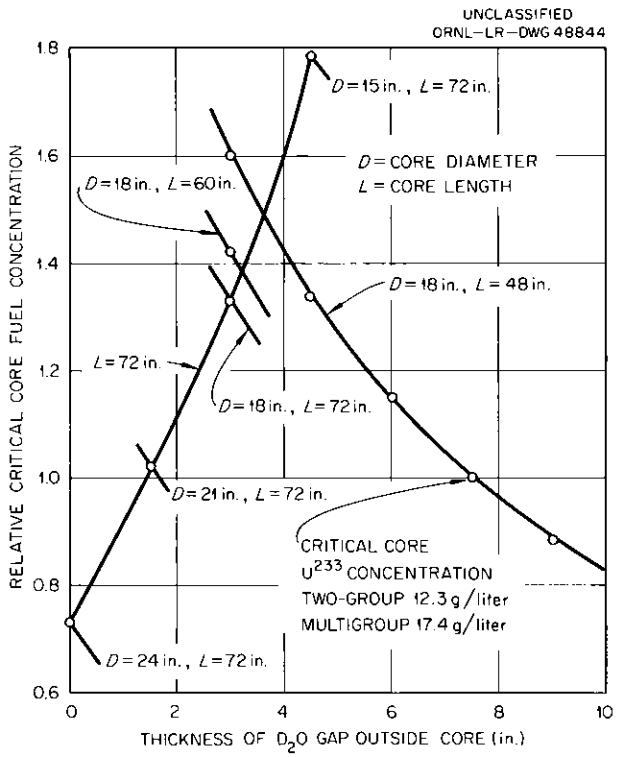

Fig. 5.1. Effect of D_2O Gap Thickness, Core Diameter, and Core Length on Critical Core Fuel Concentration (Two-Group, One-Dimensional Calculation; UO_2SO_4-D_2O Solution in Core, Thorium Pellets in Three Discrete Blanket Regions; 280°C, No Poisons).

6. DEVELOPMENT OF REACTOR COMPONENTS AND SYSTEMS

I. Spiewak F. N. Peebles

D. M. Eissenberg
C. H. Gabbard
P. H. Harley
R. J. Kedl
C. G. Lawson
J. C. Moyers
L. F. Parsly
H. R. Payne
M. Richardson
A. N. Smith
R. P. Wichner

6.1 DEVELOPMENT OF CYLINDRICAL RE-ENTRANT CORE VESSEL

The best design currently envisioned for large two-region reactors includes a vertical cylindrical core tank with a length-to-diameter ratio of about 3. Fluid is admitted in a vaned annular entry at the top of the vessel and directed at high velocity past the Zircaloy wall, thereby keeping the wall cool and reducing the corrosion rate of the metal. The main outlet is at the top, with a secondary outlet to drain the vessel at the bottom.

A test core vessel, which is a full-scale low-pressure model of a 40-Mw reactor or a tenth-scale model of a 400-Mw reactor, was fabricated to permit experimental optimization of the hydraulic design and to permit detailed measurements of velocity distribution. From the experimental data it will be possible to calculate the temperature distribution in an operating reactor of this type.

Figure 6.1 shows the vessel, which is 2 ft in diameter and 6 ft long, in place for testing; many of the 29 access holes for velocity probes are visible. Also visible are Lucite windows through which the flow may be observed. Figure 6.2 is a photograph of the inlet vane assembly, which is installed inside the top of the vessel.

Some axial and tangential velocities measured at a flow rate of 3950 gpm (two-thirds the rated flow) are shown in Fig. 6.3. At this flow rate, the superficial axial velocity at the inlet is 9.9 fps. The obvious defect in the flow pattern illustrated in Fig. 6.3 is that 47% of the inlet fluid penetrates less than 12 1/2 in. into the core. This large amount of short-circuiting is verified by visual observation of the flow.

Small solid particles, below 1/8 in. in diameter, seem to be ejected quickly from the core. However, some 1/4-in. particles remain in the core, rotating with the fluid near the bottom of the vessel, and drop out only when the flow stops.

Two new inlet vane assemblies are being designed and fabricated. These will provide higher inlet axial velocities, and it is believed the fluid by-passing can thereby be reduced to an acceptable level.

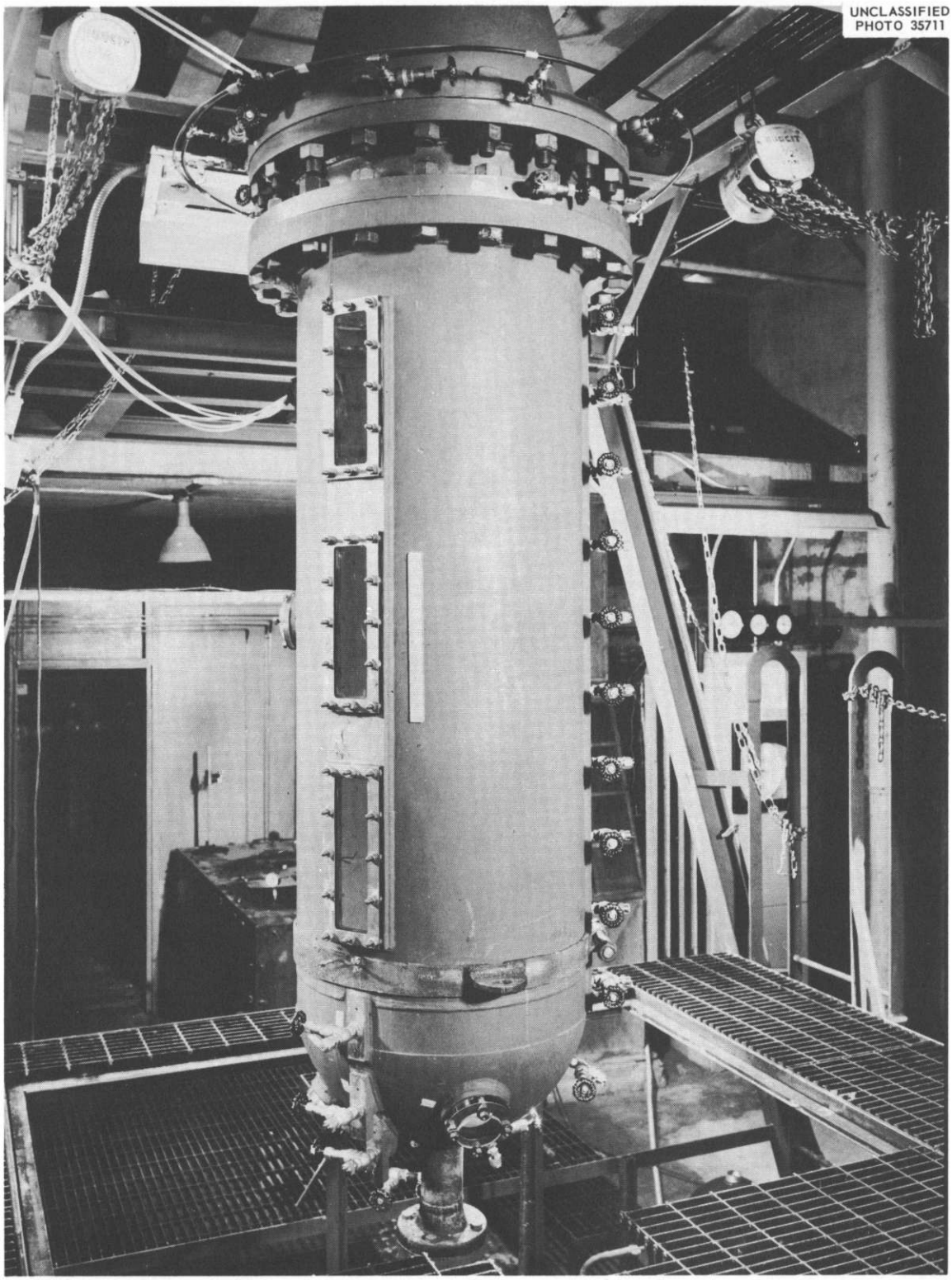

Fig. 6.1. Cylindrical Re-entrant Core-Vessel Model.

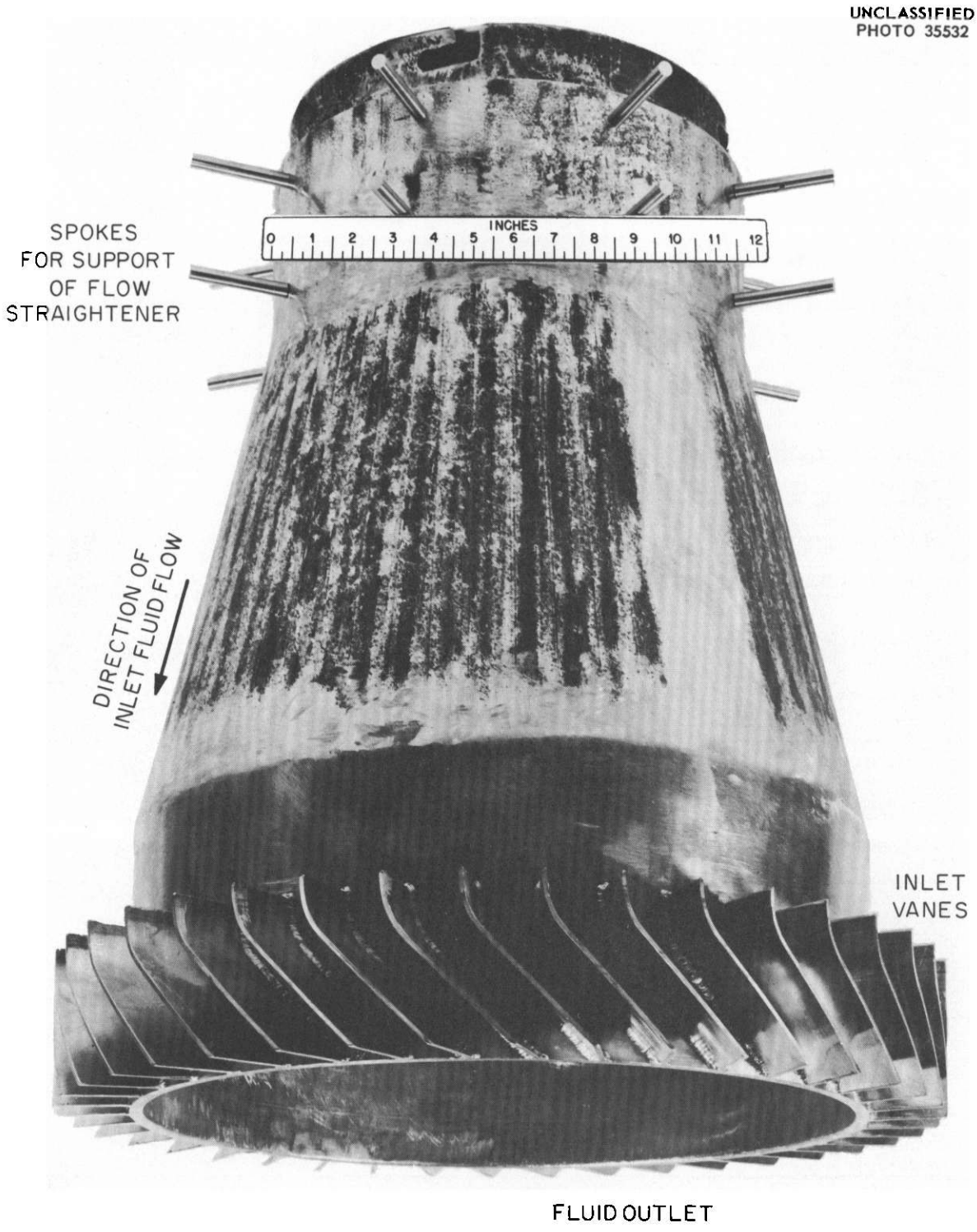

Fig. 6.2. Inlet-Vane Assembly of Core Model.

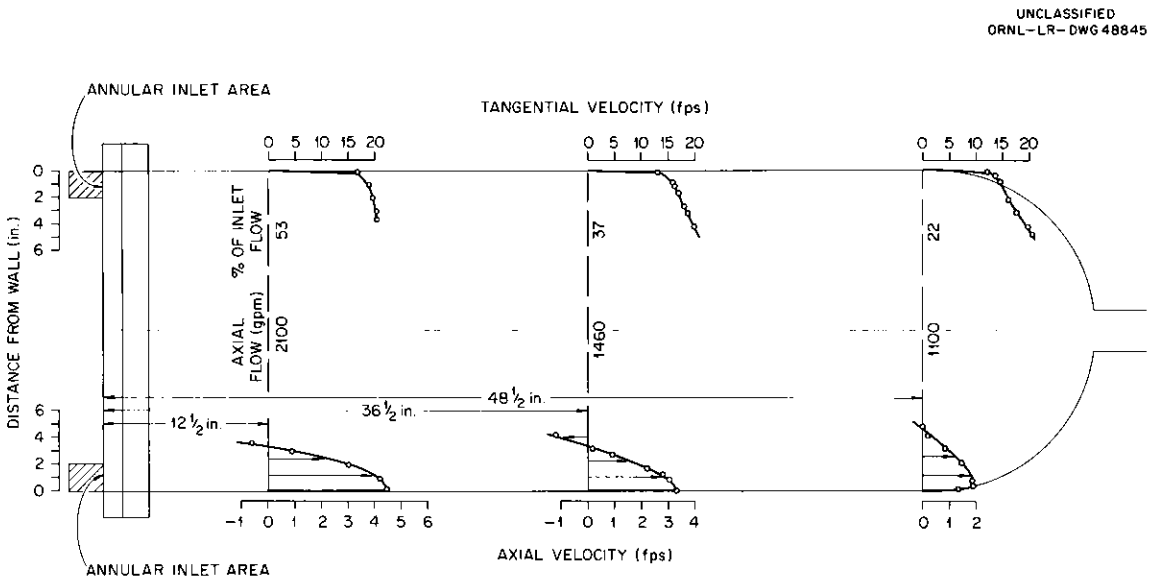

Fig. 6.3. Axial and Tangential Velocity Profiles at Three Elevations of the 2- by 6-ft Cylindrical Core, with 45° Inlet Vanes and a 3950-gpm Flow Rate.

6.2 THORIA BREEDER REACTORS WITH PELLET BLANKETS

An evaluation[1] was made of two-region thoria breeders consisting of a blanket containing thoria pellets in annular regions surrounding a cylindrical core containing uranyl sulfate fuel solution. Critical concentrations, neutron-flux distributions, core and blanket cooling requirements, chemical processing cycles and power costs were determined for 400- and 40-Mw(th) reactors. Table 6.1 gives a summary of important design data for these reactors. With the assumption that satisfactory pellets can be fabricated, it was found that a 400-Mw(th) reactor with a pellet blanket was economically more attractive than the corresponding reactor with a slurry blanket.

Figure 6.4 illustrates the pellet-blanket reactor vessel for a 40-Mw(th) reactor. The fuel solution enters at the top of the cylindrical core through a set of annular swirl-producing vanes, flows downward along the core vessel wall, turns at the bottom, and exits at the polar outlet pipe at the top. The blanket thoria is contained in concentric annular beds. These beds are cooled by heavy water, which enters at the bottom of the pressure vessel, flows upward along the outside of the core, and then radially outward through a perforated distributor shroud and the annular pellet beds in series. The heavy-water coolant leaves the pressure vessel through a side outlet nozzle.

Thoria in the innermost bed would be rearranged periodically, to regulate the irradiation of the pellets, by means of water jets. Removal of pellets from the blanket and recharging pellets to the blanket would be accomplished also by means of water jets. The means for pellet transport is based on a concept tested successfully with 1/8-in. lead shot.

6.2.1 Design of Pellet-Blanket Reactor Vessel

A general arrangement layout was started for a 40-Mw(th) reactor vessel having a 2-ft-dia, 6-ft-long cylindrical core with concentric annular beds of

Table 6.1. Design Data for Breeder Reactors with Thoria Pellet Blankets

	400 Mw(th), Nominal	40 Mw(th), Nominal
Core diameter, ft	4	2
Core length, ft	12	6
Blanket thickness, ft	2	2.25
Core power, Mw	372	40
Average core power density, kw/liter	88	76
Maximum power density at core wall, kw/liter	46	46
Core U^{233} + U^{235} concentration, g/liter	1.6	8
Core flow rate, gpm	26,600	6,000
Core inlet temperature, °C	240	250
Core outlet temperature, °C	290	274
Blanket power, Mw	92	8.5
Maximum blanket power density, kw/liter	327	50
Average thorium concentration in blanket, g/liter	1450	800
Total thorium in blanket, metric tons	26.5	7.2
Thoria pellet diameter, in.	1/8	1/8
Blanket flow rate, gpm	20,000	3,000
Blanket inlet temperature, °C	250	250
Blanket outlet temperature, °C	267	260
Blanket hot-spot temperature, °C	308	270
Total U^{233} inventory, kg	49	17
Total D_2O inventory, liters	51,000	11,400
Reactor doubling time, years	8.3	10.9

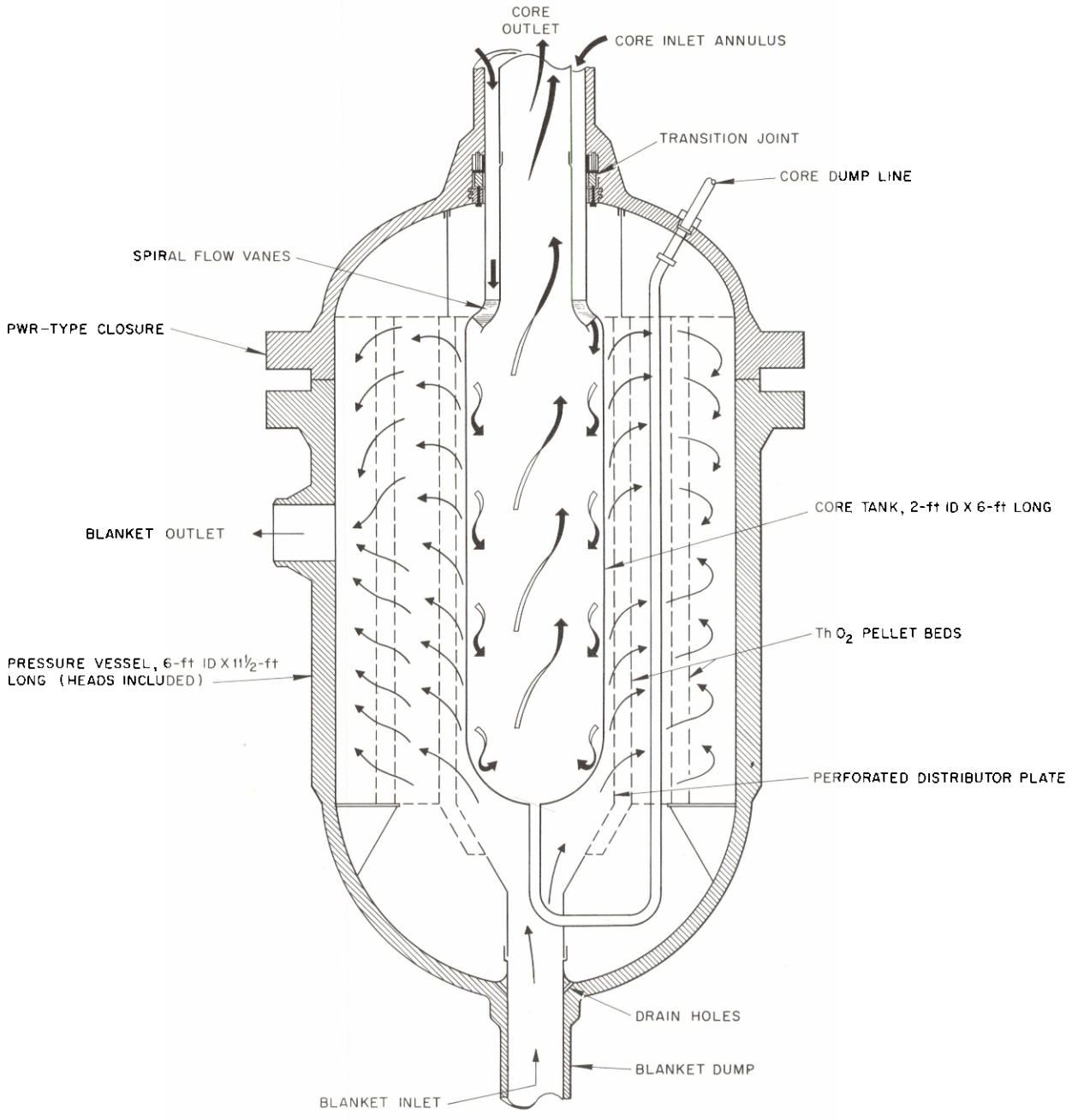

Fig. 6.4. 40-Mw Reactor with Pellet-Bed Blanket.

thoria in the blanket region. Means are provided for rearranging, removing, and recharging pellets in the innermost bed. Pellets in the two outer beds can be removed from the blanket and recharged, but not recirculated within the beds or from one bed to another. Two PWR-type seal-welded closures are provided in the pressure vessel: one to permit removal of the core vessel without removal of the blanket beds, and the other to permit removal of the pellet beds and associated pellet-handling equipment.

6.2.2 Development of Pellet-Handling Equipment

The equipment diagrammed in Fig. 6.5 was used to demonstrate the feasibility of circulating, removing, and charging thoria pellets in a reactor blanket. In the test, 1/8-in. lead-shot pellets were circulated successfully by introducing water at the jet at the bottom of the column. When the water was discharged at the top of the pellet column, through discharge line A, the pellets were disengaged by settling and returned to the pellet bed. When the water was discharged at the top of the 1-in. transfer line through discharge line B, the water velocity exceeded the pellet settling velocity at all points, and hence pellets could be removed from the column. A flapper-valve at the top of the transfer line permits charging of pellets to the column through line B.

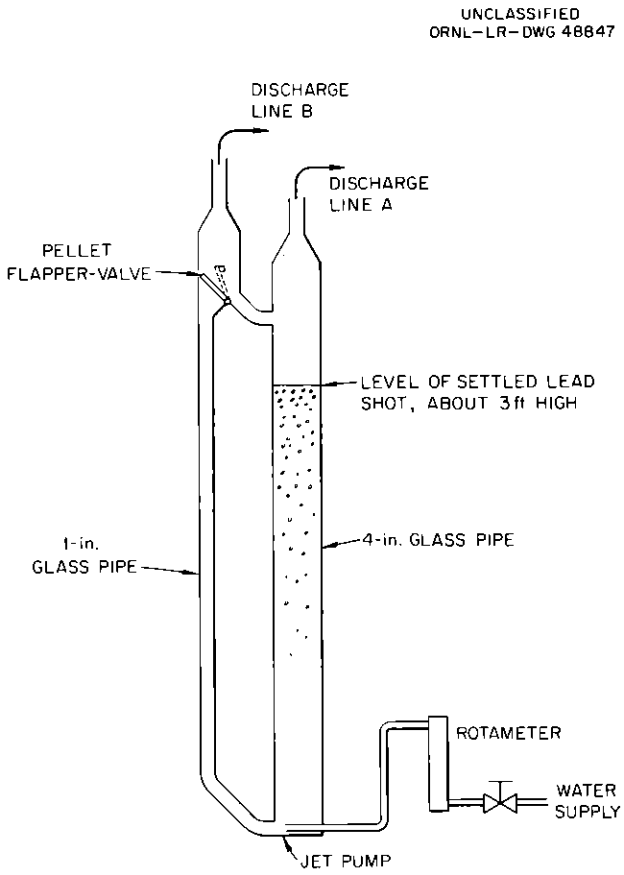

Fig. 6.5. Glass Model of Single Pellet Channel.

Attempts to circulate 1/4-in. steel shot in the test equipment were not completely successful because of occasional jamming of the large pellets in the 1-in. transfer line.

6.3 CIRCULATING-PUMP DEVELOPMENT

6.3.1 200Z Pump and Loop

The 200Z pump, which contains a motor similar to that used in the HRT circulation pumps, but which contains parts more suitable for use in circulating

thoria slurries, was operated in high-temperature water to test its alumina journal and thrust bearings. The pump continued to operate satisfactorily after 2300 hr.

6.3.2 Stator Irradiation Test

Irradiation damage to motor insulation is a potential source of pump-motor failure. A test stator, irradiated in a Co^{60} source, was previously reported[2] to have failed after a total dosage of 5.43×10^9 rads.

The test unit was removed from the source and cleaned. A low resistance from the winding to ground was found in an electrical cable near the stator. The resistance to ground of the motor insulation was then checked by connecting instruments directly to the stator leads, and it was found to be considerably lower than normal. Following baking for 48 hr at a temperature between 100 and 140°C (to remove any possible moisture present), the stator was found to have a higher resistance than before irradiation.

It was concluded from this test that pump motors having class H insulation with the end turns potted with Neonvacite (silica powder and Dow Corning resin 7521) would not be appreciably damaged by radiation in canned-motor pumps in aqueous homogeneous reactors, assuming that pump-to-motor seals did not promote excessive fluid mixing.

6.4 FEED PUMPS

Future reactors are likely to require oxygen recycle pumps, as well as fuel feed pumps of about three times the capacity of HRT pumps. Such pumps are being tested.

6.4.1 Oxygen Compressor

The high-pressure diaphragm of the three-stage diaphragm compressor, designed to recycle radioactive oxygen, has failed several times.[3] The pump was reassembled and instrumented to measure temperatures at various locations on the compressor heads. The compressor will be operated to determine if thermal stresses across the diaphragm or if differential expansion between the head and the diaphragm can be the cause of failure of the third-stage diaphragm.

6.4.2 Increased-Capacity Solution Feed Pumps

Endurance testing of feed-pump heads is continuing; the 10-3/4-in. double-diaphragm head and the 12-in. single-diaphragm head have now operated for respective totals of 14,580 and 9,966 hr.

6.5 THE 300-SM SLURRY SYSTEM

Because of the many problems which may arise in the operation of an aqueous slurry core or blanket system, a system approaching a reactor in complexity is required to demonstrate successful techniques. The 300-SM loop, following moderately successful operation with a slurry core vessel, was recently revised[4] and expanded to include a full-flow shell-and-tube heat exchanger.

Water was circulated to begin a new run. After 300 hr of water circulation, feeding of slurry to the high-pressure system with the revised feed system was

started on March 14. The concentration was brought to approximately 350 g of Th per liter in 6 hr, with a charge concentration of approximately 1000 g of Th per liter.

On March 15 excessive leakage occurred through the letdown line and the system was shut down for replacement of the letdown valves. On examination of the valves, it was found that the upper valve was not visibly damaged. It appeared that this valve had been open while the system was at pressure because of insufficient spring loading on the air operator. The lower valve, which contained similar trim consisting of a Zircaloy plug and 17-5 PH stainless steel seat, was severely eroded. As replacements, a ball valve with aluminum oxide trim was installed in the upper position, and a plug valve with tungsten carbide trim, in the lower position. During this shutdown, additional condensing surface was added to the low-pressure system to permit smoother pressure control.

The run was resumed on March 25 with most of the original solids still in the high-pressure system. On March 28, it was found that the condensate line to the pump motor was plugged with slurry, which apparently had been displaced into the high-pressure condensate receiver as a result of an operating error. The line was unplugged in place by using the high-pressure purge pump, a pressure differential of approximately 3000 psi being required to break the plug; and the slurry was flushed from the condensate receiver.

Meanwhile, it was found that the slurry stored in the dump tank contained excessive chloride contamination as a result of a cooling-water leak into the low-pressure system through the packing gland of the slurry transfer pump. Five decantations removed most of the chloride, reducing the concentration in the supernate from 30 to 2 ppm.

Slurry charging to the high-pressure system was resumed on March 31, and the circulating concentration in the high-pressure system was brought to 950 g of Th per liter on April 1, approximately 10 hr of feeding being required to increase the concentration from 350 to 950 g/liter. Slurry was circulated at 950 g/liter until April 8, when the loop was shut down to provide cooling coils on the shell side of the high-pressure heat exchanger; these were needed to run heat transfer experiments. The slurry was left in the high-pressure system until the run was restarted on April 14. The slurry was resuspended in approximately 30 sec after the pump was energized, and the loop shows no indications of plugs in any location. The run is continuing quite satisfactorily, and measurements of heat exchanger performance are being made.

The most important factor in the success of the present run, as contrasted to difficulties experienced in preceding runs, is the use of aluminum-oxide-trimmed ball valves in the feed lines. While these valves have certain limitations (they usually leak slightly, they will only hold pressure in one direction, and they will not seat satisfactorily unless there is a substantial pressure differential), they are the first of the valves tried which seem capable of shutting-off flowing slurry repeatedly.

6.6 SLURRY LOOP EXPERIMENTS

6.6.1 200B Loop Operation, Run 4B

The 200B loop has been in continuous operation during the quarter, in run 4B, pumping a 1600°C-fired 1.8-μ-dia thoria slurry (DT-12 and -13) at

temperatures between 170 and 280°C. Total run time to date is 2500 hr, and the run is still in progress. Heat transfer coefficients measured with the copper-disc heat meter[5] have been obtained as a function of concentration, temperature, pipeline velocity, and time. During this operation a capillary viscometer was used to measure the rheological constants of the slurry. The concentration was gradually reduced in the loop from an initial 860 to a low of 290 g of ThO_2 per liter.

The slurry heat transfer coefficients appeared to be proportional to the 0.8 power of velocity at low concentrations. At the highest concentration the power dependence was over 1, suggesting that fully turbulent flow was not achieved until the velocity was close to 15 fps. There was a significant increase of heat transfer resistance with time, indicating that a thoria scale might be building up.

The capillary-tube viscometer sampler was used to obtain rheological constants for various concentrations of slurry. The values of yield stress are presented in Table 6.2 for the high concentration only, since at lower concentrations the viscometer sampler indicated negligible yield stress. The yield stress reported in Table 6.2 appears to decrease with time, and is considerably

Table 6.2. Yield Stress of 200B Run 4B Slurry*

Date	Temperature (°C)	Volume Fraction Solids, ϕ	Yield Stress, τ_y (lb/ft^2)	$K = \tau_y/\phi^3$
1-21	250	0.086	0.0286	45
1-21	255	0.0855	0.0351	56
1-22	230	0.0765	0.0229	51
1-22	225	0.0765	0.0166	37
1-22	225	0.0768	0.0229	49
2-1	220	0.0850	0.0294	48
2-1	220	0.0850	0.0234	38
2-1	225	0.0850	0.0208	34
2-2	180	0.0850	0.0260	42
2-2	180	0.0850	0.0078	13
2-2	180	0.085	0.0099	16
2-3	175	0.0820	0.0169	31
2-3	175	0.0818	0.0104	19

*Coefficient of rigidity, η = 0.015 lb/ft·sec.

below that reported previously for high-temperature circulation of pure thoria slurries.[6] The value of the coefficient of rigidity for 4B slurry at the high concentration was found to be constant at 0.015 lb/ft·sec over the temperature range 175° to 250°C.

The variation of coefficient of rigidity with concentration for this slurry was investigated at room temperature in a vertical-tube viscometer. The coefficient of rigidity, η, was equal to the viscosity of water, μ, multiplied by $(1 + 10\phi)$, where ϕ is volume fraction solids. The yield stress at 1000 g of ThO_2 per liter was 0.163 lb/ft^2.

6.6.2 200A Loop Operation, Run 21A

Run 21A, in the 200A loop, was completed in February. The primary purpose of the run was to investigate the dropout behavior of an aqueous thoria slurry in a 3-in. horizontal pipe at elevated temperatures and at various flow rates and concentrations. The relative attenuation of a collimated gamma-ray beam was used to indicate concentration variations.[7]

During the run, a total of 63 stepwise scans were made with different combinations of the following variables:

Temperature, °C - 240, 260, 280
Concentration, g of ThO_2 per liter of slurry - 0, 366, 663, 909, 1200
Linear velocity, fps - 3.2, 4.3, 5.3, 6.3, 7.5, 8.5, 9.6, 12.8

Count rates of the attenuated radiation were converted into concentration values following determination of the mass absorption coefficients for ThO_2 and water in calibration runs.

A typical set of observations is plotted in Fig. 6.6. A slurry containing 900 g of ThO_2 per liter at 280°C has virtually uniform concentration at 12.8 fps, a noticeable gradient at 7.5 fps, and a very strong gradient at 3.2 fps. The data were found to correlate with an empirical relationship of the type:

$$\frac{\sigma}{\bar{c}} = \left(\frac{a - b\phi}{v}\right)^n$$

where

σ = mean deviation from average concentration,

$\bar{c}$ = average concentration of slurry,

ϕ = volume fraction of solids,

v = velocity,

a, b, n = empirical constants dependent on the slurry properties and temperature.

The relationship predicts that the concentration deviations are more marked at low concentrations. The constants change with temperature and/or slurry settling rate in a manner such that concentration deviations are more marked at elevated temperatures.

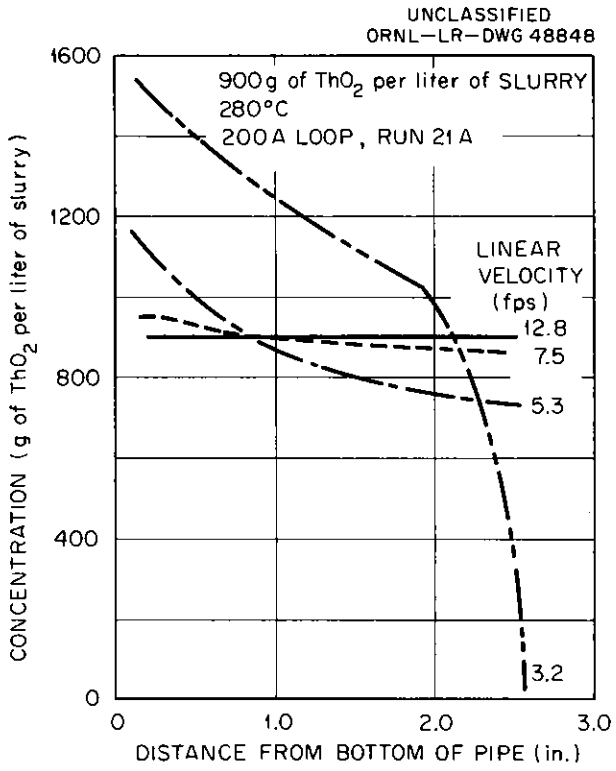

Fig. 6.6. Concentration Gradients in ThO_2 Slurry Flowing in a Horizontal 3 in. Pipe.

6.6.3 50A Loop Operation, Run 50A-1

Loop 50A operation was continued up to a total of 2300 hr, in run 50A-1, with the object of determining how various environments affect the dilatancy of a 1600°C-fired 3.65-μ ThO_2 slurry.[8] It was found by qualitative test that pumping under H_2 atmosphere for 270 hr had no effect on the moderately dilatant properties of the slurry. Since the observation had been made that complete nondilatancy had been observed only in 1600°C-fired long-pumped slurries, it was decided to add simulated corrosion-product $Fe(OH)_3$ to the circulating slurry to promote nondilatancy. Laboratory tests had indicated that $Fe(OH)_3$ alone was nondilatant. A quantity of this additive sufficient to bring the Fe-Th weight ratio up to 0.027 was added during high-temperature operation. This was a doubling of the existing ratio in the slurry. A temporary decrease in dilatant properties was observed, but the slurry returned to its former state with further pumping.

REFERENCES

1. I. Spiewak and F. N. Peebles, Tentative Evaluation of Thorium Breeder Reactors with Pebble Blankets, HRP-60-1 (Jan. 4, 1960).

2. I. Spiewak, HRP Quar. Prog. Rep. Jan. 31, 1960, ORNL-2920, p 24.

3. Ibid; p 24-25.

4. Ibid; p 43-44.

5. R. B. Korsmeyer and F. N. Peebles, HRP Quar. Prog. Rep. Jan. 31, 1959, ORNL-2696, p 61-62.

6. R. B. Korsmeyer and F. N. Peebles, HRP Prog. Rep. Oct. 31, 1959, ORNL-2879, p 67.

7. I. Spiewak, HRP Quar. Prog. Rep. Jan. 31, 1960, ORNL-2920, p 37-38.

8. Ibid; p 40-41.

7. INSTRUMENT AND VALVE DEVELOPMENT

A. M. Billings R. L. Moore

7.1 VALVE TRIM FOR THORIUM OXIDE SLURRY APPLICATIONS

Upon conversion of the 30-gpm loop to a solution system, the flushed-bellows Hammel-Dahl valve[1] was removed from service. Examination of the Zircaloy-2 plug and seat revealed no change in appearance from that reported earlier.[2] The plug and seat are shown in Fig. 7.1. Although damage to the seating region of both plug and seat is considerable, it is not catastrophic.

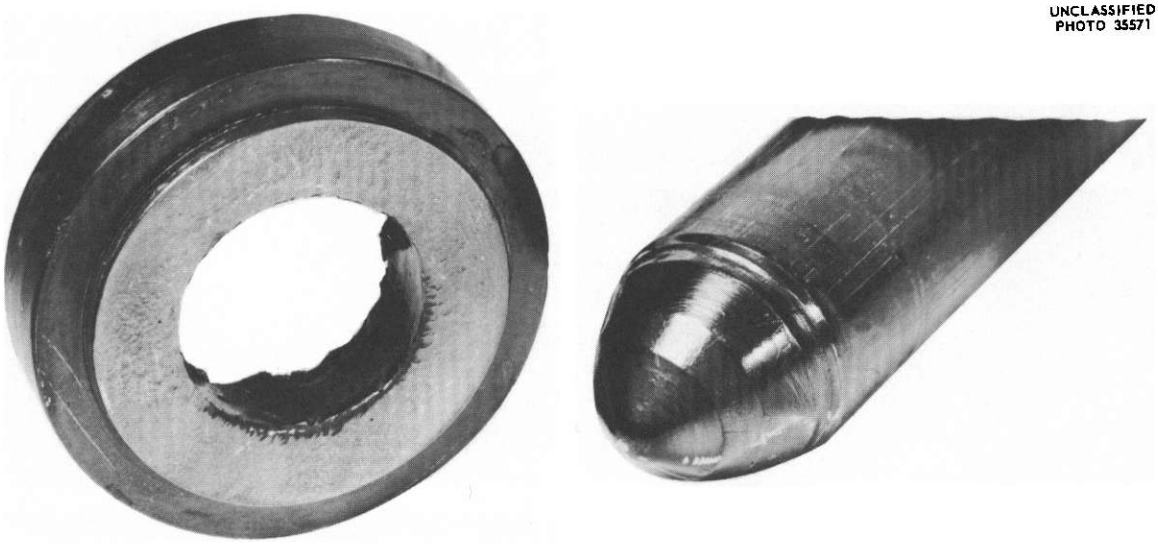

Fig. 7.1. Plug and Seat from Hammel-Dahl Valve No. 220 After Test (Feb. 17, 1960).

The set of trim was in slurry service for 5540 hr. The valve plug was in the fully opened position for approximately 4950 hr, and the remaining 590 hr was about evenly divided between plug positions of 30 to 40% closed and 65% closed. During the loop operation an additional 30 to 40 hr of water-service time was accumulated.

For high-temperature, low-differential-pressure slurry applications, Zircaloy-2 appears to be the most favorable valve-trim material tested to date.

7.2 LIFE-TESTING OF TITANIUM STEM-SEALING BELLOWS

Life-testing of titanium stem-sealing bellows[3] was completed. Twelve production-model assemblies were cycled to destruction in uranyl sulfate solution at 280°C. The stroke length was 1/8 in., and a pressure of 2300 psig

was applied externally to the assembly. Average life of the twelve units was 24,139 cycles. The Fulton Sylphon Division, Robertshaw-Fulton Controls Co., developed this bellows for a minimum life expectancy of 10,000 cycles under the conditions described above.

REFERENCES

1. D. S. Toomb et al., HRP Prog. Rep. July 31, 1958, ORNL-2561, p 143, Fig. 11.13.

2. R. L. Moore et al., HRP Quar. Prog. Rep. Jan. 31, 1960, ORNL-2920, p 48.

3. D. S. Toomb et al., HRP Quar. Prog. Rep. Apr. 30, 1959, ORNL-2743, p 100.

Part III

SOLUTION FUELS

8. REACTIONS IN AQUEOUS SOLUTIONS

M. J. Kelly M. D. Silverman
G. M. Watson

8.1 DECOMPOSITION OF PEROXIDE IN URANYL NITRATE SOLUTIONS

A study was undertaken to determine whether the decomposition of peroxide in uranyl nitrate solutions was sufficiently rapid to support consideration of uranyl nitrate solutions as potential aqueous homogeneous reactor fuels.[1] The experimental work was restricted to uranium concentrations of 0.034 M, but both H_2O and D_2O were tested as solvents, and several possible catalysts and promoters were studied within the temperature range of 40 to 100°C. Most studies were made in solutions containing 0.05 M excess HNO_3.

The problems caused by the radiolytic production of peroxide in reactor fuel solutions, the equilibrium between H_2O_2 and uranium peroxide, and the relatively low solubility of uranium peroxide have been discussed in connection with studies of the kinetics of the decomposition of peroxide in uranyl sulfate solutions.[2,3]

8.1.1 Experimental Procedure

The apparatus and experimental procedure used were those described previously,[2] but with only the chemical method of analysis employed to determine peroxide concentrations. The uranyl nitrate concentration of 0.034 M was chosen as being appropriate for reactor fuel; a concentration of 0.05 M excess nitric acid was present in all the catalytic decomposition studies for three reasons:

1. This acidity is appropriate for reactor use in the nitrate system.

2. All the catalytic species were solubilized.

3. Convenient rates were obtained.

Some experiments were performed at lower acidities in the absence of catalysts to test the effect of this variable.

8.1.2 Results and Discussion

In all previous work the decomposition of peroxide in uranyl solutions was found to be first-order with respect to peroxide; most of the results of this study followed the same pattern.

(a) Effect of Temperature.--Figure 8.1 shows the effect of temperature on the decomposition rate for various solutions. It should be noted that:

1. Energies of activation of 24 to 25 kcal/mole were calculated from the temperature dependence. These values are in agreement with those reported for the sulfate system.[2,3]

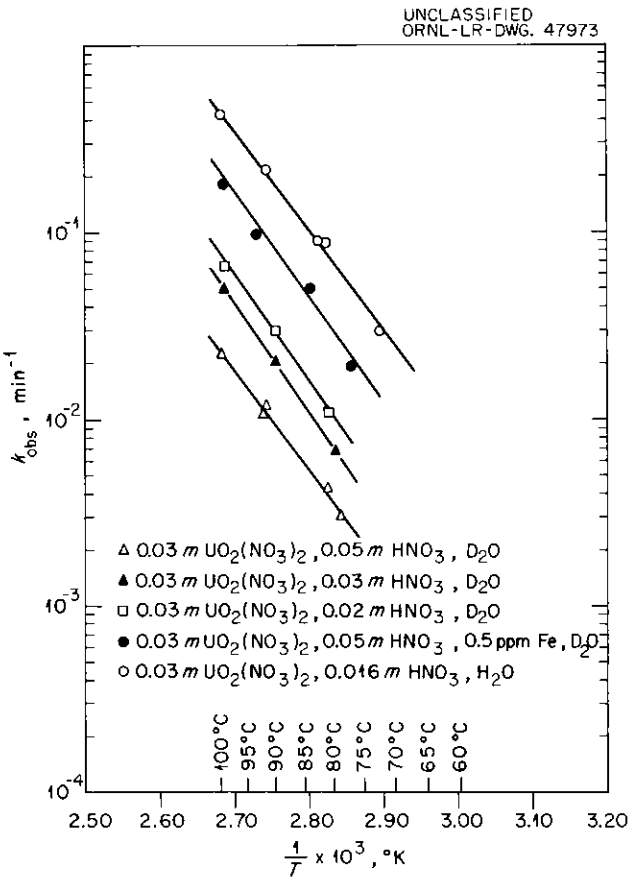

Fig. 8.1. Effect of Temperature on Decomposition Rate: Nitrate System.

2. The temperature dependence was essentially unaffected by changes in acidity or the isotopic composition of the solvent.

3. The temperature dependence was not substantially altered by the presence of small amounts of iron which were, nevertheless, sufficient to give considerable increases in the decomposition rate. This finding, analogous to results in the sulfate system, is inconsistent with the hypothesis which says that catalysts operate by providing reaction paths of lower activation energy than are available for the uncatalyzed reactions.

(b) Effect of Acidity.--The results presented in Table 8.1 show that the decomposition rate was inversely related to the acid concentration. Studies of the sulfate and perchlorate system[4] suggested that the decomposition, in solution without excess acid, proceeded largely through UO_4 as a consequence of the equilibrium

$$UO_2^{++} + H_2O_2 \rightleftharpoons UO_4 + 2H^+$$

which is displaced far to the right at low acidities. The addition of excess acid would obviously maintain the peroxide as H_2O_2 instead of UO_4, and the decomposition of H_2O_2 has been reported[5] to be much slower than that of UO_4. An analogous interpretation of these results in the nitrate system appears reasonable.

Table 8.1. Effect of Acid Concentration on the Rate of Peroxide Decomposition - Nitrate System

Solution	Solvent	Excess Acid (m)	k/k_o
I	D_2O	0.02	1
		0.03	0.62
		0.05	0.37
II	H_2O	0.016	1
		0.03	0.25
		0.16	0.114
		0.5	0.058
III	D_2O	0.02	1
		0.1	0.40
		0.34	0.23

(c) Effect of Catalysts.--Catalytic studies were undertaken, using copper, nickel, chromium, and iron as the active species. The effect of each of these species on the rate of decomposition of peroxide is shown in Fig. 8.2, where catalytic effects are represented by $\Delta k/k_o$ versus concentration. Here $\Delta k = k - k_o$, or the difference between rates in catalyzed and uncatalyzed solutions, and C is the concentration of catalyst in parts per million. It may be noted that, except for iron, only minor changes in rates were observed. In sharp contrast, iron, a very powerful catalyst for peroxide decomposition, was approximately a thousandfold more effective than the others.

The effect of ionic iron on the rate of decomposition of peroxide, as a function of temperature, is shown in Fig. 8.3. Values of $\Delta k/C$, obtained for three different solutions, are plotted versus 1/T. An activation energy of 25,000 cal/mole was calculated, in good agreement with values obtained from uncatalyzed "purified" uranyl nitrate solutions. The similar temperature dependence of the uncatalyzed and catalyzed solutions suggests that the mechanism involved in the decomposition of peroxide by added ionic iron is similar to that in the absence of a catalyst. Furthermore, it might be speculated that the decomposition of peroxide in uncatalyzed "purified" uranyl salt solutions is caused by small traces of iron, probably in concentrations $\leq$0.01 ppm.

(d) Effect of Promoters.--A reactor solution will contain, in addition to copper, measurable quantities of iron, nickel, and chromium from the corrosion of stainless steel. The effect of these mixed species on the decomposition of peroxide was therefore studied.

Nickel and chromium were added, during the course of a rate experiment, to a solution containing 0.26 ppm of iron. The results are shown in Fig. 8.4; it is evident that the addition of sizable amounts of nickel or chromium had little effect on the rate of decomposition of peroxide in the presence of ionic iron.

Previous work[2] showed that the addition of cupric ion to uranyl sulfate solutions containing iron led to much faster rates of decomposition of peroxide. Similar effects were also observed in uranyl nitrate solutions. The increased rates were much greater than could be accounted for by the product of the rate

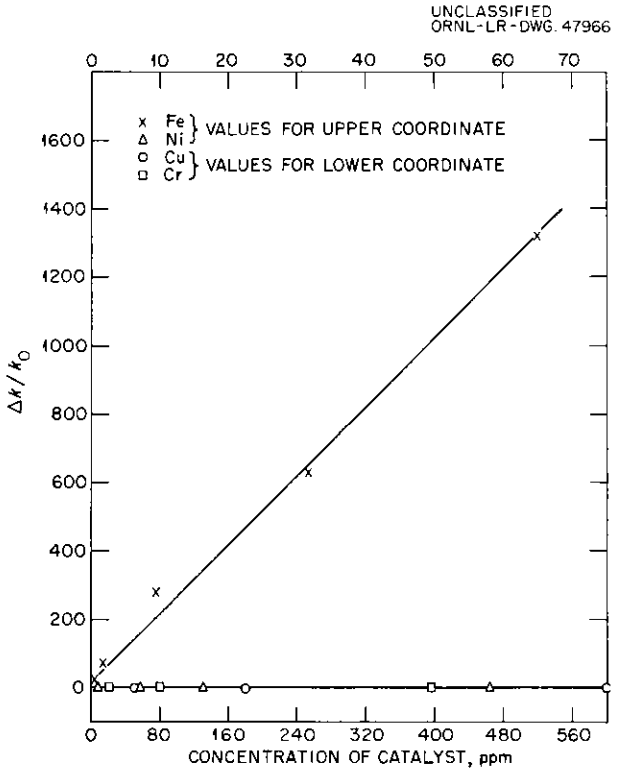

Fig. 8.2. Effect of Catalyst Concentration on Peroxide Decomposition Rate: Nitrate System.

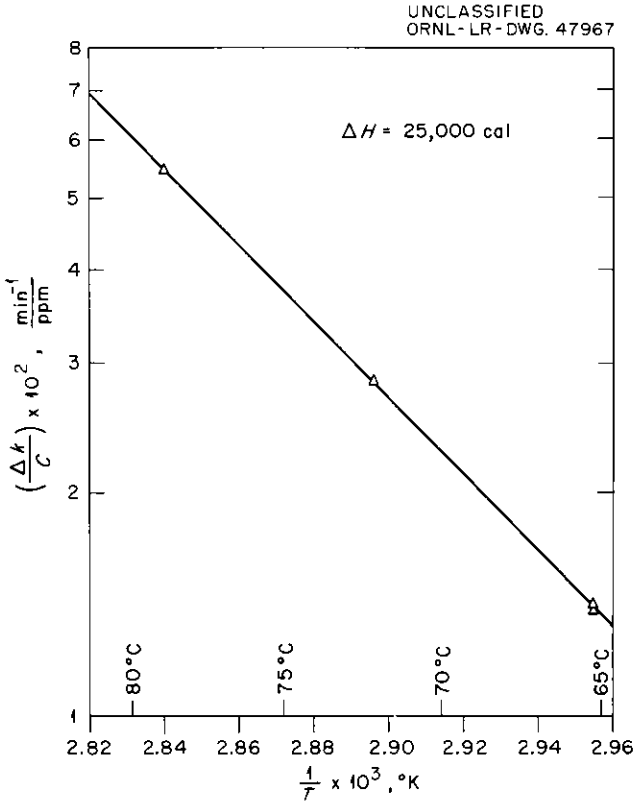

Fig. 8.3. Effect of Temperature on Iron-Catalyzed Peroxide Decomposition Rate: Nitrate System.

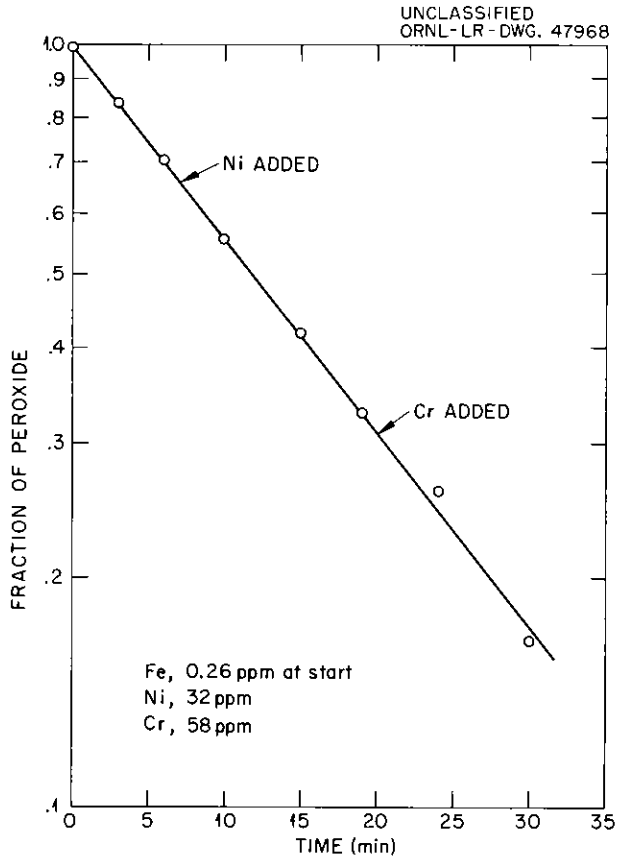

Fig. 8.4. Effect of Mixed Catalysts on Peroxide Decomposition Rate: Nitrate System.

constants obtained from Fig. 8.2. The following noteworthy results were obtained from this study:

1. Promotion increased with increasing copper concentration, reaching a plateau or saturation value at about 0.0005 M Cu^{++} (30 ppm). These results are shown graphically in Fig. 8.5, where, for fixed iron concentrations, values of k (the decomposition rate constant) are plotted against the copper concentration.

2. The rate of decomposition was first order (with respect to H_2O_2) only at low copper concentrations, but became more complex at high concentrations.

3. A square-root relationship is suggested (Fig. 8.6) when the values of k shown in Fig. 8.5 (at maximum promotion or plateau level) are plotted against the concentration of added iron. Similar results were obtained by Bohnson and Robertson[6] and interpreted by Baxendale.[7]

4. Promotion appeared to be independent of temperature, as shown in Fig. 8.7.

5. The promotion factor, $\Delta k/k_o$, decreased with increasing iron concentration (Fig. 8.8). Bohnson and Robertson,[6] whose studies were conducted in much more concentrated solutions than those used in the present work, believe that

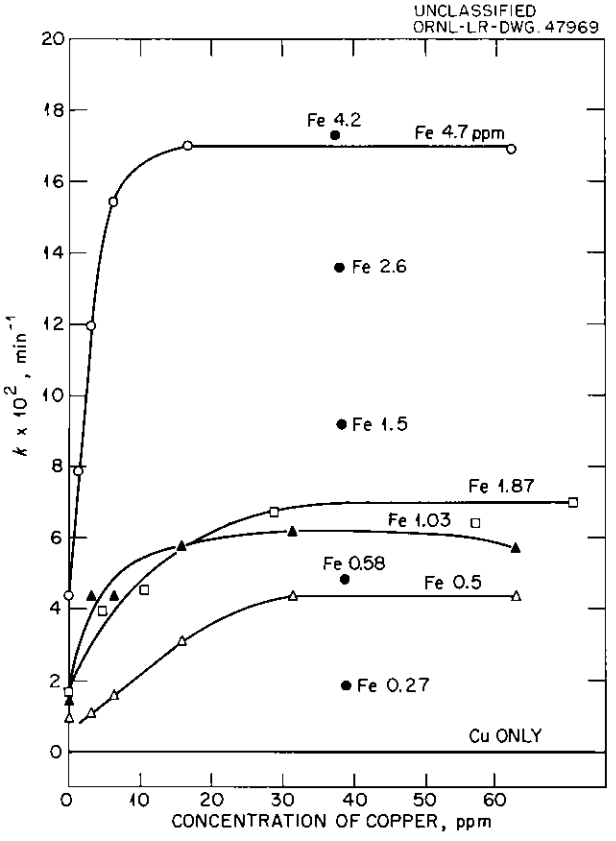

Fig. 8.5. Effect of Copper as a Promoter for Iron-Catalyzed Peroxide Decomposition: Nitrate System.

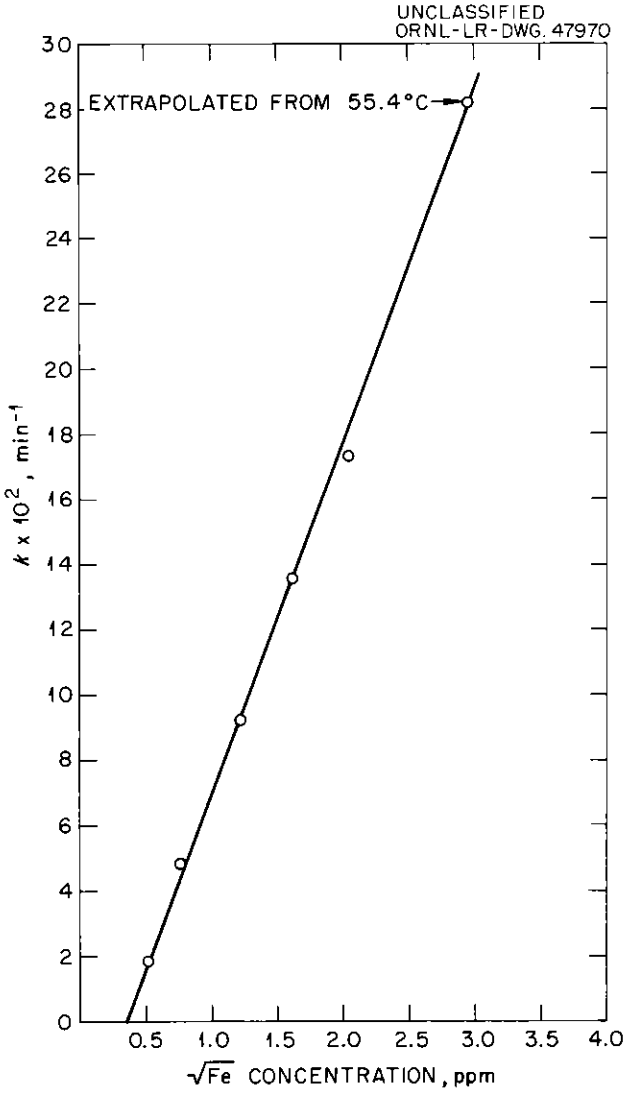

Fig. 8.6. Effect of Iron Concentration on Copper-Promoted Peroxide Decomposition: Nitrate System.

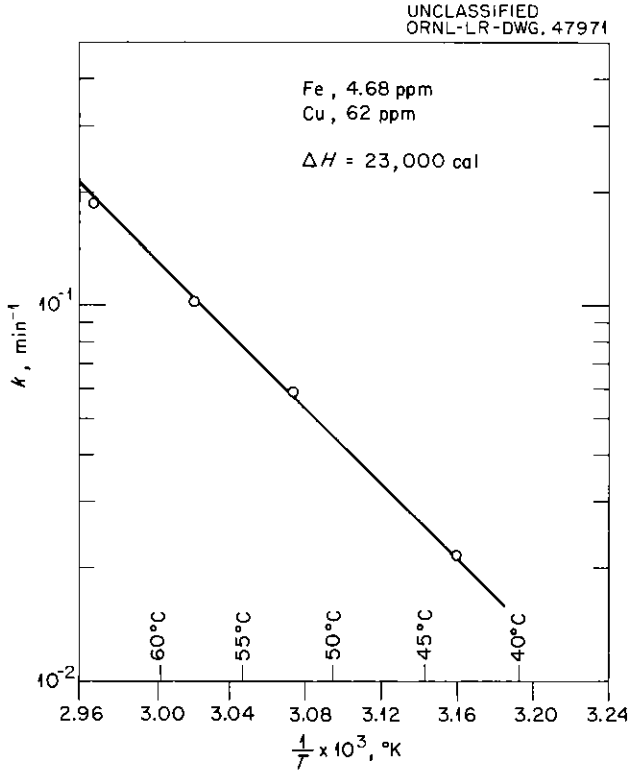

Fig. 8.7. Effect of Temperature on Peroxide Decomposition by Copper-Promoted Iron Catalyst: Nitrate System.

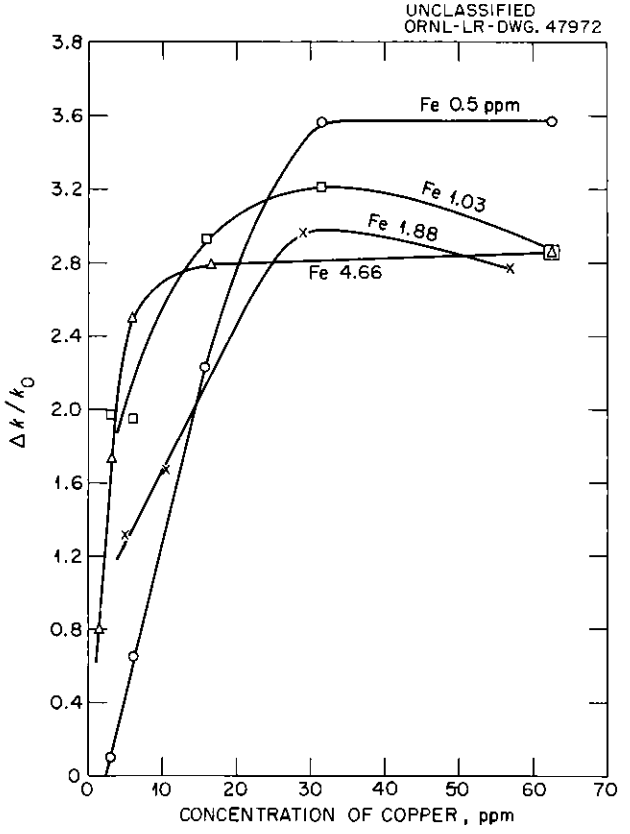

Fig. 8.8. Copper Promotion Factors in Iron-Catalyzed Peroxide Decomposition: Nitrate System.

the promotion factor probably decreases to a limiting value of 1 in concentrated solutions.

8.1.3 Conclusions

Kinetic studies conducted in uranyl nitrate solutions have given results similar to those previously reported for uranyl sulfate solutions. The rates were usually first order with respect to peroxide concentration. Of the common ions expected to be soluble in an aqueous homogeneous reactor system, only iron was an effective catalyst. The rates obtained with iron-catalyzed solutions gave an activation energy of approximately 25,000 cal/mole, practically the same as that for "purified" uncatalyzed uranyl nitrate solutions, indicating that the mechanism of decomposition is probably the same and lending strong argument to the belief that minute amounts of iron are responsible for the catalysis in "purified" solutions.

Promoter effects were observed when copper was added to iron-containing solutions. The promotion was independent of temperature and reached saturation at a copper concentration of 0.0005 M. The rates of decomposition became complex at higher copper concentration. The rate constants obtained from the promoter studies varied with the square root of the iron concentration (at constant copper concentration), in agreement with results obtained elsewhere.

Extrapolation of these results to higher temperatures suggests that peroxide decomposition rates should prove adequate under anticipated reactor conditions.

REFERENCES

1. W. L. Marshall to H. F. McDuffie, Consideration of $UO_2(NO_3)_2$-HNO_3-H_2O (D_2O) as a High-Temperature Homogeneous Reactor Fuel, ORNL CF-59-5-100 (May 26, 1959).

2. M. D. Silverman, G. M. Watson, and H. F. McDuffie, Ind. Eng. Chem. 48, 1238 (1956).

3. L. O. Gilpatrick and H. F. McDuffie, HRP Prog. Rep. July 31, 1958, ORNL-2561, p 313.

4. M. D. Silverman and C. H. Secoy, Chem. Div. Semiann. Rep. June 30, 1953, ORNL-1587, p 106.

5. M. D. Silverman, Chem. Div. Semiann. Rep. June 30, 1952, ORNL-1344, p 51.

6. V. L. Bohnson and A. C. Robertson, J. Am. Chem. Soc. 45, 2512 (1923).

7. J. H. Baxendale, "Decomposition of Hydrogen Peroxide by Catalysts in Homogeneous Aqueous Solution," p 31-86 in Advances in Catalysis, Academic Press, New York, 1952.

9. HETEROGENEOUS EQUILIBRIA IN AQUEOUS SYSTEMS

W. L. Marshall

J. S. Gill E. V. Jones R. Slusher

9.1 LIQUID-LIQUID EQUILIBRIA IN THE SYSTEM UO_3-SO_3-H_2O, ITS D_2O ANALOG, AND SIMILAR SYSTEMS CONTAINING CuO AND NiO COMPONENTS FROM 300 TO 350°C

Determinations of the equilibrium compositions of the heavy- and light-liquid phases in the system UO_3-SO_3-H_2O, its D_2O analog, and similar systems containing CuO and NiO components were continued. Detailed information on experimental techniques and earlier results were reported previously.[1]

The most recent data, together with previous results for the three-component system UO_3-SO_3-H_2O and its D_2O analog, are shown in Fig. 9.1. By plotting the saturation mole ratio, UO_3/SO_3, against the logarithm of the sulfate concentration, all data may be shown conveniently on the same figure. Since the data are not plotted on a conventional trilinear scale and are not expressed as mole or weight fractions, the lines connecting compositions of dilute liquid phases with concentrated phases are not "tie" lines in the usual sense of the word but are rather "connecting" lines. The new data extend the previously presented immiscibility curves to below 0.1 $\underline{m}$ SO_3 and, for the heavy-liquid phases, to concentrations containing an excess of UO_3 (i.e., $\underline{m}$ $UO_3/\underline{m}$ SO_3 >1). In order to anchor the ends of the liquid-liquid curves at 300, 325, and 350°C, the intersection points must be determined in which solid, presumably $UO_3 \cdot H_2O$, and two liquid phases coexist.

The extensions of the curves to higher and lower sulfate concentrations substantiate previous comments on comparative saturation mole ratios in H_2O and D_2O systems. In the light-liquid phases there is a considerable lowering of the saturation mole ratio in D_2O solutions, whereas in heavy-liquid phases there is comparatively little difference in saturation mole ratio between the two systems.

The distribution of CuO, as well as of NiO, in the heavy- and light-liquid phases of the system UO_3-SO_3-H_2O and its D_2O analog, are shown in Figs. 9.2 to 9.4. Figure 9.2 shows the distribution of CuO, NiO, and UO_3 components at 350°C for the multicomponent system UO_3-CuO-NiO-SO_3-H_2O. Due to the complexity of the system, several factors must be kept constant in order to represent the experimental data on smooth curves. In the five-component system the temperature was held constant at 300°C, the initial UO_2^{++} concentration was kept at 1.25 $\underline{M}$, and the initial concentrations of NiO and CuO were either 2.5 or 3.5 wt % each. Sets of correlating curves were drawn for solution compositions containing the 2.5 and 3.5 wt % initial concentrations of NiO and CuO. The sum of the saturation mole ratios at constant SO_3 concentration for either set was found to equal approximately the value for the saturation mole ratio, UO_3/SO_3, for the system UO_3-SO_3-H_2O not containing NiO and/or CuO components.

Figure 9.3 shows the distribution of UO_3 and CuO components at 350°C in the four-component system UO_3-CuO-SO_3-H_2O for solutions initially 1.25 $\underline{M}$ in UO_2SO_4

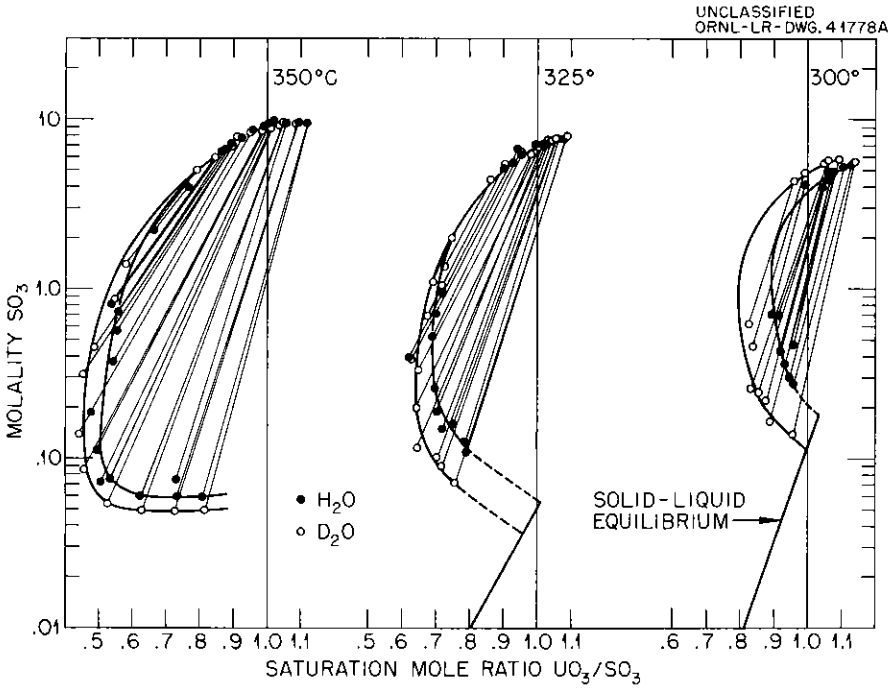

Fig. 9.1. Two-Liquid-Phase Regions in the System UO_3-SO_3-$H_2O(D_2O)$.

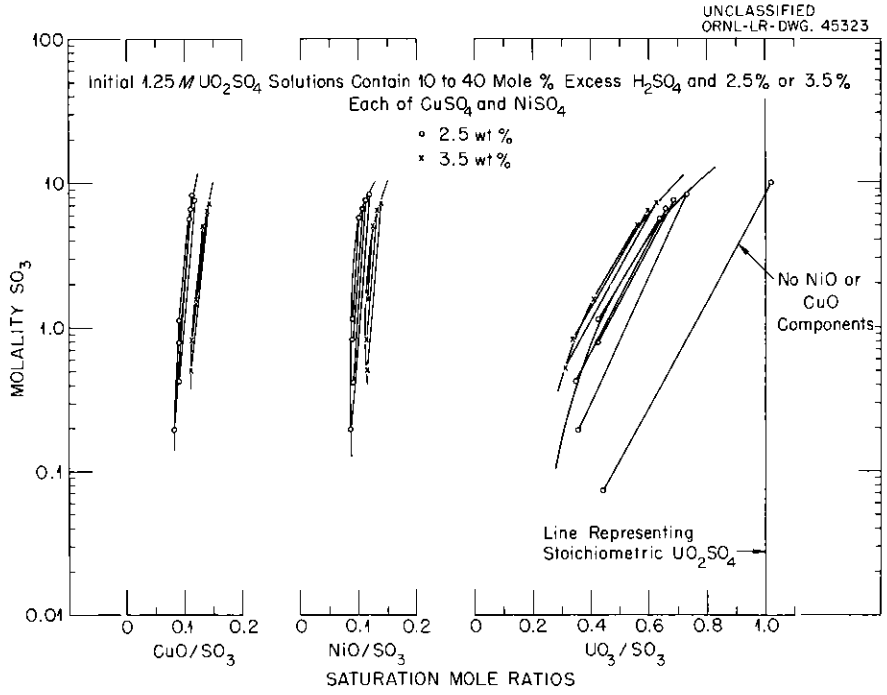

Fig. 9.2. Distribution of NiO, CuO, and UO_3 Components in Two-Liquid-Phase Region (System UO_3-CuO-NiO-SO_3-H_2O) at 350°C.

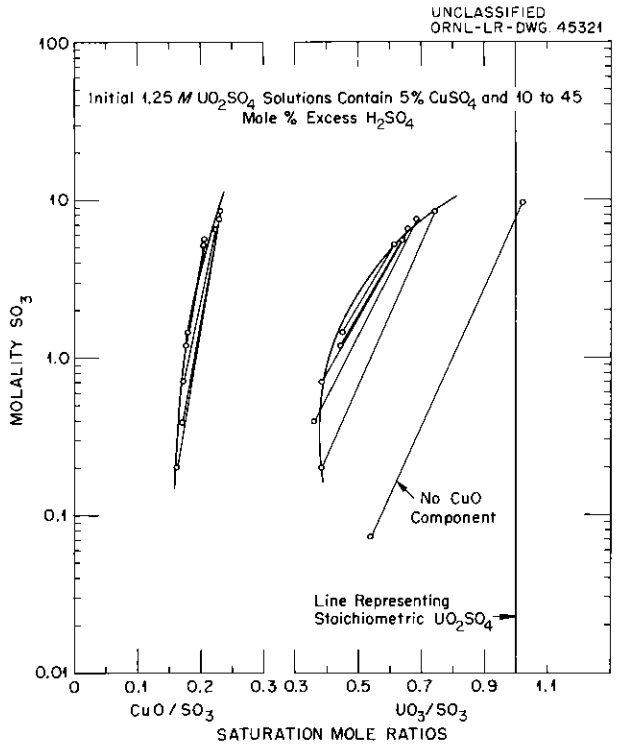

Fig. 9.3. Distribution of CuO and UO_3 Components in Two-Liquid-Phase Region (System UO_3-CuO-SO_3-H_2O) at 350°C.

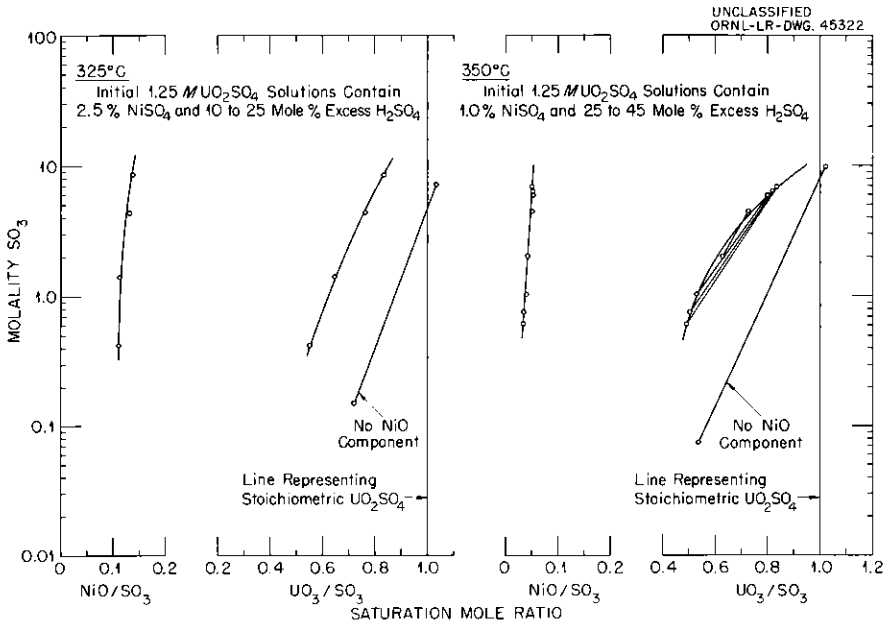

Fig. 9.4. Distribution of NiO and UO_3 Components in Two-Liquid-Phase Region (System UO_3-NiO-SO_3-H_2O) at 325 and 350°C.

containing 5 wt % $CuSO_4$ and 10 to 45 mole % excess H_2SO_4. Figure 9.4 shows a similar distribution of UO_3 and NiO components at 325 and 350°C in the system UO_3-NiO-SO_3-H_2O. The initial solutions are 1.25 M in UO_2SO_4 containing 2.5 wt % $NiSO_4$ for the 325°C data and 1.0 wt % $NiSO_4$ for the 350°C data. Excess H_2SO_4 varies from 10 to 45 mole %. In these included four-component systems, as in the five-component system, the summation mole ratios, (UO_3/SO_3 + CuO/SO_3) or (UO_3/SO_3 + NiO/SO_3), appear to fall on an immiscibility curve for the system UO_3-SO_3-H_2O (Fig. 9.1).

9.2 SOLID-LIQUID EQUILIBRIA IN THE SYSTEM UO_3-CuO-SO_3-H_2O, 300 TO 350°C

Considerable solubility information has been obtained at 300°C for solid-liquid equilibria in the five-component system UO_3-CuO-NiO-SO_3-H_2O and its included four- and three-component systems.[2] The experimental procedure consisted in the determination of saturation concentrations of solids in sulfuric acid solution in which the maximum number of solids allowable by the phase rule was always present. In this manner, monary, binary, and ternary solubility curves at 300°C were obtained as a function of sulfuric acid concentration. The experimental data, together with details of the experimental procedure and discussions, were presented previously.[2,3] Briefly, aqueous sulfate solutions in pressure vessels were saturated at 300°C with selected solids. Samples of the saturated solution were withdrawn for analysis, and the solid phases were identified by x-ray diffraction and chemical analyses after subsequent removal from the pressure vessels.

Similar investigations are being extended to 325 and 350°C. The first system under investigation is the four-component system UO_3-CuO-SO_3-H_2O in which the saturating solid phases are the new solid, $CuO \cdot 3UO_3$ (ref 4), and antlerite, $3CuO \cdot SO_3 \cdot 2H_2O$. The simultaneous solubilities of these solids in sulfuric acid solutions are being determined as a function of sulfate concentration. In this manner a binary curve can be obtained at 325 and 350°C and compared directly with the binary curve obtained at 300°C.

The preliminary solubilities at 325 and 350°C are plotted in Figs. 9.5 and 9.6, which also include the previous data at 300°C (ref 2). Figure 9.5 shows a linear plot of total sulfate in solution versus the saturation concentrations of the two components UO_3 and CuO. Figure 9.6 shows a different representation of the data in which the saturation mole ratios, UO_3/SO_3 and CuO/SO_3, are plotted against the logarithm of the sulfate concentration. It is apparent that very little change in the simultaneous solubilities of $CuO \cdot 3UO_3$ and $3CuO \cdot SO_3 \cdot 2H_2O$ occurs as the temperature is changed from 300 to 350°C at least from 0.02 to 0.1 m SO_3. The anticipated appearance of liquid-liquid immiscibility in this system at higher sulfate concentrations, however, is expected to produce a large, negative, temperature coefficient of solubility for the heavy-liquid phase.

REFERENCES

1. W. L. Marshall et al., HRP Prog. Rep. Oct. 31, 1959, ORNL-2879, p 104.
2. W. L. Marshall and J. S. Gill, Investigation of the System UO_3-CuO-NiO-SO_3-H_2O at 300°C, ORNL CF-59-12-60.
3. W. L. Marshall et al., HRP Quar. Prog. Rep. Jan. 31, 1960, ORNL-2920, p 64-68.
4. J. S. Gill and W. L. Marshall, The Compound $CuO \cdot 3UO_3$, ORNL CF-59-8-95 (1959).

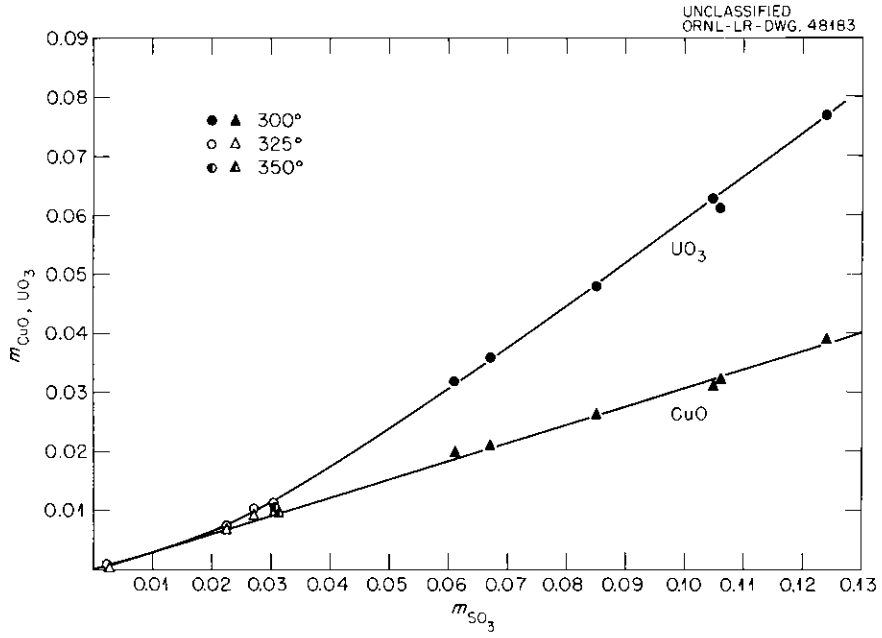

Fig. 9.5. Molal Concentrations of CuO, UO_3, and SO_3 in H_2SO_4-H_2O Solutions at 300, 325, and 350°C Saturated with $3CuO \cdot SO_3 \cdot 2H_2O$ and $CuO \cdot 3UO_3$.

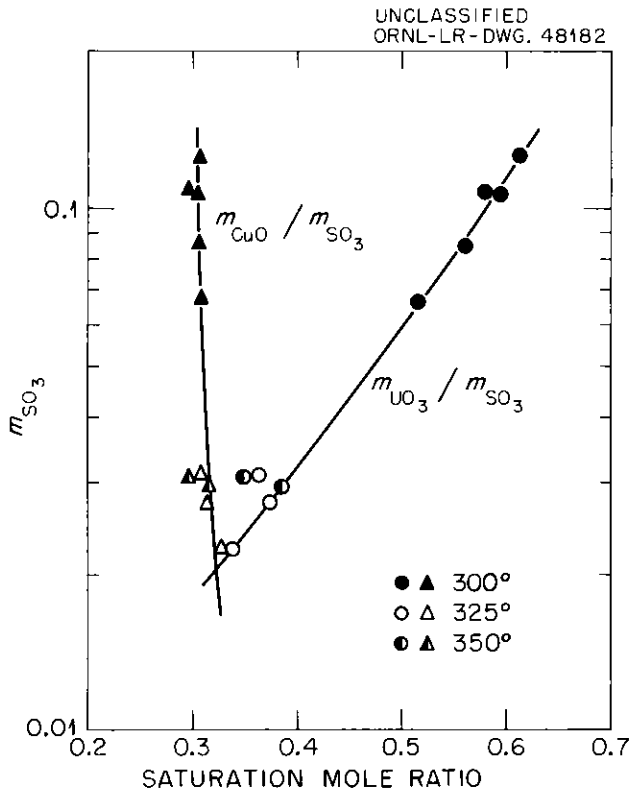

Fig. 9.6. Mole Ratios, CuO/SO_3 and UO_3/SO_3, in H_2SO_4-H_2O Solutions at 300, 325, and 350°C Saturated with $3CuO \cdot SO_3 \cdot 2H_2O$ and $CuO \cdot 3UO_3$.

10. RADIATION CORROSION

G. H. Jenks H. C. Savage

S. J. Ball R. J. Davis
S. E. Bolt V. A. DeCarlo

10.1 IN-PILE SOLUTION ROCKING-AUTOCLAVE TESTS, LITR

10.1.1 Introduction

The possibility of using $UO_2(NO_3)_2$ fuel solutions in aqueous homogeneous reactors has recently been reconsidered by Marshall.[1] He points out that the nitrate system shows some advantage over the sulfate with respect to high-temperature stability toward two-liquid-phase and solid-phase formation. Direct experimental information regarding the radiation decomposition of the nitrate ion in $UO_2(NO_3)_2$ fuel solutions was not available, but from considerations of the data of Boyle and Mahlman[2] for radiation decomposition of $Th(NO_3)_4$ solutions, Marshall suggests that the radiation decomposition of nitrate may be negligible in the dilute $UO_2(NO_3)_2$ solutions which would be employed in reactors.

In an effort to obtain experimental information of the nitrate stability and of other factors which are of importance in the evaluation of a fuel solution, an in-pile autoclave experiment with a $UO_2(NO_3)_2$ solution has been carried out. The other factors investigated were: radiolytic gas formation and copper-catalyzed recombination, and Zircaloy-2 radiation corrosion in the nitrate solution. No information has been reported previously on the radiation corrosion of Zircaloy-2 in $UO_2(NO_3)_2$ solutions. Recombination of H_2 and O_2 (ref 3) and D_2 and O_2 (ref 4) catalyzed by copper has been investigated out-of-pile by Kelley *et al*. The activation energy found was similar to that in sulfate systems. The K_{Cu} values for light-water nitrate solutions were about half those for similar sulfate solutions. D_2O as solvent reduced the K_{Cu} by approximately another factor of two. As mentioned, Boyle and Mahlman report values of G_{N_2} in rather concentrated $Th(NO_3)_4$ solutions (~0.3-3 *m* $Th(NO_3)_4$). For fission fragments, G_{N_2} was considerably higher than for fast neutrons or gamma rays, and it decreased rapidly with decreasing concentration of $Th(NO_3)_4$. Some N_2O was found; as much as about 10% of the amount of N_2. Sowden and Lynde[5] subjected $Ca(NO_3)_2$ solutions (0.21 to 4 *M* NO_3^-), to fission recoils and reported $G_{N_2} = 0.004\ (NO_3^-)^{1.5}$ for the entire concentration range. The G_{N_2} values of Boyle and Mahlman for nitrate concentration within the indicated limits are expressed fairly well by this equation as are, also, the G_{N_2} values reported[6] for $UO_2(NO_3)_2$ (~1 *M*) in Los Alamos water boilers. Gas-phase recombination of nitrogen with oxygen has been studied.[7,8] The G_{NO_2} values increase with the ratio of oxygen to nitrogen and with the addition of water vapor, and are considerably higher at elevated temperatures than at room temperature. G_{NO_2} values from 0.3 to 5 were reported. Varying amounts of N_2O were also formed, the average being about half the amount of NO_2. G_{H_2} values were also measured by Sowden and Lynde, and these results were expressed by $G_{H_2} = 2.0$ to $0.8\ (NO_3^-)^{1/3}$.

In the present work, the autoclave and the coupon specimens were made of Zircaloy-2. The initial composition of the solution, according to analyses (Table 10.2), was 0.032 *m* $UO_2(NO_3)_2$, 0.008 *m* $Cu(NO_3)_2$, 0.072 *m* excess DNO_3, and 0.17 *m* NO_3^- in D_2O, and the autoclave was about 85% full at the maximum exposure temperature of 280°C. Barton and Hebert[9] tested the stability of this solution in a quartz tube, and it appeared to be stable to 327°C. During exposure to full reactor power the solution temperature was 280°C.

Information concerning the decomposition of nitrate and the corrosion of Zircaloy-2 during irradiation was sought in the usual type of pressure measurements and in examinations and analyses of solution and samples following termination of the in-pile exposures. Radiolytic gas formation and recombination were also investigated through pressure measurements, but for these investigations the autoclave was operated at 225°C and the reactor at one-fifth of full power. Under these conditions, the rates of gas formation and recombination were slow, and the above factors could be estimated from the data for the rate of pressure change with time.

Pretreatment was done at 280°C for 185 hr. The exposure to full reactor power irradiation was performed in five successive periods. The first three and the last were of about 1 day each, and the fourth period was of about 2 days duration. The usual pressure-temperature data were obtained. Between the irradiation periods the experiment was retracted, in most cases with the reactor operating. Prior to the first and to the last irradiation periods, a series of radiolytic-gas buildup curves were obtained by short exposures at 225°C and with the reactor at 20% of full power. The initial exposure of this type was at 235°C.

After completion of the exposure, the autoclave was immediately cooled and vented, and about three weeks later was opened for examination. The solution, the autoclave rinse water, and the large amount of suspended solid material were chemically analyzed. The specimens were visually examined, then weighed. Some of them were defilmed, and others were pickled to remove a surface sample for analyses. After further pickling, two samples were used for Zr^{95} activity analysis and estimation of thermal neutron flux.

The experiment will be described in detail elsewhere.[10] A limited account is given here.

10.1.2 Results

(a) Description and General Interpretation of Pressure Results.--(1) Low-Power, Low-Temperature Measurements.--The series of short-time low-power, 225°C exposures provided smooth pressure buildup-curves from which K_{Cu} and G_{D_2} values could be estimated.

During the initial series of these exposures, small but significant increases in pressure persisted following retraction and after sufficient time had passed for the radiolytic gas to recombine. These increases amounted to 42 psi after the first exposure, which was at 235°C, and 5 and 7 psi in the two following exposures at 225°C. The exposure period for most of the measurements was less than 1 hr, and the pressure during exposure appeared to be levelling off. One exposure was continued for about 4 hr, and in this a continuing increase in pressure during exposure was apparent.

As judged from past experience with sulfate solutions, these pressure increases are not fully explained by fluctuations and/or uncertainties in pressure measurements, and thus at least part of the increases is ascribed to the formation of nitrate decomposition products during irradiation.

(2) High-Reactor-Power 280°C Measurements.--During each of the five full-power exposure periods, the pressure underwent changes qualitatively similar to those shown in the schematic diagram, Fig. 10.1, although differences in detail were observed. Also, during the hour after the start of the first of these exposures a rapid increase in pressure of about 160 psi occurred after an apparent steady-state pressure of radiolytic gas was achieved. The pressure increase was followed by a pressure decrease from the maximum of about 184 psi. Following this pressure excursion, the pressure rose as illustrated in Fig. 10.1. Pressures measured at the different points during each of the five exposures are listed in Table 10.1. Point B for exposure No. 1 was taken as the lowest pressure reached after the initial pressure excursion.

The values for the rapid changes in pressure following insertion (A-B) and retraction (D-E) increased gradually with increasing irradiation time. The pressure increase (B-C) during the first exposure was greater than that in subsequent exposures. Pressure decreases (C-D) were not observed during the

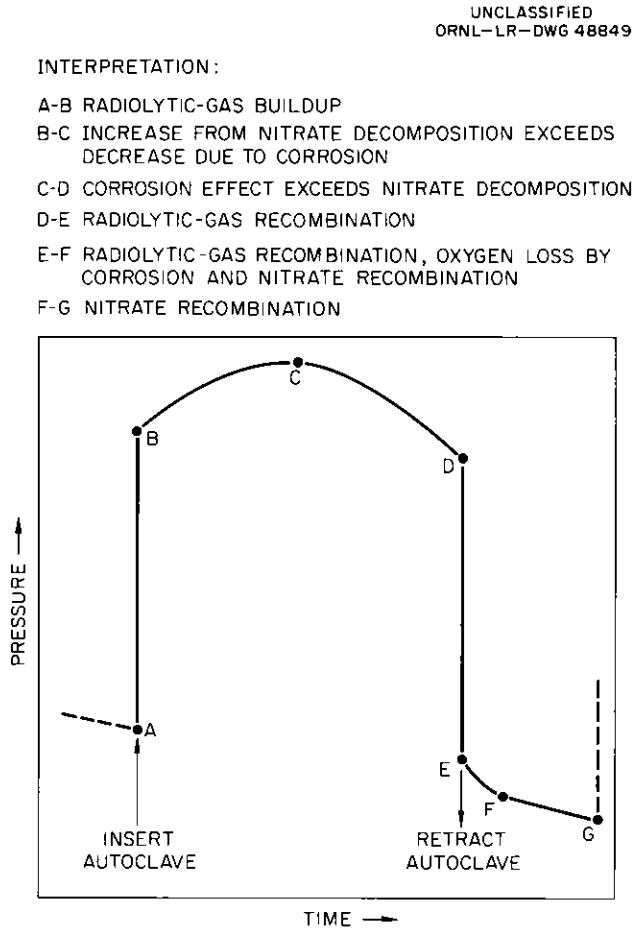

Fig. 10.1. Schematic Diagram of Progress of Pressure During Each Irradiation Period.

Table 10.1. Gas Pressures Observed at Various Times During High-Power Exposures

Exposure Time (3-Mwhr LITR Energy)	Pressure at Points Labeled on Fig. 10.1 (psi at 280°C)							Radiolytic-Gas Pressure	
	Before Insertion A	After Insertion B	Pressure Maximum C	Before Retraction D	After Retraction E	1-8 hr After Retraction F	15-20 hr After Retraction G	A to B	D to E
2-20	1048	1146[a]	1227[a]	1227[a]	1088[a]	1088[a]	1047[a]	e	139
20-45	1047[a]	1192[a]	1201[a]	1193[a]	1051[a]	1026[a]	993[a]	145	142
45-63	993[a]	1133[a]	1155[b]	1155[b]	(1010)[d]		938[c]	140	(145)[d]
63-109	938[c]	1111[c]	1133[c]	1018[c]	823[c]	800[c]	769[c]	173	195
109-134	769[c]	998[c]	1050[c]	995[c]	748[c]	718[c]	683[c]	229	247

Pressure before any irradiation (prior to the low-power, low-temperature irradiation): 975[f]

(a,b,c) Data corrected for effect of valve turns so that each value is on the same basis:

(a) correction, 24 psi;
(b) correction, 40 psi;
(c) correction, 72 psi.

(d) Estimated.

(e) Apparent value, 117 psi; but it may be confused with the initial pressure-peak phenomenon.

(f) This value calculated from a 25°C measurement.

first and third exposure, probably because of the short irradiation periods. Those observed in the other exposures increased in value with increasing time of irradiation. The pressure loss rate F-G starting a few hr after retraction was negligible for the first exposure, but was appreciable for the subsequent exposures. The total drop in pressure E-G during the 15- to 20-hr period of retraction was roughly the same in each exposure. The pressure shortly after retraction, E, for the first exposure was greater than the initial pressure, A. In each of the subsequent exposures, the pressure at E was less than that observed for the prior exposure.

The general interpretations of these pressure results based on prior experience with UO_2SO_4 solutions, G_{D_2} and K_{Cu} values determined from the low-power, low-temperature results, and the general consistency of the results are the following: The detailed explanation for the pressure excursions immediately following the first insertion is unknown. However, it appears likely that the effect is related to somewhat similar effects observed in autoclave experiments with UO_2SO_4 solutions. Some of these previous effects have been interpreted in terms of a loss of copper from solution during the initial exposure, followed by a re-solution of the copper.[11] The pressure changes A to B and D to E represent the formation and recombination of radiolytic gas upon insertion and retraction, respectively. The pressure buildup following point B was due to the formation of gaseous nitrate decomposition products. The occurrence of a maximum in the pressure was a result of a back reaction of the decomposition products, a loss of oxygen pressure due to corrosion and, probably, a decrease in the rate of nitrate decomposition as the solution became more dilute in nitrate upon decomposition. The decrease in pressure after the maximum was due primarily to oxygen loss as a result of corrosion. The pressure at point E includes the pressures of excess oxygen and that of the nitrate decomposition products. The latter pressures were probably near those which prevailed at the termination of exposure, although a small amount of recombination may have occurred. The nearly constant rate of pressure loss from F to G may have been due either to corrosion which continued after retraction or to a recombination of nitrate decomposition products under the influence of the gamma-ray field in the retracted position, or, alternatively, to both factors. The rapid pressure changes E-F after retraction and the recombination of radiolytic gas were probably also a result of oxygen loss due to corrosion which continued after retraction and recombination of nitrate decomposition products. No evaluation can be made of the relative contribution of the two possible processes.

10.1.3 Results of Examination and Analyses of Autoclave Contents

The postirradiation analyses of the solution, rinse, the part of the suspended material soluble in dilute H_2SO_4, the part insoluble or difficultly soluble in dilute H_2SO_4, and the specimen surface analyses are listed in Table 10.2.

The pH and other analytical results for the solution are consistent when it is assumed that the nitrogen was present as nitrate ion, and they show that the recovered solution contained about 39% of the original uranium and about 27% of the original nitrogen. It is assumed that the solution was not diluted or concentrated and that the unrecovered volume of solution was lost in venting or handling.

Table 10.2. Summary of Postirradiation Analyses

	Original Solution	Irradiated Solution	Autoclave Rinse	Suspended Material: Part Soluble in 25 ml of 0.1 *M* H_2SO_4	Suspended Material: Difficultly Soluble Part	Material on Surface of Dried Specimens (average of 2 values)
Sample size	5.9 ml[a]	3.9 ml[c]	4.0 ml[c]			
pH	0.95[b]	2.35[b]				
Uranium	8.3 g/liter	3.2 g/liter	0.7 g/liter	6.8 mg	9.4 mg	0.16 mg/cm^2
Peroxide				5.8 mg U[d]		
NO_3^-						
Total N	2.6 g N/liter	0.7 g N/liter	1.1 g N/liter	0.03 mg		
NH_3		0.01 g N/liter	0	0.03 mg		
Free acid	0.08 N					
Copper	0.6 g/liter	0.2 g/liter	0.02 g/liter	0.18 mg	0.44 mg	0.04 mg/cm^2
Chromium		0.002 g/liter	0.004 g/liter	0.01 mg	0.34 mg	0
Nickel		0.13 g/liter	0.07 g/liter	0.25 mg	0.20 mg	0.07 mg/cm^2
Iron		0	0.01 g/liter	0.06 mg	0.73 mg	0.64 mg/cm^2

(a) Volume of solution originally loaded into autoclave.

(b) pH values reported are glass electrode values, using buffers of H_2O solutions plus a correction of 0.25 pH units for D_2O solutions.

(c) These values are the volumes of samples collected.

(d) Expressed as milligrams of uranium, assuming that the peroxide titrated was UO_4.

The amount of nitrogen found in the rinse was greater than that found in the recovered solution, but no pH or free-acid data which are required for validating this result were obtained.

Appreciable amounts of uranium were found in the suspended material. The 6.8 mg found in the soluble part was probably mostly peroxide, which may have formed after the irradiation and prior to separation of solution from the suspended material. The 9.4 mg in the insoluble part, however, amounts to about 20% of the total uranium in the autoclave.

The analyses of specimen surfaces showed appreciable amounts of Fe, Ni, and U, and consideration of these data and of those for weight losses upon defilming show that these oxides remained on the defilmed surfaces to the extent of 1.3 mg/cm^2.

Weight losses of two defilmed Zircaloy-2 specimens average 2.4 mg/cm^2, corresponding to 0.14 mils penetration and an average corrosion rate of 9.1 mpy during exposure. However, estimations based on possible amounts of oxides remaining on the specimens after defilming indicate that the average penetration and the corrosion rate may have been 0.21 mils and 13.5 mpy, respectively.

The neutron flux during full reactor power and during insertion corresponded to a calculated solution power density of 2.6 w/ml, based on the composition of the original solution.

10.1.4 Derived Values for G_{N_2}, $G_{NO_3^-}$, K_{Cu}, and G_{D_2}; Zircaloy-2 Corrosion Rates; Nitrate Decomposition During Radiation Exposure

In using the pressure data to calculate the various factors of interest, it is assumed that the nitrate decomposition products were comprised entirely of N_2 and O_2 in a molar ratio of 2:5. As mentioned previously, the work of other investigators shows that N_2 is the major product of the decomposition, although small amounts of nitrogen oxides also have been found. It is also assumed that the solubility of nitrogen and oxygen in the $UO_2(NO_3)_2$ solution are the same as that for oxygen in UO_2SO_4 solutions of similar concentrations. Comparisons of pressure data obtained at 25°C and at the elevated temperatures in this experiment indicate that this is a reasonable assumption. It is also assumed that deuterium solubilities are the same as those employed in UO_2SO_4 solutions. No estimate of the validity of this assumption for D_2 is available.

(a) K_{Cu} and G_{D_2}.--Values for these factors calculated from the results of 225°C measurements are shown in Table 10.3. The results of the measurements made during insertion are considered more nearly valid than those obtained during retraction because of the possibility that the rates of recombination during retraction are partly controlled by diffusion processes. The results of the high-temperature exposures are not suitable for accurate evaluation of G_{D_2} and K_{Cu}, but the pressures observed during the initial exposures are in rough agreement with those predicted from the results obtained at low temperature.

(b) G_{N_2}.--Values for G_{N_2} estimated from various pressure data are listed in Table 10.4. It should be noted that the value calculated from the rate of pressure rise during the initial high-temperature exposure should be regarded as a minimum value. Some loss of pressure due to corrosion and to recombination of nitrate decomposition products may have been taking place during the rise

Table 10.3. Values for G_{D_2} and K_{Cu} Based on Low-Power Exposures at 225°C

Basis	K_{Cu} [liters (STP)·mole^{-1}·hr^{-1}]	G_{D_2} (molecules/100 ev)
Values from Data Obtained at Beginning of Irradiation		
Pressure buildup data	1600	1.3
	1600	1.3
	1700	1.4
	1700	1.4
Recombination data	1200	0.9
	1100	0.9
Values from Data Obtained After 109 hr of Irradiation		
Pressure buildup data	800	0.9
	800	0.9
Recombination data	500	0.6

Table 10.4. Estimates of G_{N_2}

G_{N_2} (molecules/100 ev)	Exposure Time (3-Mwhr LITR Energy)
Low Power, 225°C, 235°C Data	
Incremental increases in apparent equilibrium retracted pressures	
2.5×10^{-2}	0-0.3
2×10^{-3}	0.3-0.7
3×10^{-3}	0.7-1
Low Power, 225°C Data	
Approximate linear pressure increase after apparent radiolytic H_2-O_2 equilibrium	
1×10^{-2}	2
High Power, Inserted Data	
Rate of pressure buildup after apparent radiolytic H_2-O_2 equilibrium	
3×10^{-3}	5

in pressure. Also, during the low-temperature exposure, some recombination may have occurred. No corrections for these possible pressure losses were attempted. Rates of pressure increase following insertions during the exposures subsequent to the first at high temperature were less than that for the first. No attempt was made to evaluate G_{N_2} values from these subsequent exposure data.

(c) $G_{NO_3^-}$.--Rough values for the rate of recombination of N_2 can be estimated if it is assumed that the formation of a steady-state pressure during the first high-temperature exposure resulted primarily from the recombination of nitrate decomposition products. For this exposure in which the G_{N_2} was 3×10^{-3}, estimated from the initial pressure rise, the gas-phase recombination required to form a steady state at the estimated gamma ray and fast neutron fluxes prevailing in the insertion position can be estimated to be that which corresponds to a $G_{NO_3^-}$ of 1 to 3. The true $G_{NO_3^-}$ values are probably somewhat lower than the value thus obtained, since some decrease in nitrate decomposition rate would be expected as the nitrate concentration in solution decreased due to decomposition. Also, the rate of loss of oxygen as a result of corrosion may have increased as the time of irradiation exposure increased.

(d) Zircaloy-2 Corrosion Rates and Nitrate Decomposition as a Function of Time During Radiation Exposures.--Limits for the rates of Zircaloy-2 corrosion at different times during the radiation exposure can be roughly estimated from the rates of pressure decreases observed during different exposures, the total Zircaloy-2 corrosion indicated by the weight losses of defilmed specimens, the possible presence of Fe_2O_3 and other oxides on the defilmed specimens and other surfaces, and the total amount of nitrate decomposition as shown by the analyses of the final solution.

The probable minimum rates of oxygen consumption as a function of time during radiation exposure are those represented by line A of Fig. 10.2. The data points upon which the line is based are those calculated from the rates of pressure-loss measurements during the final portions of the high-temperature exposures.

The estimated maximum oxygen consumption rates illustrated by line B of Fig. 10.2 were selected such that the area under the curve corresponds to the total Zircaloy-2 corrosion which occurred if the analytical results for the

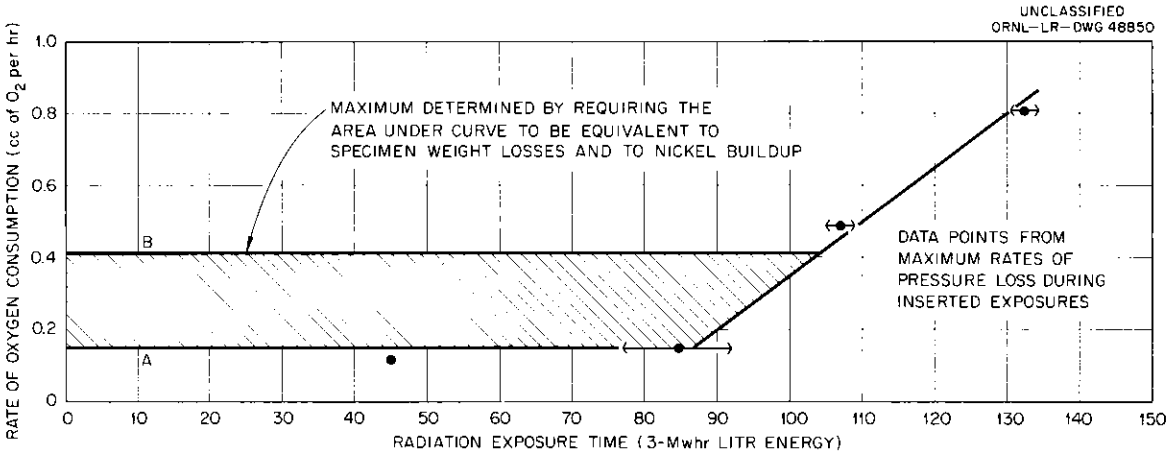

Fig. 10.2. Estimated Rates of Oxygen Consumption as a Function of Exposure Time.

amounts of Fe_2O_3 and other oxides on the coupon surfaces are considered correct and that those specimen surfaces were representative of other surfaces in the autoclave. The area under this curve also includes the amount of oxygen consumed in corroding the stainless steel capillary in the amount indicated by the nickel found in solution and on the Zircaloy-2 surfaces. The points representing the high rates of pressure loss during the two final exposures were considered as probably more nearly representative of the actual oxygen-loss rates than the other, lower-rate, points. Therefore, all the rate adjustments were applied to the first 100 hr of irradiation.

By graphical integration of the curves in Fig. 10.2, maximum and minimum values for the volumes of excess oxygen in the autoclave can be estimated to give those illustrated by curves A and B in Fig. 10.3. The difference between the values illustrated by a given one of these curves and those for the total volumes of excess oxygen plus nitrate decomposition products in the system (line C) yields the maximum and minimum values for the volumes of the gaseous decomposition products, which are illustrated by curves B' and A', respectively.

If it is assumed that the minimum rate line A in Fig. 10.2 represents rates of oxygen consumption in Zircaloy-2 corrosion, the rate for this material during the first 90 hr of radiation was about 6 mpy. The rate at the end of the final exposure was about 30 mpy. The average corrosion rate was about 10 mpy, a value in near agreement with that estimated from the weight loss of defilmed specimens.

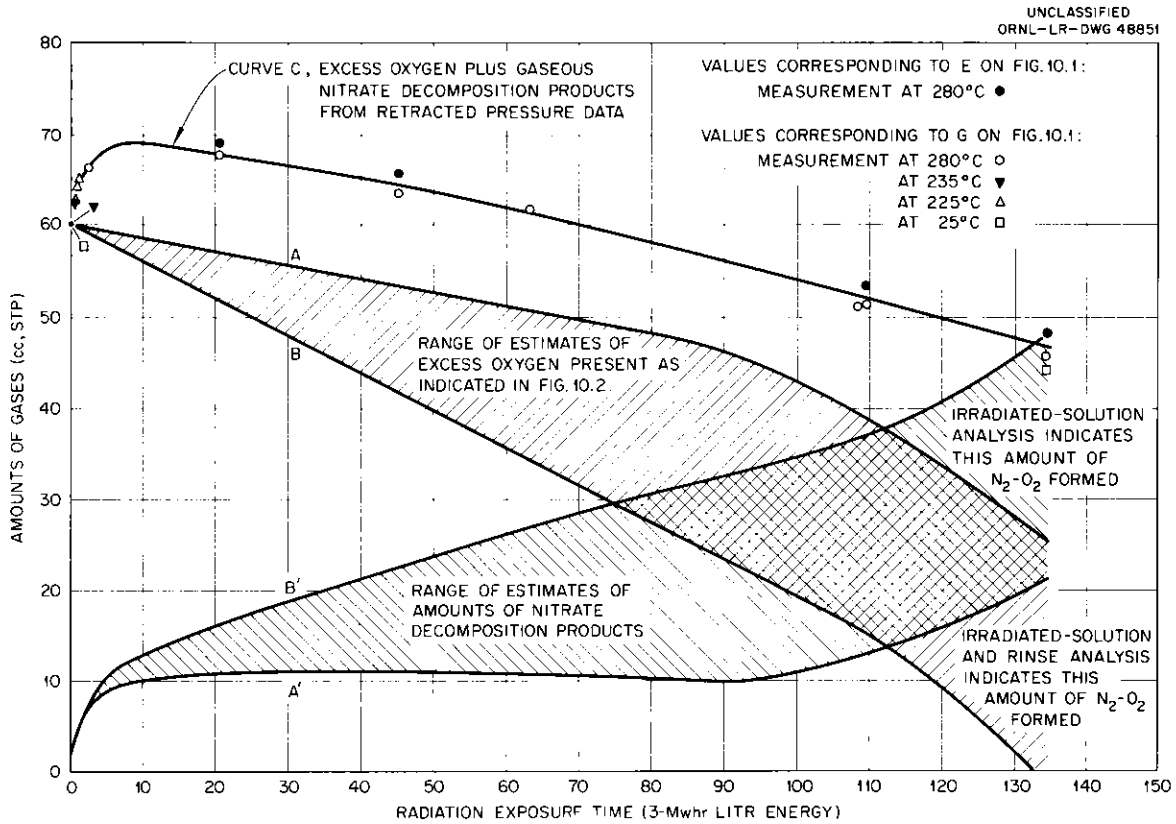

Fig. 10.3. Estimated Amounts of Excess Oxygen and Gaseous Nitrate Decomposition Products vs Exposure Time.

The corresponding curve A' in Fig. 10.3 for the minimum volumes of gaseous nitrate decomposition products shows that the volumes increased rapidly to about 10 to 12 cc (23 to 25% decomposition) during the initial exposures and then remained nearly constant until the final exposure, during which the volume of decomposition products increased to about 20 cc (47% decomposition). It may be noted that the indicated amount of gaseous decomposition products at the end of the experiment is in fair agreement with that indicated by the analytical results for the total amount of nitrogen in the solution and rinse. These results showed about 27% of the original nitrogen to be in the solution and 28% in the rinse. A discrepancy in the interpretation of the final two rate values in Fig. 10.2 is apparent in this treatment of the data. The treatment indicates that the pressure of nitrate decomposition products was increasing at the time the total pressure in the system during exposure was increasing; therefore, the rates of oxygen consumption may have been greater than those calculated from the rate of pressure decrease.

The proper correlation of these facts is not apparent. It is possible that the oxygen-consumption rates were greater than those employed. It is also possible that the rates did not increase regularly with exposure time in this region and that the high rates occurred only during the time that the observed pressures were decreasing rapidly. Other treatments of the data to include these possibilities do not appear worthwhile in view of other appreciable uncertainties in the results.

The estimated maximum rates of oxygen consumption due to corrosion, illustrated in line B, Fig. 10.2, corresponds to a Zircaloy-2 corrosion rate of about 12 mpy during the 100 hr of radiation when it is assumed that the steel corrosion rate remained constant throughout the 134 hr of exposure. Curve B' in Fig. 10.3, illustrating the estimated maximum amounts of gaseous nitrate decomposition products, shows a rapid rise to about 12 cc during the initial exposures and then a slower but steady increase during subsequent exposures to a value of about 48 cc. This volume is slightly more than that which would be produced by 100% decomposition of the nitrate in solution. Again the interpretation of the final two rate points in Fig. 10.2 is in question because the indicated pressures of nitrate decomposition products were increasing at the times the pressures were decreasing and, again, attempts to resolve these discrepancies by other treatments do not appear worthwhile because of over-all uncertainties in the results.

The true amounts of corrosion and of gaseous decomposition products probably fall between the limits indicated in Figs. 10.2 and 10.3, with the exception that during the final 30 hr of exposure, oxygen consumption rates greater than those indicated in Fig. 10.2 may have occurred.

10.1.5 Summary and Discussion

Although appreciable uncertainty exists in the interpretation of some of the results obtained in this experiment, the factors comprising the objectives of the experiment were evaluated, but with limited accuracy.

All the results are consistent with the occurrence of nitrate decomposition during radiation exposure. The results of pressure measurements during the initial 225 to 235°C exposures and during the initial 280°C exposure provide evidence that the initial nitrate decomposition rate was greater than that predicted by the reported results of Sowden and Lynde, mentioned in the introduction, by factors of from about 7 to 70. A back reaction of the nitrate decomposition products is indicated by the results of the first 280°C radiation exposure.

The $G_{NO_3^-}$ value of about 1 to 3 for gas-phase recombination, estimated from these results by assuming that NO_3^- is the sole product of recombination, is within the range of values which have been reported by others. It should be noted, however, that the conditions of pressure, temperature, and gas phase composition in this experiment differ from those employed in the other reported studies, and the $G_{NO_3^-}$ for this present experiment cannot be accurately predicted from the other studies.

The initial K_{Cu} values (225°C) are about three times as large as those found out-of-pile by Kelly et al.[4] The initial G_{D_2} value of 1.3 is near agreement with the value of about 1.5 found for nitrate solutions by other workers. The apparent decreases in K_{Cu} and G_{D_2} throughout the exposure can be ascribed to a loss of uranium and copper from solution.

The Zircaloy-2 corrosion rates during the initial 100 hr of radiation at 280°C were probably in the range 6 to 12 mpy. A corrosion rate in the same range would be expected for uranyl sulfate solutions of similar concentrations. During the final 34 hr, the rate was greater than 12 mpy and was probably as high as 30 or more. The large amount of sorbed uranium (0.16 mg/cm^2) indicates that a high effective power density prevailed in the system and probably accounts for the high rate near the end of exposure.

REFERENCES

1. W. L. Marshall, Consideration of $UO_2(NO_3)_2$-HNO_3-$H_2O(D_2O)$ as a High Temperature Reactor Fuel, ORNL CF-59-5-100 (May 26, 1959).

2. J. W. Boyle and H. A. Mahlman, Radiation Induced Decomposition of Thorium Nitrate Solutions, Nucl. Sci. and Eng. 2, 492-500 (1957).

3. M. J. Kelly et al., The Effectiveness of Cupric Ion as a Homogeneous Catalyst in the UO_3-HNO_3-H_2O System for the Recombination of Hydrogen and Oxygen Produced by Radiolytic Decomposition, ORNL CF-59-9-15 (Sept. 3, 1959).

4. M. J. Kelly, Reactor Chem. Div., ORNL, private communication.

5. R. G. Sowden and Elizabeth M. Lynde, The Effect of Fission Recoil Energy on Calcium Nitrate Solutions, A.E.R.E. C/R 2480 (Feb. 1958).

6. R. M. Bidwell, L. D. P. King, and W. R. Wykoff, Nucl. Sci. Eng. 1, 452 (1956).

7. C. G. Edwards and F. Moseley, The Production of Chemicals from Reactors, Part 1. The Fixation of Atmospheric Nitrogen by Fission Fragments, A.E.R.E., C/R 2710 (Oct. 1958).

8. P. Harteck and S. Dondes, Producing Chemicals with Reactor Radiations, Nucleonics 14(7), 22-25 (1956).

9. C. J. Barton, Sr., and G. M. Hebert, ORNL, private communication.

10. R. J. Davis et al., report in preparation.

11. G. H. Jenks et al., HRP Quar. Prog. Rep. July 31, 1958, ORNL-2561, p 234-236.

Part IV

SLURRY FUELS

11. ENGINEERING AND PHYSICAL PROPERTIES

H. W. Hoffman

C. S. Morgan D. G. Thomas

11.1 SUSPENSION TRANSPORT STUDIES

Previous studies[1,2] of the minimum velocity required to transport a flocculated suspension in horizontal pipes have shown two regions of flow, depending on the concentration. In the first region, the suspension is sufficiently concentrated to be in the compaction zone and hence has an extremely slow settling rate. The second region is observed with more dilute suspensions which are in the hindered-settling region and settle 10 to 100 times faster than slurries which are in compaction. An unresolved problem was the definition of the critical concentration separating the two flow regions, although it was clear from the data presented that the critical concentration increased with tube diameter.

In order to obtain additional evidence on the effect of tube diameter and concentration on the onset of compaction, a series of hindered-settling studies were made (Fig. 11.1). For sufficiently dilute concentrations, the hindered-settling rate is independent of tube diameter, decreasing regularly as the concentration is increased. However, for any given tube diameter, there is a certain critical concentration beyond which the settling rate decreases sharply to a value 1/10 to 1/50 of that expected if there were no wall effect. The decrease in settling rate is due to the suspension being in compaction and, as shown by the family of curves on Fig. 11.1, there is a regular increase of the critical concentration with tube diameter. The critical concentration is also a function of the degree of flocculation, and hence the diameter-concentration relation must be determined for each particular suspension.

The compaction concentration determined from hindered-settling measurements is compared with the compaction concentration from minimum-transport studies in Fig. 11.2. The good agreement observed indicates that critical concentrations determined from a simple series of hindered-settling tests can be used to determine the range of applicability of minimum-transport relations developed for the compaction region.

Previous studies[2] have indicated that minimum-transport data for a dilute suspension can be correlated by an expression of the form:

$$\frac{U_t}{(u_{*_w})_c} = \Psi\left(\frac{D_p (u_{*_w})_c}{\nu} \right). \qquad (1)$$

Among the possible mechanisms, two appeared to be susceptible to analysis, provided that conditions were restricted to include only those particles with diameters smaller than the thickness of the laminar sublayer and which settled according to Stokes' law. The two hypotheses were that the minimum-transport condition for particles resting on the bottom of the pipe occurs:

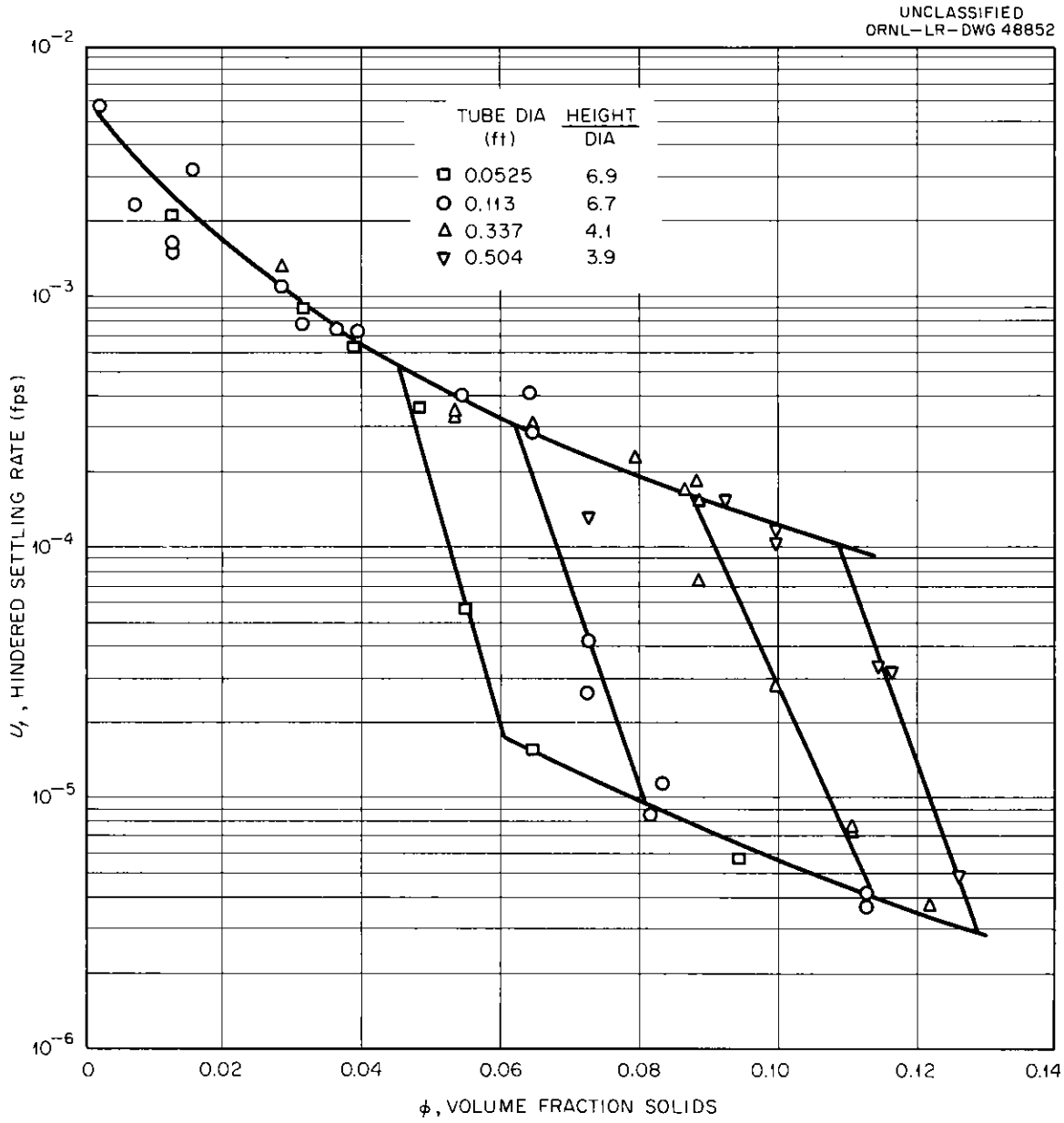

Fig. 11.1. Hindered-Settling Rate as a Function of Suspension Concentration for Flocculated ThO_2 Suspension (Series I), Showing Effect of Container Diameter on Onset of Compaction.

(1) when the lift force due to the velocity gradient is equal to the gravitational force, or

(2) when the turbulent-velocity fluctuations at a distance of one particle diameter from the wall equals the terminal settling velocity.

Assumptions implicit in the first hypothesis are:

(1) $\frac{u}{u_{*_w}} = u^+ = y^+ = \frac{y\, u_{*_w}}{\nu}$,

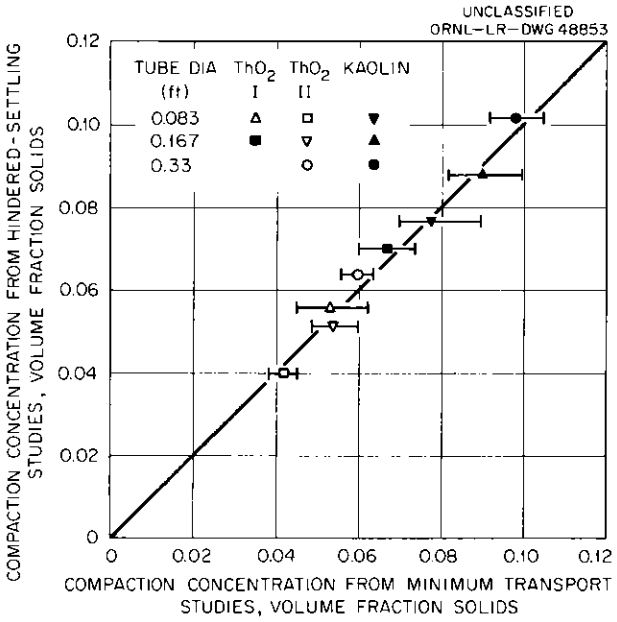

Fig. 11.2. Comparison of Compaction Concentrations Determined from Hindered-Settling and from Minimum-Transport Studies.

(2) the lift coefficient is equal to the drag coefficient,

(3) the ratio of lift force to gravitational force is unity at the minimum-transport condition.

The second assumption is supported by data taken by Fage and recalculated by White.[3] The line calculated on the basis of these assumptions is shown in Fig. 11.3a, compared with the data previously reported.

Assumptions implicit in the second hypothesis are:

(1) Turbulent fluctuations extend through the classical laminar sublayer, becoming zero only at the pipe wall.

(2) The expression for the decay of the fluctuations in the proximity of the wall is that derived by Deissler[4] in his analysis of mass transfer at high Schmidt numbers.

The first assumption is supported by experimental observations[5,6] and has been used successfully in interpretation of heat[7] and mass-transfer data.[8] The line calculated on the basis of these assumptions is shown in Fig. 11.3b, compared with the data previously reported. As can be seen, there is little to choose between the agreement of the data with the two different lines.

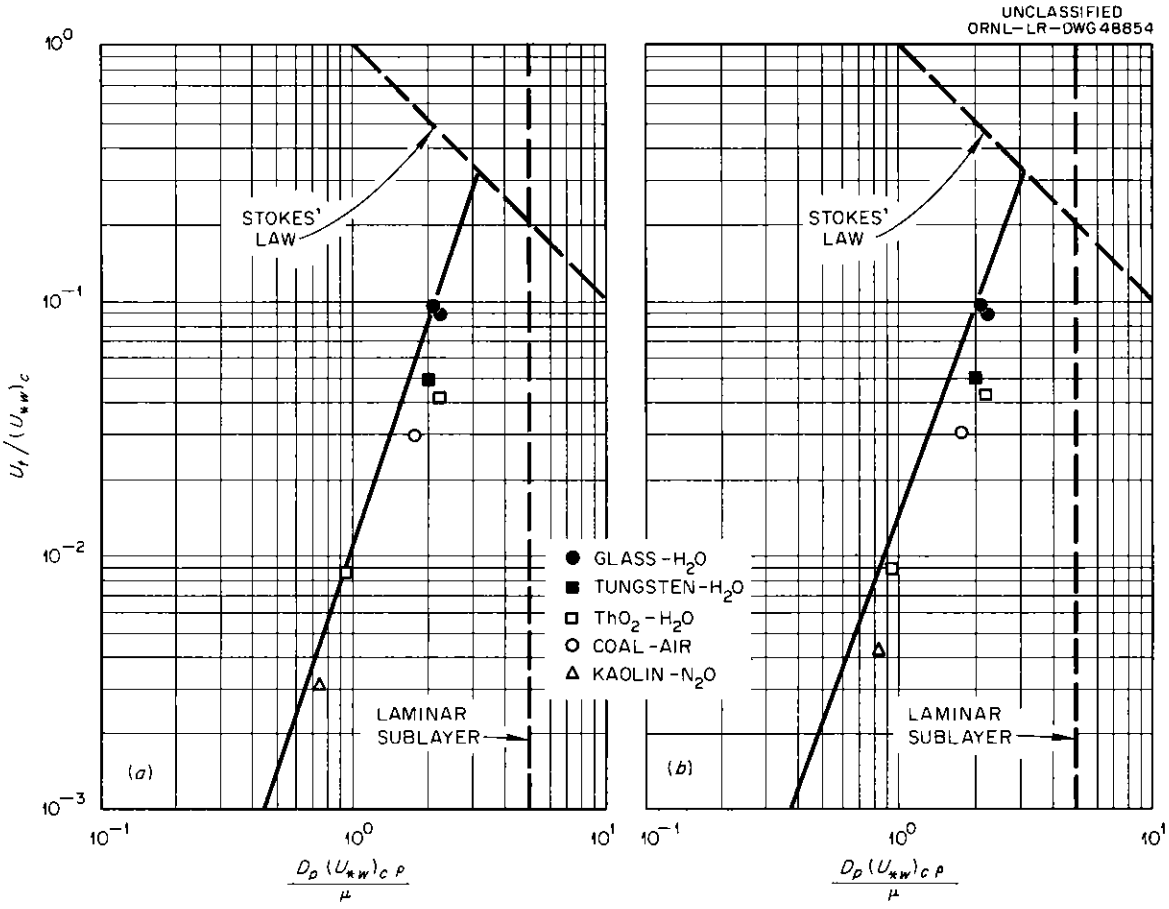

Fig. 11.3. Minimum-Transport Correlation for Flocculated Suspensions.

11.2 THORIA CAKING STUDIES

11.2.1 Thoria Dispersing Agents

The addition of dispersing agents to flocculated ThO_2 suspensions produces many desirable effects, ranging from virtually eliminating the non-Newtonian flow characteristics to possibly preventing the formation of cakes on loop surfaces. However, most electrolytes either decompose or lose their effectiveness at elevated temperatures.

During a series of screening tests, it was observed that thoria slurry, contained in a quartz tube, was maintained as a dispersed suspension for more than two weeks at 250°C after addition of Li_2SO_4. The dispersing effect was marked over a wide Li_2SO_4 concentration range. Since no other electrolyte that had been tested in this series had exhibited a strong dispersing capacity, it was desirable to test the effectiveness of Li_2SO_4 in preventing caking in a high-temperature loop test.

The cake prevention test was made in the 30-gpm loop using ThO_2 spheres, material which had caked in all previous tests even in the presence of such electrolytes as chromic acid, sulfuric acid, or sodium aluminate.[9] The ThO_2 concentration was about 400 g of Th per kg of H_2O, and the circulation temperature was 250°C. The initial Li_2SO_4 concentration was 2000 ppm based on ThO_2. This was increased to 3000 ppm after 50 hr circulation and to 7000 ppm after 170 hr. After circulation was complete, there was no cake in the impeller vanes or weep holes although such deposits had always occurred in prior sphere-circulation runs. The multidiameter sample barrel (three different velocity sections) had no deposits in the 20- or 10-fps sections. There was thin (<1 mil), soft ThO_2 film covering the entire 5-fps section. The film had been deposited in two layers, the upper of which peeled off in some places on drying, suggesting that oxide deposition occurred after additional Li_2SO_4 was added to the loop. It is believed that this represents definite evidence that addition of Li_2SO_4 to a high-temperature circulating-thoria loop inhibits cake formation. However, the optimum concentration of electrolyte and the exact mechanism responsible for cake inhibition are yet to be determined. It is known that addition of Li_2SO_4 to ThO_2 at room temperature gives very high zeta potentials, with values up to -195 mv as determined by microelectrophoretic measurements.[10] Both the high zeta potential and the apparent effectiveness in reducing cake formation may result from adsorption of $SO_4^{=}$ on the particle surface with highly hydrated Li^+ ions forming a strong counter-ion layer.

11.2.2 Concentration of Small ThO_2 Particles Required for Cake Formation

It is believed that ThO_2 cake formation occurs when 1- to 3-micron particles degrade, producing fine fragments which may be deposited on container surfaces as a hard cake. The quantity or concentration of fine fragments required to produce cake formation is not known. A qualitative test was made by circulating thoria spheres diluted with 1600°C-calcined ThO_2. These spheres provide fragments for cake formation, while the 1600°C oxide does not form cakes. Circulation of slurry containing 50 wt % of each oxide type resulted in reduced cake formation compared to that normally occurring during sphere circulation. There were ThO_2 films on impeller faces and in the multidiameter sample barrel, but almost no cake was in impeller vanes or weep holes. Thus, although the substantial quantity of noncaking oxide apparently did not serve as an alternative site for fine-fragment deposition, it may have acted as a scrubbing agent, removing deposits from the most turbulent regions of the system.

11.2.3 Properties of ThO_2 Containing a Coprecipitated Oxide

Studies of slurry caking phenomena have demonstrated the importance of particle integrity in the prevention of caking. One method of achieving particle integrity of pure ThO_2 is by calcination at a temperature of 1600°C. An alternative procedure for achieving integrity, with the added advantage of a lower calcination temperature, is by incorporating a suitable metallic oxide in the thorium compound to be calcined. In order to study the effect of different metals, thorium hydroxide or oxalate was coprecipitated with Si, Al, Pb, Zr, or Mg and then calcined stepwise to 800°C. Particle integrity was determined after Waring blendor treatment of 1 hr and 10 min, using the Cake Resuspension Index (CRI) procedure previously described.[11] (Briefly, the CRI procedure yields an empirical number, varying from 0 to 10, which is inversely proportional to particle integrity.) The results for ThO_2 with additives of Al, Pb, and Si, prepared by coprecipitation as the hydroxide, are:

Additive, Mole Fraction	CRI
None	6
Si, 0.1	4.6
Al, 0.1	2
Pb, 0.1	1

The results for ThO_2 with Zr additive, prepared by coprecipitation as the oxalate and followed by digestion for 4 hr, are:

ZrO_2, Mole Fraction	CRI
0	4
0.05	1
0.05 (calcined at 1000°C)	0
0.1	0.5
0.25	0

Results with MgO addition were very unfavorable with respect to particle integrity.

A CRI of 2 or less gives qualitative evidence of high particle integrity, and on this basis it is apparent that oxide additives of Al, Pb, and Zr may produce increased particle integrity although there are insufficient data to specify the exact concentration and calcination schedule required.

REFERENCES

1. P. R. Kasten et al., HRP Quar. Prog. Rep. Apr. 30, 1959, ORNL-2743, p 63-65.
2. H. W. Hoffman et al., HRP Prog. Rep. Oct. 31, 1959, ORNL-2879, p 159-63.
3. C. M. White, Proc. Roy, Soc. (London) 174A, 322-38 (1940).
4. R. G. Deissler, NACA Report 1210 (1955).
5. A. Fage and H. C. H. Townend, Proc. Roy. Soc. (London) 135A, 656 (1932).
6. J. J. Keyes and J. E. Mott, An Investigation of Thermal-Transient Decay at a Fluid-Solid Interface and in Turbulent Flow Through Circular Ducts, ORNL-2603 (Dec. 2, 1958).
7. R. A. Suehrstedt et al., Application of Concepts of Penetration Theory to Heat Transfer, KT-378 (Dec. 1, 1958).
8. T. J. Hanratty, AIChE Journal 2, 359 (1956).
9. H. W. Hoffman et al., HRP Prog. Rep. Oct. 31, 1959, ORNL-2879, p 163-64.

10. C. M. Boyd, H. P. House, and O. Menis, Micro-Electrophoretic Determination of the Zeta Potential of Thorium Oxide, ORNL-2836 (Nov. 10, 1959).

11. C. S. Morgan, Status Report on ThO_2 Caking Studies, ORNL CF-57-9-102 (Sept. 26, 1957).

12. THORIUM OXIDE IRRADIATIONS

J. P. McBride
O. O. Yarbro

Work on the effect of reactor irradiation on the properties of thorium oxide continued, with the recovery for examination of two series of thoria powders irradiated in aluminum capsules in a lattice position in the LITR; the recovery of a slurry of >25-μ Houdry spheres irradiated in a settled condition in the LITR (C-43); and the start of the irradiation at 250°C of a settled bed of thoria pellets, 0.196-in. diameter, under D_2O in the C-43 facility.

12.1 IRRADIATIONS OF THORIA POWDER

During the month of February, 1958, personnel of the Solid State Division initiated the irradiation of two series of thoria powders (C and D) in aluminum capsules in the C-52 lattice position of the LITR. The powders were prepared from 650°C-fired D-16 thorium oxide by refiring them in platinum crucibles for 24 hr at 650, 800, 900, 1100, and 1500°C. The solids were recovered for examination after having been irradiated 16 months (series D) and 21 months (series C). Series C samples are now being examined. The 650, 800, and 900°C-fired samples in both series were red, and the particles had agglomerated into hard, glossy clinkers (Fig. 12.1). The 1100°C- and 1500°C-fired oxides were powders of off-white and blue colorations, respectively (Fig. 12.2). Specific surface areas for all series D samples (series C samples have not yet been measured) except the 1500°C-fired material were markedly decreased by the irradiation (Table 12.1), despite the fact that the estimated maximum temperature of the powders during irradiation, based on calculations assuming 25% theoretical density for the powders, was less then 300°C.

The powders were canned in aluminum capsules, about 2-1/2 in. long and of 1/2-in. OD and 1/4-in. ID. They were irradiated in such a way that the reactor cooling water flowed over the outside of the capsules. The capsules contained cobalt and titanium flux monitors.

The only contaminant found in the oxides after irradiation was aluminum (100 to 5000 ppm), most of which probably came from powder that dropped into the oxides during the grinding required to open the capsules. The marked decrease in surface areas with all except the high-fired oxides suggests that the irradiation produced much the same effect as firing an oxide to about 1500°C. The results of density measurements of the irradiated oxides were erratic, and the measuring technique will have to be modified. Measurements of average particle sizes will be made on all the irradiated samples as time and radiation level permit.

12.2 IRRADIATION OF HOUDRY-SPHERE SLURRY

An aqueous slurry with 5 g of >25-μ Houdry spheres containing 0.5% natural uranium was irradiated for 52 days in a settled condition at a thermal neutron

Fig. 12.1. 650°C-Fired ThO_2 Powder Irradiated 16 Months in the LITR; Maximum Temperature 300°C.

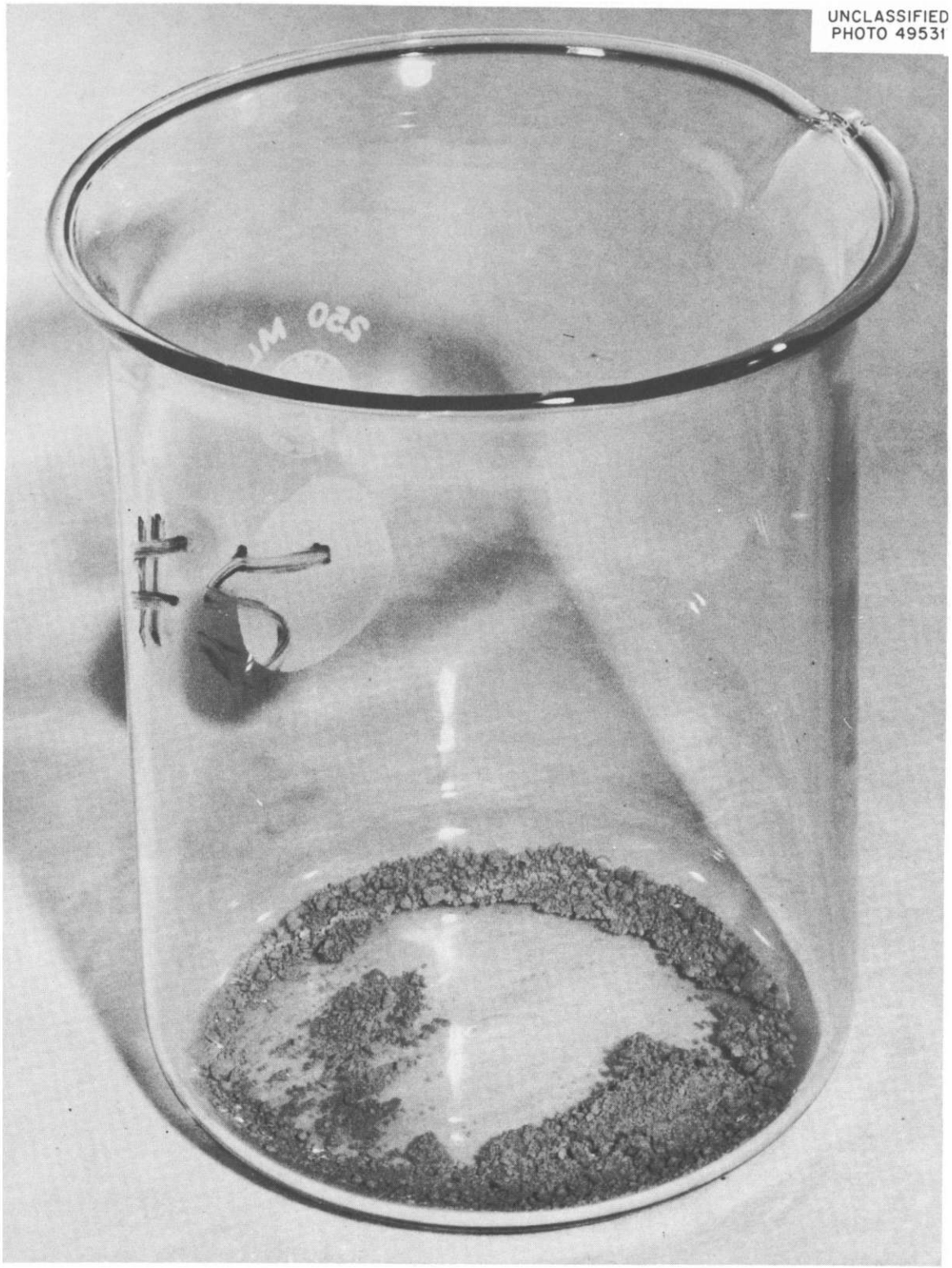

Fig. 12.2. 1500°C-Fired ThO_2 Powder Irradiated 16 Months in the LITR; Maximum Temperature 300°C.

Table 12.1. Thoria-Powder Irradiations in LITR

Irradiation time: 489 days
Maximum temperature: <328

Oxide Firing Temp. (°C)	Neutron Flux: Thermal: Average $\frac{Pa^{233}*}{Th}$	Neutron Flux: Thermal: $\frac{U^{233}*}{Th}$	Neutron Flux: Thermal: $\frac{Sr^{89}*}{Th}$	Neutron Flux: $Co^{59}(n,\gamma)Co^{60}$	Neutron Flux: Fast, ~5.0 Mev $Ti^{46}(n,p)Sc^{46}$	Surface Area (m^2/g) Before	Surface Area (m^2/g) After	Description of Irradiated Oxide
		$\times 10^{10}$		$\times 10^{13}$	$\times 10^{3}$			
650		2.5		2.5	1.6	28.4	1.0	Red clinkers
800		2.1		2.3	1.3	15.2	<0.5	Red clinkers
900		2.2		1.7	1.6	7.9	<0.5	Red clinkers
1100		1.9		1.8	1.4	3.3	1.9	Off-white powder
1500		1.7		1.8		0.8	0.8	Blue powder

*Flux based on neutron capture or fission yield as related to total thorium present.

flux of ~2 x 10^{13} in hole C-43 of the LITR.[1] The container was a stainless steel autoclave equipped with mild-steel cooling fins to increase the efficiency of the air cooling used in C-43 to control temperatures. Water was apparently lost from the autoclave after only four days' irradiation, and the autoclave temperature increased from 180 to 280°C. More water was added after an additional 21 days' irradiation, reducing the temperature from 280 to 230°C. The autoclave temperature continued to rise slowly under the ordinary conditions of cooling, probably because of increased fission heating, and at the end of the experiment the lowest temperature that could be maintained under ordinary conditions of temperature control was 270°C.

When the autoclave was opened, a dried plug of yellow solid containing more than half the original material was found at the top. This solid was apparently deposited as a result of the refluxing introduced by air cooling: air flows down over the top of the bomb, and the top is the coolest position. Approximately 1.3 ml of slurry was drained from the autoclave after the plug was broken away. Portions of the slurry and plug have been submitted for chemical, radiochemical, and physical analyses.

12.3 IRRADIATIONS OF THORIA PELLETS

Irradiation under D_2O at 250°C of a settled bed of 50 thoria pellets 0.196 in. in diameter was initiated in the C-43 facility in the LITR. The pellets were prepared by treating the Davison-prepared pellets (1450°C fired) with dibasic aluminum nitrate solution and refiring at 1750°C (see Sec. 15.1.2). Hot-cell equipment to measure pellet wear in a spouting-bed test and the crushing strength of the irradiated pellets is being developed.

REFERENCE

1. J. P. McBride and N. A. Krohn, HRP Quar. Prog. Rep. Jan. 31, 1960, ORNL-2920, p 91.

13. DEVELOPMENT OF GAS-RECOMBINATION CATALYSTS

J. P. McBride L. E. Morse

Further studies were carried out on the catalytic combination of hydrogen (or deuterium) and oxygen by thoria and thoria-urania slurries containing a "sol-prepared" palladium-thoria catalyst. The sol method of preparing the palladium catalyst, described below, has given the most active palladium catalyst and appears to be reproducible. Specific activity of the sol-prepared catalyst seems to be independent of the type and concentration of slurry solids. Laboratory tests of the catalyst in thoria-urania slurries being used in-pile radiation-corrosion studies indicated that the activity was more than adequate for use in these systems. Tests on a slurry sample from a pump-loop gas-recombination study showed a lower specific activity than is obtained with unpumped slurries and confirmed qualitatively the drop-off in catalytic activity observed during the loop run. The decline in activity during pumping was coincident with a slurry-solid degradation process.

13.1 PALLADIUM CATALYST DEVELOPMENT

The sol preparation method consisted in refluxing a 650°C-fired thorium oxide in an aqueous solution of palladium nitrate (0.5 g of $Pd(NO_3)_2$ to 10 g of ThO_2) to form a sol and then reducing the sol with hydrogen. Treatment with hydrogen (or deuterium for heavy-water preparations) reduced the palladium, destroyed the bulk of the nitrate, and flocculated the sol. The catalyst preparation was a flocculated, slow-settling suspension, an aliquot of which was added to the slurry under test. Preparations were made in both ordinary water (P-23) and heavy water (P-28 A and P-28 B-C).

The rate data showed reproducible activities of the catalyst in the cases where the slurry was pretreated with oxygen (Table 13.1). It was active in both thoria and thoria-urania systems. Assuming an average blanket power level of about 10 kw/liter, slurries containing only a few hundred ppm of palladium should have sufficient activity to keep the radiolytic-gas partial pressure below 150 psi at 280°C even under an excess-oxygen overpressure. Included in Table 13.1 are data obtained from an in-pile slurry experiment with a thorium - 8% enriched-uranium oxide at a power level of 20 w/ml, which showed a specific catalyst activity about four times greater than that observed in out-of-pile studies. Pretreatment of the slurry-catalyst system with hydrogen or maintaining an excess-hydrogen overpressure resulted in an increase in specific activity of many orders of magnitude. The limits of hydrogen or oxygen overpressure or H_2/O_2 ratios under which catalytic activity is maintained have not been explored, but preliminary information suggests that some limitations may exist.

The order of the recombination reaction has not yet been established. Apparent over-all reaction orders of 0 to 2 based on total gas pressure in excess of steam have been observed. An effort is under way to determine the order of reaction with respect to hydrogen and oxygen partial pressures by

Table 13.1. Palladium Catalysis of Hydrogen-Oxygen Reaction in Thoria Slurries

Catalyst: sol-prepared
Temperature: 280°C

Catalyst Preparation	Description of Slurry: g Th/kg H_2O	Description of Slurry: Oxide Firing Temp. (°C)	Catalyst Concentration: ppm of Pd, Based on Thorium	Catalyst Concentration: m of Pd	Pretreatment Gas or Gas in Excess	Reaction Rate, P_{H_2}=100 psi, (moles H_2/liter·hr)	CPI[a] at 0.001 m Pd, P_{H_2}=100 psi (w/ml)
P-23	100	1600	275	0.00024	H_2	25	460
P-28 A	100	1600	117	0.00010	O_2	0.23	9
P-28 A	500	1600	23.4	0.00010	H_2	~50	~2000
P-28 A	100	1000 (Th - 8% U oxide)[b]	59.3	0.00005	O_2	0.11	9
P-28 A			118.6	0.00010	O_2	0.34	13
P-28 A			170	0.00015	O_2	0.59	16
P-28 A	1080 (in LITR)	1000 (Th - 8% U oxide)[b,c]	59.3	0.00055	O_2	5.5	40
P-28 B-C	69.2	1000 (Th - 16% U oxide)[b]	133	0.00008	O_2	0.42	22

[a]Catalyst performance index = $\frac{\text{reaction rate at 0.001 m Pd and } P_{H_2} = 100 \text{ psi}}{(0.38)\ (0.6)}$, where 0.6 is the G value for gas production.

[b]Thorium - 8% uranium oxide and thorium - 16% uranium oxides are equivalent to U/Th mole ratios of 0.08 and 0.16, respectively.

[c]See Sec. 14.2.2 of this report.

determining the initial reaction rate with various H_2/O_2 ratios under various over-all gas pressures.

13.2 EFFECT OF SLURRY CONCENTRATION ON CATALYTIC ACTIVITY

A series of experiments was carried out in which the P-28 A catalyst preparation was first added to a slurry (100 g of Th per kg of H_2O) of 1600°C-fired oxide at a concentration of 117 ppm of palladium, based on thorium. The catalytic activity was measured, and then the thoria concentration was charged in increments of 100 g of Th per kg of H_2O and the activity again measured. Increasing the thoria content to 500 g of Th per kg of H_2O without adding any more palladium did not significantly change the specific activity of the catalyst at either 250 or 280°C, the two reaction temperatures investigated (Table 13.2).

The water produced during recombination tests at any one concentration was removed prior to the addition of fresh thoria. Initially and after each thoria addition, the suspension was heated at 280°C for at least 24 hr under oxygen

Table 13.2. Effect of Thoria Concentration on Catalyst Activity

Slurry Concentration (g Th/kg H_2O)	Palladium Concentration (ppm Pd/Th)(m x 10^{-4})	No. of Expts.	Initial H_2/O_2 Ratios	Apparent Reaction Order	CPI,* P_{H_2}=100 psi (w/ml)
		Reaction Temperature, 250°C			
100	117	1.1	3	0.56 - 0.64	0-1	0.3 - 1.2
200	58.5	1.1	3	0.52 - 0.53	0	0.4 - 1.2
300	39.0	1.1	3	0.56 - 0.62	1	0.2 - 0.3
400	29.25	1.1	4	0.40 - 0.50	1	0.2 - 0.3
500	23.4	1.1	4	0.33 - 0.40	0.5-1	0.2 - 0.5
		Reaction Temperature, 280°C			
100	117	1.1	3	0.61 - 0.64	0-2	0.3 - 0.9
200	58.5	1.1	3	0.60 - 0.62	0-1	0.7 - 1.4
300	39.0	1.1	3	0.57 - 0.63	1-1.5	0.3 - 0.5
400	29.25	1.1	5	0.25 - 0.59	1-1.5	0.5 - 1.2
500	23.4	1.1	5	0.29 - 0.34	1-1.5	0.8 - 1.3

*Catalyst performance index = $\dfrac{\text{reaction rates in moles } H_2/\text{liter}\cdot\text{hr at } P_{H_2}=100 \text{ psi}}{(0.38)(0.6)}$,

where 0.6 is the G value for gas production.

(200 psi at room temperature) prior to its use in recombination tests. Excess oxygen over stoichiometric H_2 + 1/2 O_2 was maintained in all experiments.

Over-all reaction orders, based on total gas pressure in excess of steam, were from 0 to 2, but the majority of reactions showed a first-order dependence. Of 27 experiments, 15 showed first-order dependence; nine, zero order; three, 1.5 order; and one, second order. Twelve of the reactions measured were preceded by an initial reaction, too fast to measure, which consumed part of the gas mixture.

Further experiments are planned in which the thoria concentration will be held constant and the palladium concentration increased in successive steps. Some insight should be gained as to whether or not the concentration of the slurry to which the palladium is added is an important variable in the utilization of the catalyst.

13.3 PALLADIUM CATALYSIS IN THORIA-URANIA SLURRIES

Work on gas recombination in thoria-urania slurries (Table 13.1) was carried out primarily in support of the in-pile slurry-corrosion studies of the REED corrosion section. The same thorium-uranium oxide preparations containing enriched uranium used or planned for use in the in-pile work were used. The thorium-uranium oxides contained U/Th molar ratios of 0.08 and 0.16. The experiments were run after pretreatment of the slurries with oxygen (200 psi at room temperature) at 280°C for 60 hr. An initial overpressure of 200 psi of oxygen at room temperature was added to the reaction autoclave prior to heating the system to 280°C for the recombination experiments. Stoichiometric quantities of hydrogen and oxygen were then added at temperature, and the reaction was followed by noting the decrease in gas pressure with time.

Comparison of the data obtained with the thorium - 8% uranium oxide in-pile (Sec. 14.2.2) and out-of-pile (Table 13.1) indicates that the specific activity obtained in-pile was about four times greater than that obtained out-of-pile. No importance is attached to this difference because the out-of-pile experiments were carried out at about one-tenth the slurry concentration used in the in-pile work, and the comparison is based on a linear extrapolation of recombination activity with slurry concentration.

13.4 PALLADIUM CATALYSIS IN PUMPED SLURRIES

The slurry corrosion group of REED has carried out gas-recombination tests in a mockup of an in-pile slurry loop, using a thorium - 0.5% uranium oxide (Sec. 14.3.10). In general, for similar slurries, the specific catalyst activities in the loop were 10 to 20 times lower than those in the laboratory tests in autoclaves. In addition, the activity dropped off with pumping time, coincident with slurry degradation.

A sample of a slurry used in the mockup (1000°C-fired thorium - 0.5% uranium oxide; 1800 ppm Pd, based on thorium, showed a CPI of ~1 w/ml at 280°C and P_{H_2} = 100 psi (G = 0.6) in a laboratory test. A synthetic mixture of the original charge gave a CPI of >30 w/ml, confirming qualitatively that the catalytic activity did decrease in the loop run. As yet no explanation has been found for either the unusually low specific activities observed in the loop or the drop-off in activity. A laboratory effort to investigate these discrepancies is under way.

14. SLURRY CORROSION AND BLANKET MATERIALS TESTS

E. L. Compere H. C. Savage

J. M. Baker
S. E. Bolt
V. A. DeCarlo
R. B. Gallaher
R. A. Lorenz
R. E. McDonald
A. R. Olsen
M. L. Picklesimer
S. A. Reed
A. J. Shor
L. F. Woo

14.1 THORIA-PELLET TEST PROGRAM

14.1.1 Introduction; Laboratory and 100A Loop Tests of Experimental Thoria Pellets

The use of thoria pellets as a possible blanket material in a two-region breeder reactor was investigated at ORNL in 1953-54 in a series of preliminary tests using fluidized beds of ThO_2 cylinders and washers.[1] Recent renewed interest in a pellet blanket (see Sec. 6.2) has stimulated a more comprehensive investigation of methods for preparing suitable thoria compacts and of development of tests for estimating the attrition of the pellets under simulated reactor conditions.

In one proposed 400-Mw breeder reactor (Sec. 6.2), the blanket would contain approximately 27 metric tons of thoria pellets. If the pellets were attrited at the rate of 0.0004 wt %/hr as a result of periodic agitation of the beds, thermal ratcheting, etc., approximately 100 g/hr of fine material would result. If pellets are moved only a few times during the course of their exposure, losses due to pellet attrition incident to movement from one reactor region to another are probably momentarily higher but are much less frequent. Such movement may involve fluidization, jet-pumping, or other schemes.

The size distribution and chemical behavior of the degradation products are of considerable interest in studying their disposition. While in the reactor system, the nature, extent, and locality of their accumulation will be important, potentially involving hot spots, reduced heat transfer, maintenance problems, etc. Removal procedures are also of interest, both to avoid the above problems and because of potential processing advantages.

Efforts during the past quarter have been concerned with the development of tests appropriate for the characterization of pellet preparations, and the examination of experimental preparations from several sources. Approximately 50 experimental pellet preparations have been tested. The majority of the preparations were fabricated in the Chemical Technology Division. Several samples were also prepared by the Ceramics Group of the Metallurgy Division. Five samples obtained at various times were from outside vendors: two from Davison Chemical Company, two from the American Lava Corporation, and one from Norton Company. The experimental pellets, which were calcined in the range 1000 to 1750°C, included 0.2-in.-dia spheres and right cylinders and cylinders with hemispherical ends, approximately 0.2 in. diameter by 0.2 in. in length. Details of pellet fabrication are discussed in Sec. 15.1.1. Major fabrication variables included

pellet density, calcination temperature, initial thoria calcination temperature and particle size, additives (CaO, Al_2O_3), pressing pressures, die lubricants, and binders.

A summary of major preparation variables and results of the evaluation tests is presented in Table 14.1.

14.1.2 Test Methods

Early preparations usually consisted of one to five pellets, which were exposed in static autoclave tests of 17 to 350 hr duration in pure water at 260°C. This test served to reveal susceptibility to leaching effects. The effect on the preparations was evaluated from weight changes, dimensional changes, differences in general appearance as observed with an optical microscope and by chemical analysis of the supernatant liquid for leachable additives originally in the samples.

When 25 or more pellets were available, a portion of them was also subjected to 24-hr rocking-autoclave tests in 260°C water, using the same postrun examinations. The 2.5-liter autoclave was rocked ±60° at 38 cycles/min. Rocking-autoclave tests served to inidicate susceptibility to attrition due to pellet agitation as well as leaching in high-temperature water. Low values on this test would be expected to imply satisfactory handling qualities for reactor exposure.

Sufficient quantities of two preparations were available for exposure in 100A loop tests conducted at 260°C using D_2O and nitrogen overpressure. Pellets were contained in cylindrical holders 1 in. in inside diameter, which were inserted in the test loop as packed static beds placed in a horizontal position or as free-moving fluidized "pulsating" beds placed in a vertical position. Superficial velocities through the beds were 2 and 0.2 fps, respectively. Periodic samples were withdrawn from the test loop and submitted for chemical analyses. Quality of the pellets was determined as noted above.

As preparation techniques improved and higher quality pellets were made, autoclave tests alone were not sufficient to distinguish slight differences between small lots of pellet preparations. Therefore an accelerated test using the spouted-bed[2] technique was employed. The method consisted of consecutive 1-hr exposures at room temperature using 10 pellets in a bed when the superficial liquid velocity was 0.2 fps and the jet velocity was 24 fps. Quality of the pellets was determined after each 1-hr exposure by measuring weight loss and dimensional changes and by microscopic examination.

Fluidized-bed and ball-mill tests at room temperature were run in one case where sufficient pellets were available. In the fluidized-bed test, 1500 pellets (744 g), which formed an 8-in. settled bed in a 2-in. Pyrex pipe, were fluidized at 0.7 fps superficial velocity resulting in a bed expansion of 40 to 50%. Four successive 2-hr tests were made.

In the ball-mill test, 10 pellets and 250 ml of H_2O were placed in a 3.75-in.-dia 750-ml rubber-lined ball mill rotated at 155 rpm, for eight successive 1-hr exposures. Particle size of attrited material from this test corresponded to the size of thoria-powder particles used in the preparation of the pellets.

14.1.3 Pellet Quality

Weight-loss rates ranged widely in static autoclave tests, from 0.2%/hr to 0.0001%/hr, as preparation procedures advanced (Table 14.1). A few preparations

Table 14.1. Preparation Variables and Attrition Rate of Experimental Thoria Pellets

Additives, Original (wt %)	Treatment	Final Calcin. Temp. (°C)	Density (Hg Immersion) (g/cc)	Mfg. Meth.	Shape	No. of Preps. Tested	Average Attrition Rate (wt %/hr)		
							Autoclave, 260°C		Spouted Bed
							Static, 17-350 hr	Rocking, 24 hr	25°C, 2 hr
None	-	1750	8.0-9.6	P	Cylinder	24	0.0001-0.03	0.02-2	2-4
None	-	1750	9.0	P	Cyl-hemisph	3	0.0001-0.0005	0.7	3
None		1450	5.0	P*	Sphere	1	0.2	-	30
None	$Th(OH)_4$ sol	1200	5.6	P*	Sphere	1	-	-	25
None	$Th(NO_3)_4$ soln	1200	-	P*	Sphere	1	-	-	17
None	-	1750	6.0	P*	Sphere	1	0.001	-	10
None	$Th(OH)_4$ sol	1750	6.7	P*	Sphere	1	-	-	3
None	$Th(NO_3)_4$ soln	1750	6.6	P*	Sphere	1	-	-	5
None	$AlOH(NO_3)_2$ soln	1750	7.4	P*	Sphere	1	-	-	1
0.25-0.5 CaO	-	1750	8.8-9.7	P	Cylinder	7	0.0001-0.02	0.09-0.7	2-5
0.3 Al_2O_3	-	1750	9.7	P	Cyl-hemisph	4	-	0.08-1.3	0.8-3
0.3-5 Al_2O_3	-	1750	7.8-8.9	P	Cylinder	6	0.0001-0.0003	0.05-0.12	1.4-3
0.2 CaO + 0.4 Al_2O_3		-	-	(BM)	Sphere	1	-	-	0.9
0.25 CaO + 0.5 Al_2O_3		1750	8.9	P	Cylinder	1	0.0001	0.2	-
0.5 CaO + 5.0 Al_2O_3		1750	8.3	P	Cylinder	1	0.0008	-	3

P - pressed
P* - pressed in spherical die by Davison Co.
(BM) - pellets apparently finished by ball milling, Norton Co.

displayed weight gains. Materials which displayed weight losses greater than 0.0003%/hr generally had failed due to spalling, leach-out of additives, or partial or complete disintegration. Of 47 batches tested, 31 showed weight losses below 0.0003%/hr. Pellets which gained weight during exposure were usually discolored, and some suffered dimensional changes. Such changes appeared to be the result of high-temperature water reactions with additives (e.g., CaO) or impurities present in the pellets as a result of fabrication variables.

Attrition rates in rocking-autoclave tests at 260°C ranged from 0.05 to 1.7%/hr based on 24-hr weight-loss data. Of 12 preparations tested, 5 displayed rates less than 0.1%/hr.

The spouted-bed test was a rapid screening test indicating susceptibility to attrition due to agitation. Rates ranged from 30%/hr to 0.3%/hr, after various exposure times on various preparations. Of 12 preparations tested, half displayed rates of 1%/hr or less. After ten consecutive 1-hr exposures, attrition rates were frequently a factor of 3 to 4 lower than the initial 1-hr rate, but subsequently appeared to become relatively steady in value. This was attributed to pellet surfaces becoming rounded and smoother.

A few preparations were carried through 25 or more consecutive 1-hr tests. Data from these are shown in Fig. 14.1 in which the logarithm of weight (as percentage of original) is plotted against time. Linearity after the first few hours implies a constant-percentage weight-loss rate. A number of characterization tests of a recent preparation (batch P-39) were made. The material consisted

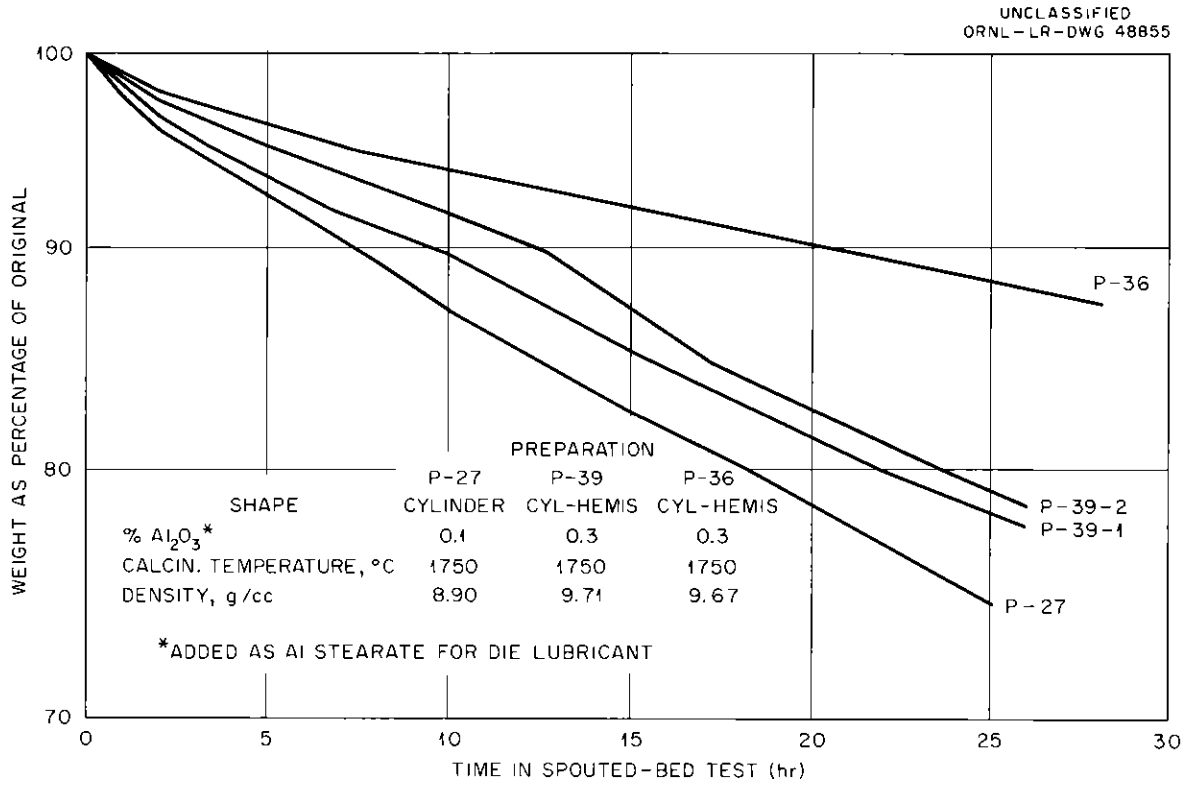

Fig. 14.1. Pellet Weight Loss in Extended Tests in Spouted Bed.

of 0.2-in. cylinders with hemispherical ends, prepared from pure thoria with the addition of 5% aluminum stearate (equivalent to 0.3% Al_2O_3 in the pellet) as lubricant. After pressing, the material was fired at 1750°C to a density (Hg immersion) of 9.7. Results by various test procedures were:

Static autoclave, 260°C	0.0005-.0012%/hr
Rocking autoclave, 260°C	1.2%/hr
Fluidized bed, 25°C	0.2-0.1%/hr
Ball mill, 25°C	2.3-1.1%/hr
Spouted bed, 25°C	1.4-3%/hr (first hr)
(see Fig. 14.1)	0.8%/hr (steady)

The effects of pellet shape were of interest, as both techniques of manufacture and handling qualities were involved. Initial preparations were cylinders varying in size from 0.1 to 0.2 in. in height and diameter. Later compacts had been fabricated as cylinders with hemispherical ends. Two preparations were nearly spherical in shape. Right cylinders and modified cylindrical shapes were fabricated by conventional pressing techniques using an appropriately shaped die and ejecting plunger. A number of the preparations contained pressing defects. Early batches of cylinders were laminated (see Fig. 14.2). These pellets failed generally along planes of lamination, and some chipping and spalling were observed. This batch was used in the first loop test.

Some cylinders with hemispherical ends had stress planes along the boundaries between the cylindrical body and domed ends. Localized erosion occurred in these areas as shown in Fig. 14.3. Several preparations which appeared satisfactory by macroexamination were found to contain numerous pores and microcracks (Fig. 14.4) when they were mounted and polished using conventional metallurgical techniques. High weight losses occurred with such preparations during exposures in both static- and rocking-autoclave tests.

Pellet density appeared to be a factor with pellets of lower density. The series (given in Table 14.1) in which pellets of density 5.0 were treated with $Th(OH)_4$ sol, $Th(NO_3)_4$, or $AlOH(NO_3)_2$, and recalcined, resulted in pellets of varied density up to 7.4. The attrition rate diminished exponentially in this series from 30%/hr to 1%/hr.

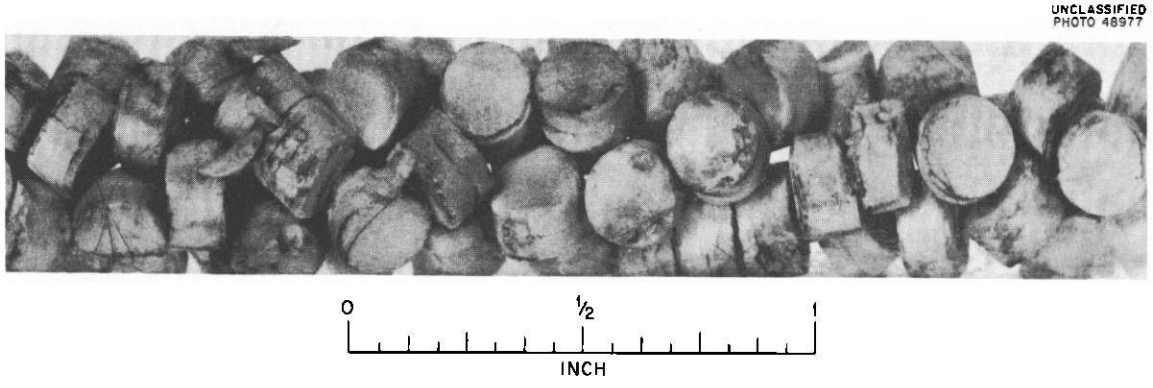

Fig. 14.2. Photograph of P-12 ThO_2 Pellets Showing Laminations Resulting from Improper Pressing Conditions.

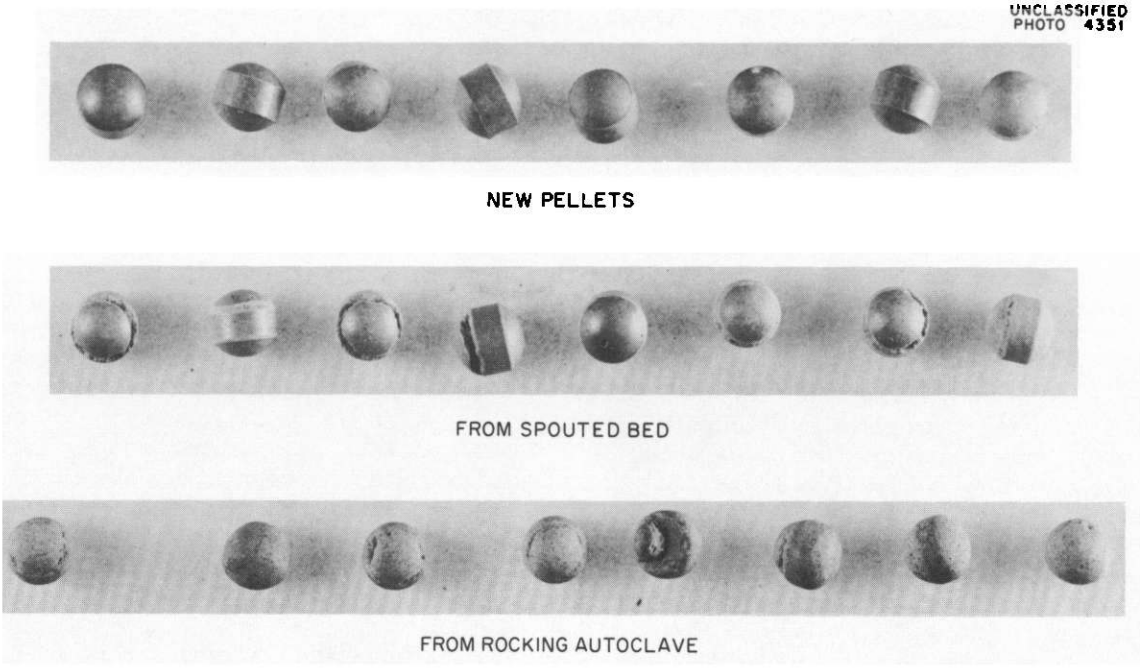

Fig. 14.3. Photograph of P-37 Pellets Showing Areas of Localized Attrition as a Result of Stress Planes.

With other preparations prepared in different ways, in which the pellets were of higher density, from about 8 to 9.7, no strong correlation of attrition rate with density was evident.

14.1.4 Loop Tests

A 100A pump-loop test was carried out on the pellets shown in Fig. 14.2, which were exposed in randomly packed, static, horizontal beds at D_2O superficial velocities of 2 and 0.06 fps. In the 350-hr test, attrition rates averaged 0.006 and 0.004%/hr, respectively. Of the material lost as fines, 53 and 54%, respectively, remained in the beds. The remainder was deposited in quiescent areas of the main loop. Only trace amounts of thorium were detected in the circulating D_2O. During exposure, laminations in the compacts were enlarged. One per cent of the pellets disintegrated. These pellets had shown weight-loss rates at 260°C in static and in rocking autoclaves, respectively, of 0.002 and 1.7%/hr.

A second loop test was made with 0.1-in. cylindrical pellets (American Lava Corp.) which contained 0.5 wt % CaO as additive. These pellets had been prepared a number of years ago.[1] Static autoclave tests at 260°C on single pellets gave weight-loss rates which ranged between 0.0002 and 0.02%/hr. Two consecutive 24-hr rocking-autoclave tests gave attrition rates which averaged 0.7%/hr.

For the loop test, pellets were exposed in a horizontal, packed bed as described for the previous test and in a vertical column in which the pellets were fluidized. With uniform cylindrical pellets, under geometries such as that of the experiment, a pulsating action may develop in fluidized beds. This effect was observed in the present experiment. The superficial velocity through the

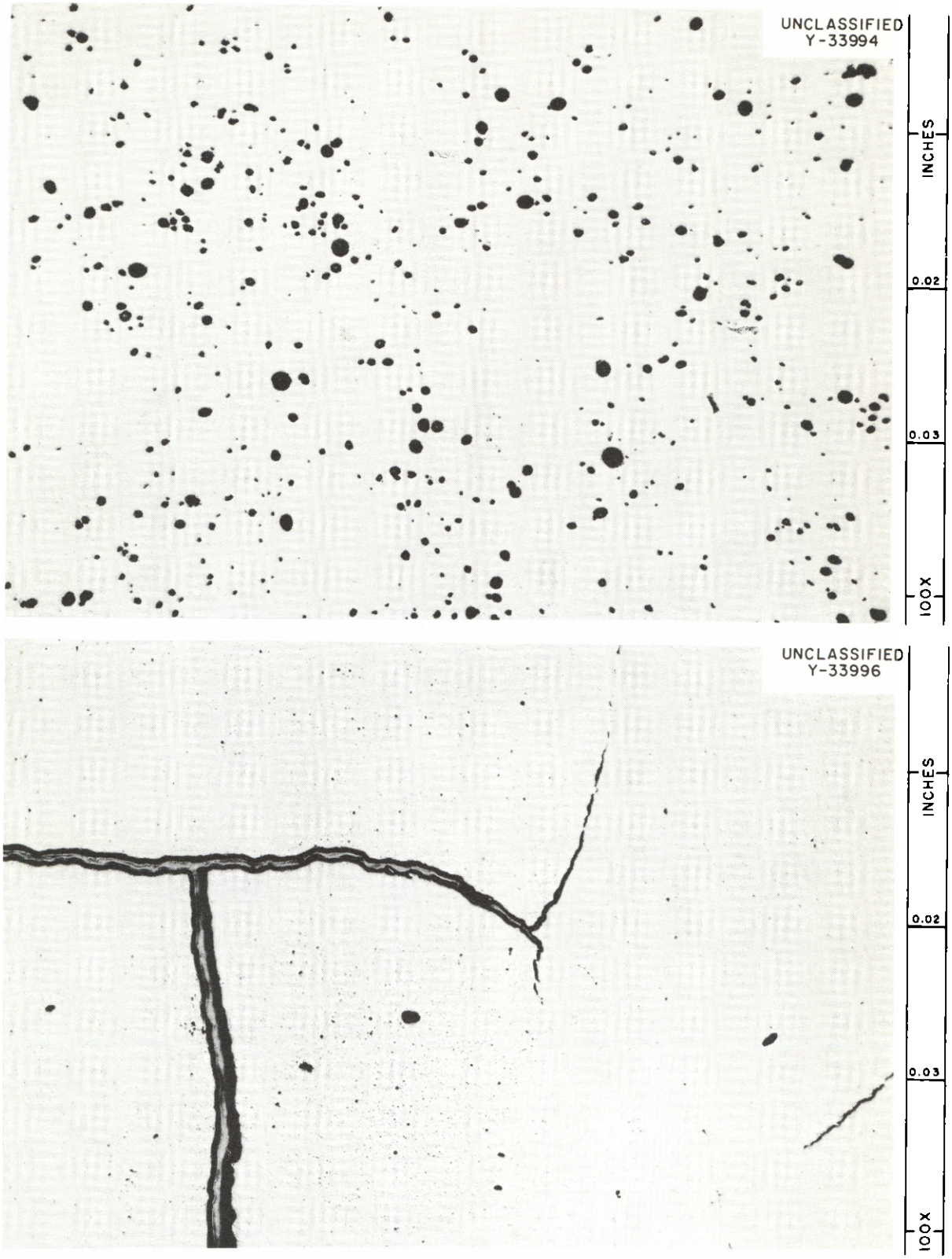

Fig. 14.4. Photomicrographs Showing Microcracks and Pores in ThO_2 Pellets.

horizontal bed was 1.3 fps, and a velocity of 0.2 fps was maintained through the pulsating fluidized bed. A television x-ray unit was used periodically to observe that there was constant movement of the pellets in the vertical bed.

During the 288-hr test at 260°C, the attrition rate in the horizontal bed was 0.008%/hr. In the pulsating bed the rate was 0.02%/hr. Seventy-seven per cent of the material lost from cylinders in the horizontal bed remained as fines within the bed. No fines remained in the pulsating bed.

Approximately 7% of the calcium was leached from the pellets. Although a total of 26 g of ThO_2 and 0.2 g of Ca were released from the beds, only trace quantities (see Fig. 14.5) of the materials were detected in the circulating D_2O. The bulk of the attrition products was deposited in the loop piping. The material was recovered by a circulating rinse of the loop using 5% nitric acid at 200°C.

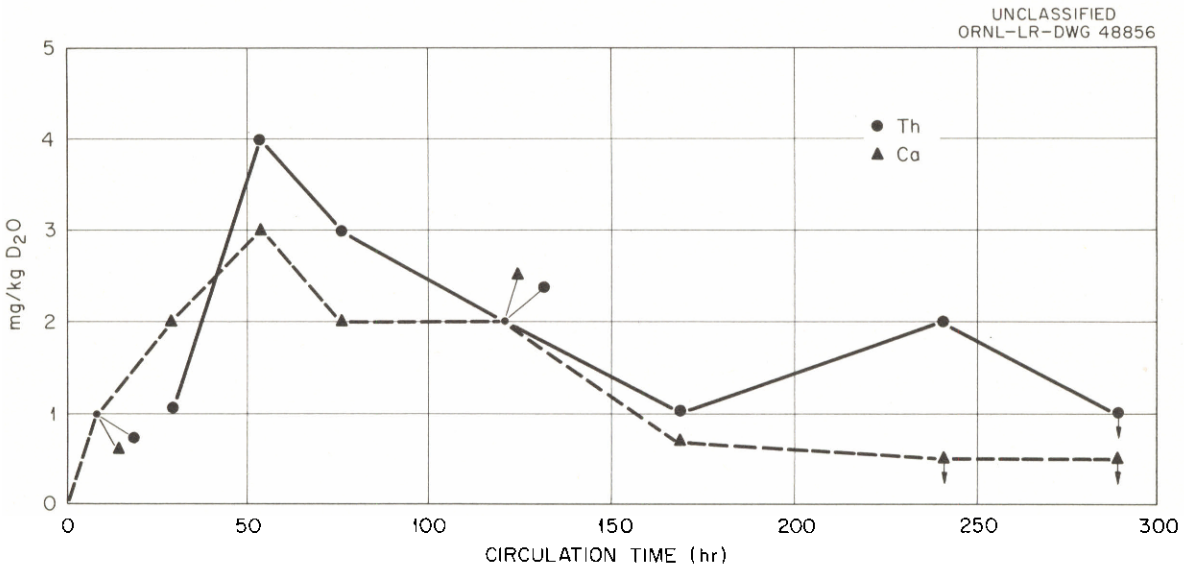

Fig. 14.5. Concentration of Thorium and Calcium in Circulating D_2O During 100A Loop Test with ThO_2 Pellets Containing 0.5% CaO.

14.2 IN-PILE AUTOCLAVE SLURRY CORROSION STUDIES

14.2.1 Introduction

The Zircaloy-2 autoclave slurry corrosion experiment discussed below resulted in achieving the highest fission power density yet developed in slurry systems, estimated to be 20 w/ml. During the short in-pile period, corrosion was slight and catalytic recombination satisfactory. However, the experiment was terminated earlier than planned because slurry plugging of the 20-mil-ID capillary connecting tubing prevented obtaining further sensitive pressure readings. The thoria - 8% enriched-urania slurry had given out-of-pile evidence of a tendency to form deposits, and there was some evidence of similar behavior in-pile.

Interest in the hydriding of Zircaloy-2 prompted the examination of in-pile autoclave corrosion specimens exposed in various experiments to radiolytic gas and oxygen or deuterium atmospheres.

14.2.2 Exposure of In-Pile Experiment L5Z-152S

Operation.--In-pile Zircaloy-2 autoclave experiment L5Z-152S was loaded with thoria-urania slurry at a concentration of 1080 g Th per kg of D_2O, with 7.9 wt % enriched uranium with respect to thorium, and 0.0006 m Pd added as a recombination catalyst. At an assumed flux in LITR beam hole HB-5 of 1×10^{13} neutrons/cm^2·sec, the fission power density in the autoclave in the fully inserted position was 20 w/ml at 280°C. The experiment was operated at 280°C out-of-pile for 673 hr, and in-pile for 65 hr, of which 42 hr was irradiation time.

A 60-psi overshoot during the initial heatup out-of-pile to 280°C led to examination of the location of the slurry in the autoclave at temperature by gamma-ray radiography. This revealed that a tenacious slurry plug was formed in the lower end of the autoclave when it was heated up to 280°C in one step without rocking. It was further shown that the slurry remained suspended when the autoclave was heated in 30°C steps, each followed by 5 min of rocking (36 cycles/min rather than 19).

After insertion into LITR beam hole HB-5, the autoclave was irradiated 17 hr (overnight) in the fully retracted position (flux, 3% of 1×10^{13} neutrons/cm^2·sec) before being moved into the fully inserted position. After 5 hr of smooth operation in this position, the temperature indication of the internal thermocouple rose from 280 to almost 300°C, and the experiment was retracted. A deposition of thoria - enriched-urania slurry around the thermowell was suspected. The following day, during a reactor shutdown, the autoclave was cooled to 25°C; and slow response of the Baldwin pressure cell to the pressure changes involved implied a partial plug in the 20-mil-ID capillary connecting tubing. A brief insertion at 280°C, during subsequent reactor operation, to a flux of 15% of fully inserted flux confirmed this, although no unusual temperature effects associated with the thermowell were observed. The experiment was terminated after pressure readings were obtained at 25°C.

Catalyst Performance.--From two of the three step-wise insertion experiments, total radiolytic-gas pressures of 220 and 140 psi in the fully inserted position were estimated. Based on a fission power density of 20 w/ml, catalyst performance indices of 14 and 21 w/ml per 100 psi D_2, respectively, resulted. The disparity of the two values might be a result of wide temperature oscillations that the autoclave experienced on insertion due to the large shifts in load of the heater-cooler.

Postrun Observations.--When the autoclave was dismantled, no loss of D_2O from the autoclave during the high-temperature operation was indicated by slurry samples recovered. Also, no significant deposits of slurry were observed around the thermowell of the autoclave, although a deposition of slurry had been suggested by the rapid rise in temperature of the internal thermocouple during the fully inserted irradiation. However, a light, chalky coating of slurry was observed on the weld at the base of the thermowell, which extended approximately one-fourth the length of the thermowell down from the weld region, indicating that deposition of slurry around the thermowell may have been an ephemeral occurrence.

14.2.3 Corrosion in Experiment L5Z-152S

Time and Radiation Effect on Generalized Corrosion.--Generalized corrosion in Zircaloy-2 autoclave experiment L5Z-152S was followed in the usual way from the decrease in oxygen pressure as determined from gas measurement during reactor shutdowns at 25°C (refs 3 and 4), and the results from this experiment are presented in Fig. 14.6. During the initial 25 hr of pre-irradiation operation, a

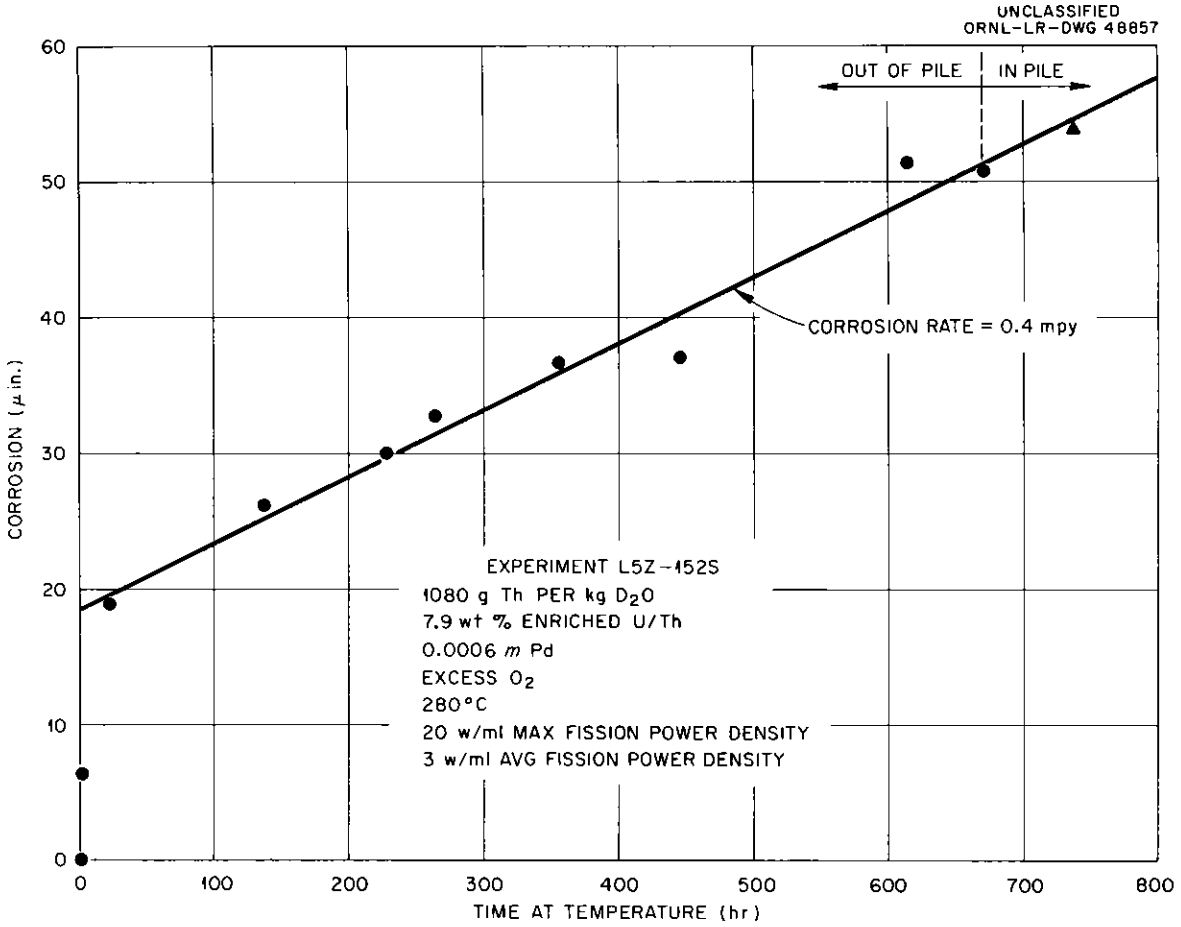

Fig. 14.6. Radiation Corrosion of Zircaloy-2 Autoclave by Thoria-Urania Slurry.

fairly rapid decrease in oxygen pressure, equivalent to a corrosion of 19 μ in. was observed. This initial consumption of oxygen may have been due, in part, to an oxidation of uranium in the slurry. Thereafter, the corrosion appeared to be linear with time, with the average corrosion rate observed being 0.4 mpy. No appreciable response to irradiation during the short in-pile period was indicated.

Coupon Corrosion Specimens.--The corrosion results of coupons, determined by weight lost, in experiment L5Z-152S are presented in Table 14.2. The Zircaloy-2 specimens lost weight in the experiment, and corrosion rates were calculated from the loss without correction for zirconium oxide remaining on the specimen. Consequently, the values given represent a minimum estimate of attack, and the true corrosion was undoubtedly greater. Gains in weight are usually experienced with Zircaloy-2, and attack is calculated by attributing such gains to the formation of oxide corrosion product.

14.2.4 Hydrogen Pickup in Zircaloy-2 Specimens from Previous Experiments

Results of hydrogen pickup by Zircaloy-2 corrosion pin specimens exposed at 280°C in Zircaloy-2 autoclaves containing thoria or thoria-urania are presented in Table 14.3. With the exception of control experiment Y6Z-128S, the experiments were irradiated in the HB-6 facility of the LITR. No significant

Table 14.2. Radiation Corrosion of Coupon Specimens in Zircaloy-2 Autoclave Experiment L5Z-152S

Temperature, °C	280
Concentration of slurry, g Th per kg D_2O	1080
Wt. % enriched U, with respect to Th	7.9
Concentration of catalyst, m of Pd	0.0006
Atmosphere	Excess O_2
Type of autoclave	Zr-2
Hours at temperature out-of-pile	673
Total hours at temperature	738
Hours irradiated	42
Effective fraction of full irradiation time, fully inserted flux	0.151
Assumed flux, neutrons/cm^2·sec (in the fully inserted position)	1×10^{13}
Maximum power density, w/ml, at 280°C	20
Average power density while irradiated, w/ml, at 280°C	3
Autoclave generalized corrosion,[a] μ in.	
Out-of-pile	51
Total	54
Coupon-specimen corrosion, μ in. (Based on weight loss)	
Zircaloy-2[b]	13, 17
Type 347 SS	28
Titanium-75A	29

[a]Based on oxygen measurements.
[b]In a number of experiments Zircaloy-2 has been observed to gain in weight as a result of in-pile exposure. Consequently, the above Zircaloy-2 figures represent the least amount of corrosion that could have occurred.

change in pickup of hydrogen by the pin specimens as a result of in-pile exposure or atmosphere is noted, but exposure to high-temperature water quite generally resulted in a small uptake (20 to 110 ppm).

14.3 IN-PILE SLURRY LOOP

14.3.1 Introduction

Test results obtained from operation of a prototype 5-gpm in-pile loop indicate that the loop is now capable of circulating thorium oxide slurries at temperatures at least to 280°C. During the past report period the loop core section was replaced with a coiled-pipe core design which eliminated slurry deposition of thoria previously observed in the core region. A slurry sampling system which will allow samples of the slurry to be removed from the loop during in-pile operation was designed and satisfactorily tested in a mockup facility.

Operation of the loop with a thorium oxide slurry containing 1/2 wt % enriched uranium, which is the material proposed for use in-pile, and measurements of the recombination kinetics and stability of a palladium catalyst during

Table 14.3. Hydrogen Pickup In Zircaloy-2 Autoclaves

Expt.	Thorium (g/kg D_2O)	Uranium (g/kg D_2O)	Atmos.	Hrs. at Temp.	Hrs. Irrad.	Avg. Fis. Power Density (w/ml)	Total Corr. Based on Gas Meas. (μ in.)	Zr-2 Spec. No.	Zr-2 Item No.	Spec. Corr. (μ in.)	Hydrogen After Exposure (ppm)[a]	Hydrogen Pickup (ppm)[a]
L6Z-122S	990	5	O_2	1074	765	0.6	105	L	1212	35	120	60
								M	1212	44	130	70
L6Z-125S	950	5	D_2	1232	1044	0.5	62	L	1212	118	160	100
								M	1212	94[b]	120	60
L6Z-126S	980	50	D_2	314	140	1.8	53	L	1212	55	130	70
								M	1212	40[b]	170	110
L6Z-127S	400	20	O_2	1122	732	0.8	100	M_1	1215D	104	150	40
								M_2	1215D	8[b]	140	30
Y6Z-128S	410	20	O_2	1143	0	0	33	M_1	1215D	6[c]	160	50
								M_2	1215D	0[c]	130	20
L6Z-129S	1090	54	O_2	1660	1260	3.2	175	S_2	1215G	145[b]	210	90

[a]Hydrogen content expressed as ppm H with no distinction between H and D atoms.
[b]Un-defilmed specimen.
[c]Specimen corrosion based on weight loss here; all others based on weight gain.

this run indicate that the loop is satisfactory for in-pile operation with this slurry.

Based on these test results as well as more than 4000 hr out-of-pile loop operation which have been accumulated during the in-pile slurry loop development program, an in-pile loop has been fabricated and is now being tested out-of-pile.

14.3.2 Slurry Circulation

Following run 4, previously reported,[5] the velocity in the core section was increased from 4 to 6 fps by incorporating a coiled-pipe core section (described below) in the loop. For run 5 the thoria used was of the same batch as for run 4 (DT-18 with 1/2 wt % uranium) except it was refired to 1500°C (from 1225°C) in an attempt to reduce or eliminate the particle-size degradation which occurred during pumping in runs 3 and 4. However, during run 5 the refired DT-18 thoria underwent even more degradation than the slurry previously tested. The mean particle size had decreased from 1.7 to 0.56μ after 650 hr of operation at 280°C, with slurry concentrations ranging from 450 to 900 g of Th per kg of D_2O. However, during run 5 no thoria deposition occurred in the core section as previously observed,[6] and the circulating-slurry concentration as determined from samples removed from the loop was in good agreement with that calculated from the thoria inventory. Run 5 was terminated after 870 hr because of pump overheating.

The pump was replaced, and for run 6 the loop was charged with thorium oxide, batch DT-22, containing 1/2 wt % enriched uranium, which is the material proposed for use in the first in-pile loop experiment. After 700 hr of circulation at 280°C, this thoria has undergone much less particle-size degradation than other slurries previously tested in this loop. The mean particle size has decreased from 1.9 to 1.6μ . The activity of the palladium recombination catalyst has also remained more stable than in other runs, as discussed in Sec. 14.3.10.

The loop was initially charged with sufficient slurry to give a circulating concentration of 1400 g of Th per kg of D_2O; slurry samples removed during the run, which are replaced with D_2O, have reduced this to 700 g of Th per kg of D_2O. Analyses of these samples indicate that all thoria in the loop is in circulation. Periodic radiographic examination of the core section shows that there is no thoria deposited there.

14.3.3 Core Section

The core section which had been used through run 4 is similar to that of the ORR in-pile solution loop.[7] This core geometry and flow rate (2 to 4 fps) allowed settling and resultant loss of thoria from the circulating stream.

Following run 4, the core was replaced with one fabricated from 1/2-in. sched-40 pipe as shown in Fig. 14.7. This type of core was designed to improve core geometry for fluid flow and to increase the flow velocity to~ 6 fps to prevent slurry settling. The particular configuration used was the result of several considerations: (1) to provide sufficient volume (300 cc) to expose an appreciable fraction (35%) of the slurry to maximum neutron flux, (2) to provide space for corrosion test specimens, and (3) to fit within the dimensions of the existing loop-container jacket.

A mockup of the coiled-pipe core section was installed in the prototype loop prior to run 5, and no deposition of slurry in this core has occurred in more than 1500 hr of slurry operation.

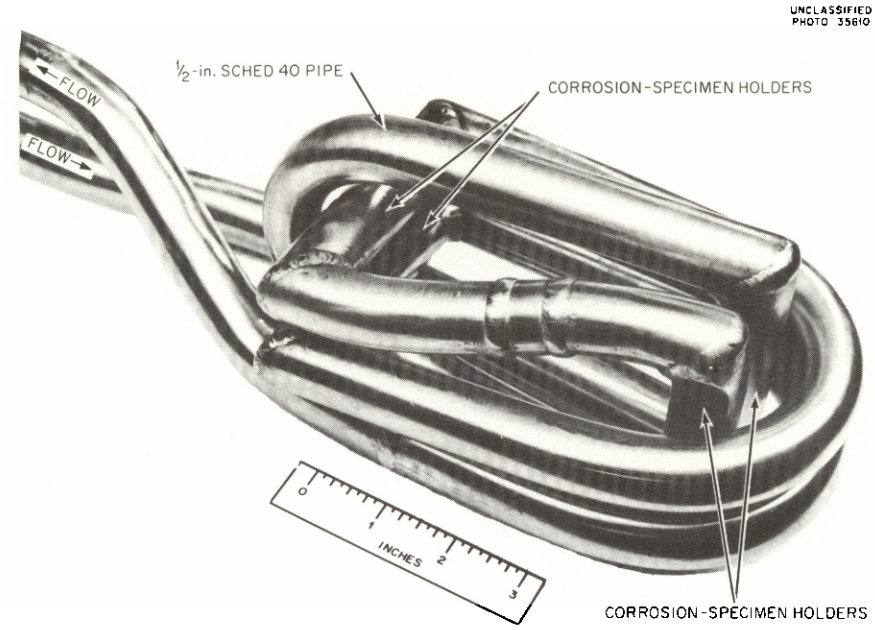

Fig. 14.7. Coiled-Pipe Core for the In-Pile Slurry Loop.

14.3.4 Corrosion Test Specimens

Corrosion test specimens of Zircaloy-2, type 347 stainless steel, titanium 45A, and titanium 110AT are incorporated in the coiled-pipe core section. These specimens are in the form of flat plate coupons 5/8 in. x 1/4 in. x 1/16 in. thick, and eight test coupons are located in each of the six holders (a total of 48 specimens).

The coupons form a continuous septum through the center flow channel of each holder, and holders with flow velocities of 22 and 8 fps are located in the high- and low-flux regions of the core and in the pump discharge line in order to obtain information on the effect of reactor irradiation on corrosion by thorium oxide slurry.

14.3.5 Circulating Pump

The 5-gpm canned-rotor pump used in the in-pile slurry loop is equipped with aluminum oxide bearings and journal bushings and is identical to the pump used in the in-pile uranyl sulfate solution loops.[8] After 3500 hr of operation in the prototype slurry loop, the pump was removed because of excessive temperature and noisy operation. Inspection revealed that the bearings and journal bushings were worn. Considering that a portion of the pump operation was without bearing purge, which allowed thoria to enter the bearing region, the pump performance was excellent, and a 3500-hr operating life is considered more than adequate for a first in-pile loop experiment. Visual examination of the pump impeller and impeller housing revealed no excessive corrosion or erosion.

14.3.6 Slurry Filter

The sintered-metal filter of 8-μ mean pore diameter used to provide thoria-free filtrate for the pressurizer feed and pump purge continues to perform satisfactorily after more than 4200 hr of operation with thorium oxide slurries at concentrations to 1400 g of Th per kg of D_2O and at temperatures to 280°C.

14.3.7 Over-All Loop Corrosion

Over-all loop corrosion rates for runs 4, 5, and 6 in the prototype in-pile loop, L-2-26S, have been low. More than 2100 hr of slurry operation was accumulated in these three runs. All runs were at a loop temperature of 280°C, in an oxygen atmosphere, at a flow rate of ~8 fps in the main loop stream, and with thoria concentrations of from 450 to 1400 g of Th per kg of D_2O. Stainless steel corrosion was calculated from analyses of chromium content of the slurry and from oxygen consumed, and the following over-all loop stainless steel corrosion rates (based on the superficial loop area contacted by circulating slurry) were obtained. The low corrosion rate was qualitatively confirmed by visual inspection of the pump impeller and housing following run 5.

Run Number	Thoria Concentration (g Th/kg D_2O)	Time (hr)	Corrosion Rate (mpy)	
			Chromium in Slurry	Oxygen Consumed
4	550-800	1500	0.5	0.4
5	450-900	870	0.6	0.7
6	700-1400	700	0.1	0.3

14.3.8 Sampling System

A sampling system designed to remove slurry samples from the loop while operating in-pile has been fabricated and tested in conjunction with out-of-pile operation of loop L-2-26S. This system consists of a sample tank interconnected with the loop through valves and capillary tubing. The sampler is capable of removing 15-ml samples of slurry from the loop main stream. The quantity removed is replaced with D_2O in order to maintain a constant D_2O inventory in the loop.

The sampling system has performed quite satisfactorily in removing 21 slurry samples from loop L-2-26S, and the thoria concentration of these samples has not deviated more than 10% from that calculated from the loop inventory of thoria and D_2O. There has been no incidence of plugging of any of the sampler valves or lines to date.

14.3.9 In-Pile Slurry-Loop Package

The first slurry loop, L-2-27S, scheduled for in-pile operation has been fabricated and is now undergoing out-of-pile tests. The loop is designed for operation to 300°C and 2000 psia; it contains an ORNL 5-gpm canned-rotor pump with aluminum oxide bearings and journal bushings, a type 347 stainless steel sintered-metal filter, a coiled-pipe core section (Fig. 14.7), pressurizer, and a heater. Figure 14.8 is a drawing of the loop, which also shows the loop-container jacket and beam-hole liner. The sintered-metal filter provides a thoria-free filtrate which is used as a pressurizer feed stream and a pump-bearing purge.

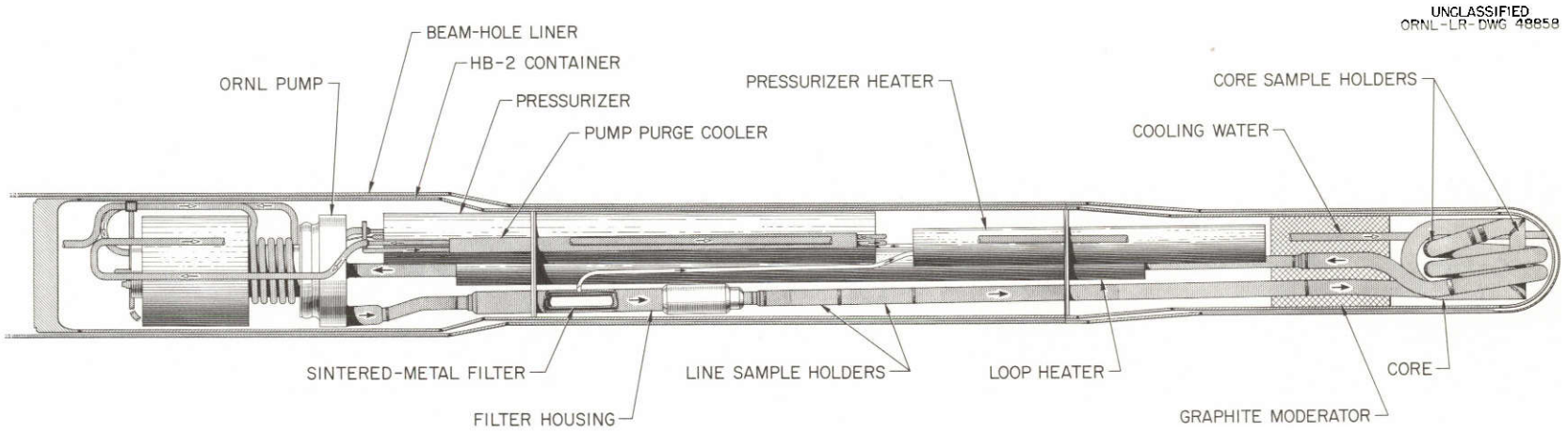

Fig. 14.8. Slurry In-Pile Loop.

The loop contains corrosion test specimens of Zircaloy-2, type 347 stainless steel, titanium 45 A, and titanium 110AT in the core and in the pump discharge line. For the pump output of 5.5 gpm, the slurry flow rates in the loop are: loop piping, 9 fps; core, 5.8 fps; corrosion specimen holders, 8 and 22 fps.

14.3.10 Catalysis Studies

The study of the activity and stability of palladium catalysts for the recombination of radiolytic gas in an in-pile slurry loop continued in a series of tests made with each of three different slurry preparations. These were performed in conjunction with the out-of-pile development runs in the prototype loop.[9]

The first series of tests, in loop run L-2-26S-4, made with a slurry prepared from batch DT-18 thoria - 0.5% urania (1250°C-calcined), have been described[10] previously in part. Additional data are presented here in graphical form, together with data from runs involving two additional thoria-urania preparations: batch DT-18, refired at 1500°C, used in loop run L-2-26-5; and batch DT-22, used in loop run L-2-26-6, which was prepared in a manner identical to DT-18, fired at 1250°C, but containing highly enriched uranium. Batch DT-22 is to be used in the actual in-pile test.

The procedure[11] for measuring the catalytic activity consisted of the rapid injection of a quantity of D_2 gas into the pressurizer vapor space while the loop operated with oxygenated slurry at 280°C, followed by observation of the rate and manner of pressure decay.

The gross recombination rate varied with the catalyst loading. To correct for variations in palladium concentration during the course of a run, due to sampling of the constant-volume system, the behavior of the catalyst was expressed as specific catalytic activity. Specific catalytic activity was defined as the rate of recombination in moles of D_2 per hour, at 100 psi partial pressure of D_2, per gram of palladium in the loop. This is a good unit for describing the effect on in-pile radiolytic-gas equilibrium pressure, since as solids are removed from the loop, gas generation and recombination will vary in the same proportion.

The catalyst activity varied with palladium circulation time. Data for the various runs are plotted in Fig. 14.9. It may be seen that a general decline in catalyst activity occurred as circulation was continued. This was most rapid in run L-2-26S-5 using the 1500°C-calcined thoria. It is perhaps significant that this run also showed rapid degradation in particle size (see Sec. 14.3.2). Batch DT-22, to be used in-pile, showed in run L-2-26S-6 the highest stability of all, requiring over 600 hr to lose half its activity. The radiolytic-gas generation rate for the in-pile experiment was estimated[12] as 0.06 to 0.08 moles of D_2 per hour. It has been concluded that sufficient activity may be achieved and maintained by the palladium catalyst to permit the in-pile experiment to be operated without requiring unduly frequent supplemental additions of catalyst. About 1 g of palladium will be loaded initially.

REFERENCES

1. I. Spiewak and J. A. Hafford, Abrasion Test of Thoria Pellets, ORNL CF-54-3-44 (March 9, 1954).

2. Max Leva, Fluidization, p 169-178, McGraw-Hill, New York, 1959.

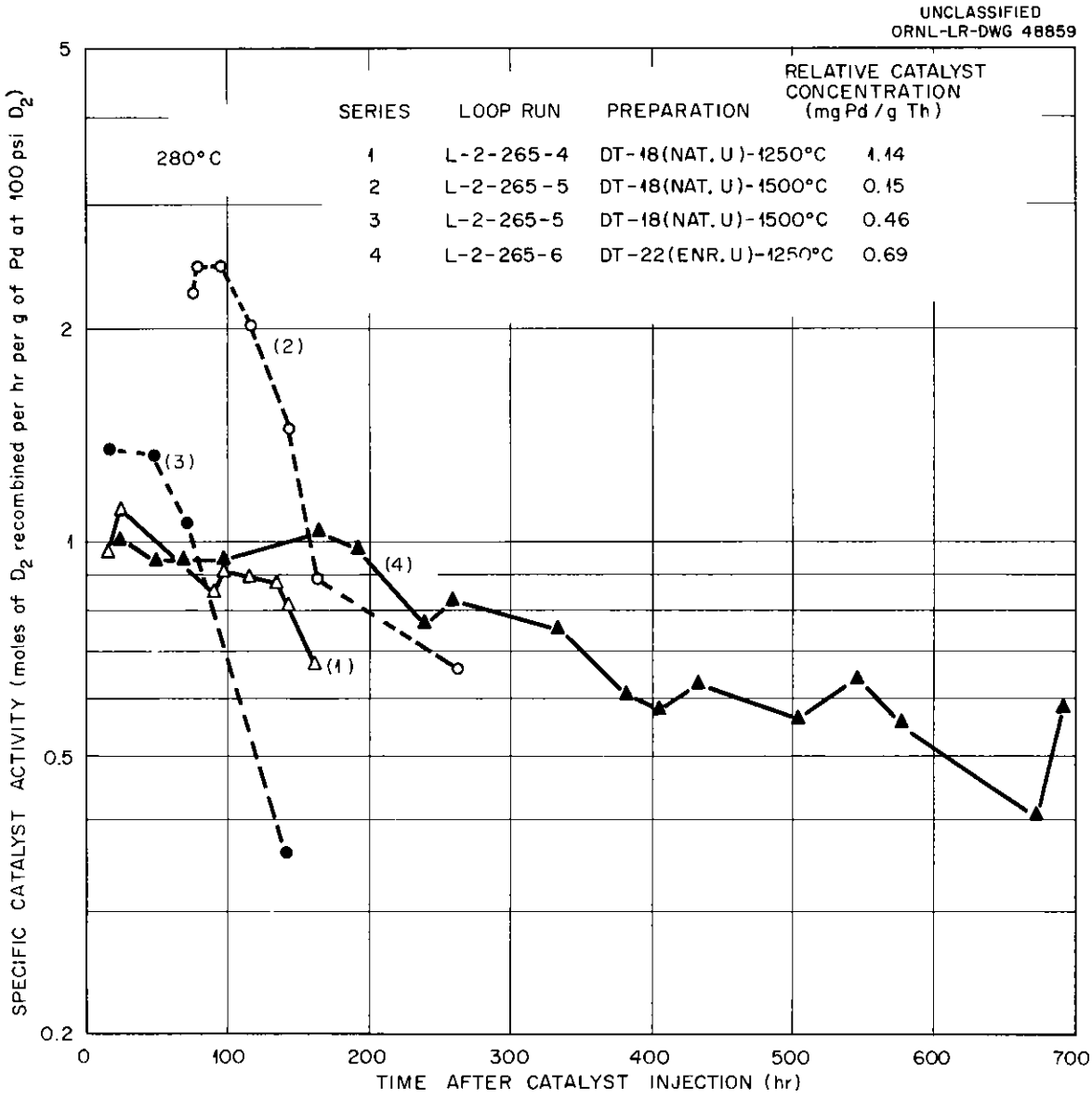

Fig. 14.9. Effect of Circulation on Palladium Recombination-Catalyst Activity in Slurry In-Pile Loop Mockup.

3. E. L. Compere et al., HRP Quar. Prog. Rep. Jan. 31, 1958, ORNL-2493, p 113.

4. K. S Warren and R. J. Davis, In-Reactor Autoclave Studies - LITR. I - Outline of Methods and Procedures, ORNL CF-57-5-110.

5. H. C. Savage et al., HRP Quar. Rep. Jan. 31, 1960, ORNL-2920, p 108-110.

6. Ibid., p 109.

7. H. C Savage et al., HRP Quar. Rep. Oct. 31, 1958, ORNL-2654, p 165, Fig. 15.5.

8. H. C. Savage, Sintered Alumina as a Pump Bearing and Journal Material, ORNL CF-57-11-122 (Nov. 26, 1957).

9. E. L. Compere et al., HRP Prog. Rep. for Periods Ending July 31 and Oct. 31, 1959, ORNL-2879, p 205.

10. E. L. Compere et al., HRP Quar. Prog. Rep. Jan. 31, 1960, ORNL-2920, p 108.

11. Ibid., p 111.

12. E. L. Compere et al., HRP Prog. Rep. for Periods Ending July 31 and Oct. 31, 1959, ORNL-2879, p 208-209.

Part V

FUEL MANUFACTURE

15. THORIUM OXIDE PREPARATION

O. C. Dean P. A. Haas

C. C. Haws A. T. Kleinsteuber
K. O. Johnsson J. W. Snider

15.1 PREPARATION OF THORIUM OXIDE PELLETS

For the pebble-bed blanket, thoria spheres 0.20 to 0.25 in. in diameter and of sufficient strength to resist attrition under reactor conditions are required. Various oxalate powders, binders and lubricants, granulation and pressing techniques, and firing temperatures were investigated for making small batches of rounded thoria pellets that would meet the above requirements. Aluminum or thorium nitrate additives were developed for strenthening and densifying weak pellets of low density.

15.1.1 Preparation of Thoria Spheres for the Pebble Blanket

Five-kilogram batches of pellets are desired for initial feasibility studies. A tentative spouting-bed test to determine resistance to attrition has been established (Sec. 14.1). After exposure of ten test pellets in this test apparatus for 2 to 5 hr, a somewhat uniform hourly weight loss is established. To be of interest, pellets should uniformly lose less than 1%, and preferably less than 0.5% of their original weight.

By use of a variety of powders, granulation procedures, binders, lubricants, forming pressures in the Stokes model E automatic press, and final firing temperatures, about 20 preparations were made from oxalate-precipitated thoria powders. Only three of these batches had sufficiently high resistance to attrition in the spouting bed to be of interest for further testing: preparations P-35, P-36 and P-39 (see Table 15.1). The properties of powders used in pellet preparation are shown in Table 15.2.

The best ceramic powder used was LO-38 P-1, precipitated under oxalate-deficient conditions at 70°C, digested 1 hr, and washed three times on the filter with deionized water at 70°C. The oxalate was calcined by increasing the temperature to 180°C for 1.5 hr, to 380°C for 0.5 hr, and then to 800°C for 1 hr. Powder LO-38 P-2 was precipitated and washed by the same procedure but was fired at 800°C for 4 hr instead of 1 hr. Pellets formed from this powder had markedly less green strength and less resistance to attrition when fired than those made from LO-38 P-1. A blend of P-1 and P-2 powders was less satisfactory than the P-1 alone. The blend of well-crystallized powders (30% DT-83 and 70% DT-73) was almost as satisfactory as the LO-38 P-1 when fired to 1000°C for 1 hr prior to pellet fabrication. The blend was significantly superior to either powder alone.

Wide particle-size distribution, which is a function of firing temperature, appears to be necessary for a good ceramic-grade powder. Powders fired below 800°C produced pellets that cracked on firing at 1750°C or were brittle, and those fired above 1000°C (DT-78-1400) produced poorly sintered powder, leading to a porous product.

Table 15.1. Fabrication Conditions and Properties of Some Thoria Sphere Preparations Formed from Oxalate-Precipitated Thoria Powders in a Stokes Model E Automatic Tablet Press

Pellet Batch No.	Powder[a]	Binder-Lubricant	Additive to Pellet Before Firing	Final Firing Temp. (°C)	Density (g/cc)		Spouting Bed Loss (wt %/hr)	
					As Pressed	As Fired	Initial	Final
P-35	Blend, 30% DT-83, 70% DT-78, fired 1000°C, 1 hr	5% Al stearate[b] (3.4% Al)	None	1750	5.82	9.64	2.1	0.43
P-36	LO-38 P-1	5% Al stearate (3.4% Al)	None	1750	4.51	9.67	1.2	0.25
P-39	Blend, 80% LO-38 P-1 and 20% LO-38 P-2	5% Al stearate (3.4% Al)	None	1750	4.80	9.70	2.9	0.60
P-45	Davison, ceramic grade, 800°C-fired	1% PVA[c] in kerosene	None	1450	----	5.05	30.2	21.5
P-46	Davison, ceramic grade, 800°C-fired	1% PVA in kerosene	None	1750	----	6.01	10.6	6.4
P-48	Davison, ceramic grade, 800°C-fired	1% PVA in kerosene	Diban[d]	1750	----	7.42	1.2	0.83
P-49	Davison, ceramic grade, 800°C-fired	1% PVA in kerosene	Thoria sol[e]	1200	----	5.61	25.5	24.3
P-50	Davison, ceramic grade, 800°C-fired	1% PVA in kerosene	Thoria sol	1750	----	6.74	3.5	1.8
P-51	Davison, ceramic grade, 800°C-fired	1% PVA in kerosene	2 M $Th(NO_3)_4$	1200	----	5.48	18	15.7
P-52	Davison, ceramic grade, 800°C-fired	1% PVA in kerosene	2 M $Th(NO_3)_4$	1750	----	6.62	6.6	3.5

[a] See Table 15.2 for properties of powder.

[b] Aluminum stearate prepared by the reaction of aluminum chloride with 100% excess stearic acid in isopropyl alcohol, followed by water precipitation and washing to remove HCl.

[c] Polyvinyl alcohol.

[d] Dibasic aluminum nitrate solution, 5 M aluminum NO_3/Al ratio = 1.2.

[e] Ammonia-neutralized to NH_3/Th = 3/1; 1.7 M thorium.

Table 15.2. Properties of Thorium Oxide Powders Used in Preparation of Thoria Pellets

Powder No.	Firing Temp. (°C)	Firing Time (hr)	Surface Area (m^2/g)	Crystallite Size (Å)	Average Particle Size (μ)	Percentage of Particles >10 μ	Size Distribution (σ_g)
DT-83	650	4	24.9	132	0.9	0.08	1.36
DT-78-650	650	4	21.5	135	6.3	36.4	1.28
DT-78-1400	1400	4	0.69	2500	7.9	10	1.31
LO-38 P-1	800	4	21.2	146	7.0	20	~0.5
LO-38 P-2	800	4	16.9	196	7.2	39	~2.5

Relic weakness appears to be important because it sets the limits of pressing pressures usable. The LO-38 P-1 powder had relatively weak relics which broke down at pressures greater than 8000 psi and permitted close packing for good sintering conditions. It was probably nearly ideal for the production of cylindrical pellets, where pressing pressures were uniform over the cross section of the punch faces. When pressing pressures were not uniform, as with the formation of spherical pellets, or were higher than 1200 psi, planes of slip developed which led to formation of laminar cracks. The cracks in spherical pellets invariably appeared at the junction of the hemisphere with the cylindrical section. When higher-strength powders were pressed (P-35, Table 15.1), greater pressures were required to form strong green pellets. A blend of strong and weak powders (DT-83 with DT-78-1400) showed minimum cracking in spherical pellets. An attempt to reproduce LO-38 P-1 powder by complete oxalate precipitation resulted in a powder with the characteristics of DT-78. It is thought that nitrate occluded on LO-38 P-1 powder prior to firing was important in furnishing its special properties.

Granulation of the powder prior to pressing is essential in developing the good flow properties necessary to uniform filling of the die and uniform density of the green pellet. The procedure involves applying uniformly a small percentage of binder and/or lubricant to the powder, pressing, light grinding, and sieving. The conventional binders, polyvinyl alcohol (PVA) and carbowax, were used with or without kerosene as a die lubricant. Stearic acid, thorium stearate, and aluminum stearate were also used. Aluminum stearate gave the best results with powders having weak relic structures. The presence of aluminum appeared to strengthen and vitrify the fired pellets. It is known that alumina and thoria form a liquid at 1750°C, which is a likely reason for the strengthening effect.

The aluminum stearate was prepared by dissolving aluminum chloride and 100% excess of stearic acid in anhydrous isopropyl alcohol and then adding water to precipitate it. Water-washing removed chloride, and the vacuum-dried residue was redissolved in isopropyl alcohol for application to the thoria powder. Five weight percent aluminum stearate in sufficient isopropyl alcohol to wet the whole powder mass was added to the thoria, and the mixture was thoroughly stirred. The isopropyl alcohol was evaporated under vacuum at 80-90°C. The powder was pressed at less than 8000 psi and then screened through a 20 mesh sieve three times. After being rolled for a few minutes, the powder was ready to press in the Stokes automatic press. The amount of aluminum in the aluminum stearate was 3.4 wt %, and application of a 5% solution added

0.17 wt % aluminum to the thorium. Smaller amounts of aluminum stearate were tried but with less satisfactory results.

In order to find reasons for the existence of preferred planes of weakness in spherically pressed thoria pellets which led to cracked fired pellets, the granulation step was studied briefly. Powders that had poor flow properties produced weak pellets most likely to contain cracks. Bridging would occur, preventing uniform filling of the die, and the fired pellets had large voids. When polyvinyl alcohol, stearic acid, or stearate soap binders were used in granulation, powders flowed poorly if 20% of the granules were below 80- to 100-mesh U.S. Sieve size.

In an alternative granulation technique, oxalate powders fired to 650°C were treated with 2 M thorium nitrate solution or 2 M and 16 M nitric acid to disperse the relics. The resulting sols were dried at 100 to 165°C and ground lightly. When fired to temperatures above 470°C, hard granules were produced. This granulated powder was pressed to strong pellets having high densities (5.8 to 6.6 g/cc), which then were fired at 1750°C to strong pellets having densities of 8.3 to 8.5 g/cc. Quantitative data on attrition resistance are not yet available, but the pellets resisted breakage and chipping in a bottle shake test. This method of granulation has the advantage of working equally well for all oxalate powders fired below 800°C.

15.1.2 Davison Thoria Spheres

Five kilograms of thoria spheres were prepared by the Davison Chemical Company and delivered for evaluation. The pellets were made from a ceramic-grade thoria prepared from low-temperature-precipitated thorium oxalate which was then fired to 800°C. The powder was granulated with 1% PVA and lubricated with 0.5% kerosene. The pellets were formed by extremely light pressing in a Stokes spherical ball-face die modified by Davison and were then fired to 1450°C. These pellets were chalky and weak (Table 15.1, P-45). When a sample was fired to 1750°C, the density and strength were greatly improved, but they were still too weak to be of use for the pebble blanket. Filling the pores of the pellets under vacuum with thorium nitrate solution or thoria sol or 5 M dibasic aluminum nitrate (diban) solution followed by drying and refiring to 1750°C increased both density and attrition resistance. The diban treatment gave the most significant improvement (Table 15.1, P-48). Refiring to only 1200°C did not give a significant improvement for any treatment. When the diban treatment was applied to cracked pellets from the P-39 preparation, some increase in pellet strength was also noted.

15.1.3 Pellet-Firing Studies

Data were obtained on the effects of firing time and temperature on the density of ThO_2 pellets. The firings were made in a 2500-w Globar furnace capable of producing temperatures up to 1500°C. Approximately 600 pellets with 5% aluminum stearate binder were made for the tests. The green densities of 32 pellets average 4.62 g/cc and ranged from 4.55 to 4.70 g/cc. Three firings at 1270, 1400, and 1500°C were made in an argon atmosphere. The maximum density obtained for the 1270°C firing was 8.34 g/cc after 23 hr of firing (Fig. 15.1). Melting of the platinum crucibles during the 1500°C firing may have resulted in inaccurate data, as the fired pellets were of poor quality. Pellets taken out at 1470°C while bringing the furnace up to temperature had a density of 9.0 g/cc. In 4 more hours of firing, 2 of which were at 1500°C, the density did not increase.

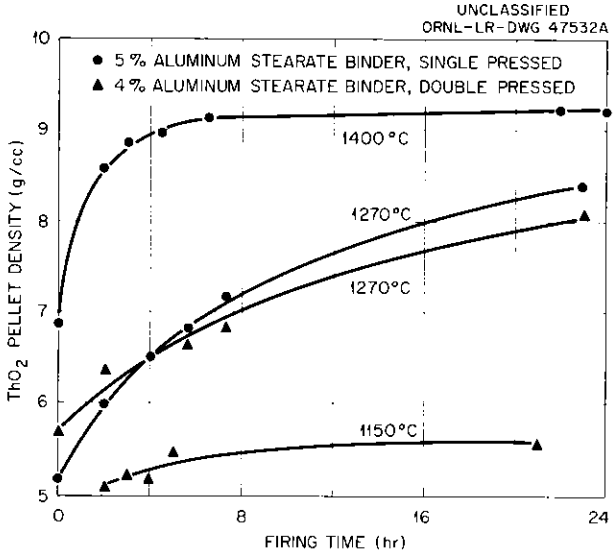

Fig. 15.1. Pellet Density vs Firing Time in Argon Atmosphere.

15.2 PREPARATION OF THORIUM OXIDE POWDER

Present emphasis is on the preparation of spherical flame-calcined thoria particles with a mean diameter of 5 to 8 μ. After completion of the thoria-beryllia run,[1] the entire calcination system was cleaned and the reflector replaced to eliminate any possible spread of beryllium contamination. A study of variables affecting particle size has been undertaken.

Since most of the oxide that has been prepared thus far from the drying and calcining of the alcohol-solution droplets has had a mean particle diameter of 1.0 μ, it was assumed that the torches used were producing liquid droplets of 5 to 10 μ diameter. This estimate was based on the concentration of the feed solution and the assumption of droplet integrity through the firing process. Increasing the size of droplets fed to the combustion zone from 50 μ (containing salt equivalent to a solid of 12 μ dia) to 150 μ (containing salt equivalent to 35 μ dia) had no significant effect upon product particle size. It is thought that explosive subdivision of droplets occurs within the flame and that above some critical size the droplets are mechanically unstable in the flame. Thus, final particle size may only be related to droplet size up to some critical value.

A reduction of maximum reflector temperature from 1600 to 900°C doubled the particle size, from 1.0 μ to 2.0 μ. Substitution of water for methanol as the feed solvent and nitrogen for propane-oxygen as the atomizing gas had no significant effect on particle size.

REFERENCE

1. P. A. Haas, C. C. Haws, and K. O. Johnsson, HRP Quar. Prog. Rep. Jan. 31, 1960, ORNL-2920, p 119; Chem. Tech. Div. Unit Operations Jan. 1960 Monthly Rep., ORNL CF-60-1-49.

Part VI

METALLURGY

16. METALLURGY

A. Taboada

T. M. Kegley, Jr. P. L. Rittenhouse
W. J. Leonard R. L. Stephenson
M. L. Picklesimer A. J. Taylor
C. H. Wodtke

16.1 PHYSICAL METALLURGY OF ZIRCALOY-2

Resistance measurements were made on Zircaloy-2 at temperatures ranging from 100 to 1050°C during continuous heating and cooling cycles at nominal rates of 2, 5, and 10°C per minute. Measurements were also made at the maximum obtainable rates of heating and cooling, approximately 70°C per minute, at a temperature of 800°C. The resistance of Zircaloy-2 (and thus the resistivity) was unaffected at any temperature between 200 and 780°C by heating and cooling rates of 2, 5, or 10°C per minute. The alpha/alpha-plus-beta temperature was 827 ± 1°C on heating at 2, 5, or 10°C per minute, and somewhat greater than 830°C at the maximum rate of heating. The beta/alpha-plus-beta temperature was approximately 980°C on heating at all rates, but the change in resistance with temperature at this temperature is too gradual to permit a more accurate determination of the phase boundary at this time. The beta/alpha-plus-beta temperature determined on cooling was found to vary too greatly with prior thermal history and with soaking time at 1050°C to report at the present time. The alpha/alpha-plus-beta temperature found on cooling was strongly affected by the cooling rate, being 785 ± 1°C for rates of 2 and 5°C per minute, 781 ± 1°C for 10°C per minute, and 760°C ± 3°C for the maximum cooling rate obtainable, approximately 70°C per minute.

Two deviations of the resistance-temperature curve from that expected were observed. In the temperature range from 250 to 450°C, the resistance-temperature curve is abruptly about 2% higher than it should be if the curves above and below this temperature range are extrapolated to meet. The temperature limits of this deviation are shifted by variations in heating and cooling rates, by heating or cooling, and somewhat by prior thermal history. Also, a "bump" in the resistance-temperature curve occurs in the region of the two-phase field (alpha-plus-beta phases), varying in magnitude, temperature range, and temperature limits with heating or cooling cycle, heating and cooling rates, and prior thermal history. Neither observation can be explained by the present knowledge of the physical metallurgy of Zircaloy-2. It is definitely known that hydrogen did not cause either of the "bumps" observed, for the specimen was vacuum-annealed to a content of less than 5 ppm H_2.

Calibration resistivity equipment has been built which will permit the conversion of the resistance-temperature or resistance-time data to resistivity data so that different specimens, alloys, or heat treatments can be compared on a relative basis. The calibration equipment is now being tested.

16.2 ZIRCONIUM-ALLOY DEVELOPMENT

Zirconium-base alloys containing niobium and copper have shown promise in the development of a more corrosion-resistant alloy to replace Zircaloy-2 as the core-tank material for aqueous homogeneous reactors. The information necessary for the development of these alloys is being procured by basic physical metallurgical studies and in-pile corrosion tests. Considerable data have been obtained and reported[1,2] on the beta-quench and reheat transformations.

Transformation kinetics and morphological studies of the Zr-15Nb-1Cu system have been in progress during the past quarter. Both beta-quench and reheat and true isothermal transformations are being studied. It has been established that the transformation sequence occurring on reheating the quenched beta structures is essentially that of the Zr-15Nb binary alloy, but the shape of the TTT curve so far determined is not similar. Apparently, appreciably more omega phase is formed in the ternary alloy during the time required to heat to the aging temperature, causing much higher hardnesses in the early stage of the transformation sequence. The behavior of the ternary alloy is similar to that of the parent binary on isothermal transformations at temperatures at and above 400°C, there being no appreciable hardness increase on transformation. The transformation product appears in the microstructure as a nodule which grows grain by grain, each grain added transforming to a certain stage of completion before a neighboring grain starts to transform.

Transformation kinetics and morphological studies of binary alloys of the Zr-Cu and Zr-Mo systems have been started. Both beta-quench and reheat and isothermal transformations are being studied. Specimens of both alloy systems have been aged or transformed for times of 1/4, 1/2, and 1 hr at temperatures of 400, 500, 600, and 700°C. Hardness data have been obtained, but the data are inconclusive. Further studies at both shorter and longer times are being made. The development of suitable metallographic polishes and etchants has been difficult, but some success for the Zr-Cu specimens has shown a nodular transformation product occurring in the grain boundaries and growing into the grains for those specimens isothermally transformed. No transformation product has yet been delineated for those specimens which have been quenched and aged.

16.3 ThO_2 PELLET FABRICATION

As part of the general program to produce sound, abrasion-resistant, ThO_2 pellets for use as reactor blanket material, an effort was made to study the variables connected with fabricating round-ended pellets from D-40 ThO_2 powder.

Flat-ended pellets were readily produced with densities of 9.3 g/cm^3, by using powder additions of 0.5 wt % CaO and 2 wt % Carbowax. However, when this powder was used for fabricating round-ended pellets, stresses were generated by the upper punch which caused laminations at the transition of the round end and the cylindrical section. This lamination condition was improved by changing the die design and by reducing the forming pressure; however, when the pressure was reduced sufficiently to eliminate laminations the sintered density was lowered excessively.

An attempt to eliminate laminations was made by calcining the powder in order to reduce elastic springback of the pellet material when pressure was released in the pressing operation. In order to retain as high a sinterability as possible, the material was ball-milled after calcination. The tendency to

laminate was greatly reduced when the calcined powders were used; however, it was necessary to control forming pressures. Even powders calcined as high as 1425°C exhibited laminations when the forming pressure was sufficiently high.

Pellets with a variety of composition and fabrication variables have been submitted for testing to determine the combination of manufacturing conditions that will result in maximum abrasion resistance. Both flat-ended and spherical-ended pellets were made from materials calcined at three different temperatures. One set of these contained 0.5 wt % CaO to check the effect of sintered density, while another was pure ThO_2. Half the above specimens were pretumbled to remove easily abraded projections; the duplicate specimens were submitted without rolling. In all, 24 sets of pellets were produced with varying conditions.

16.4 UNDERWATER ARC-CUTTING OF REACTOR SCREENS

The underwater constricted-arc cutting process[3,4] utilizing a special torch was applied successfully in cutting five diffuser screens into strips for removal from the HRT core vessel (see Sec. 1.1.4).

REFERENCES

1. G. M. Adamson et al., HRP Quar Prog. Reps. Oct. 31, 1956, ORNL-2222, p 114-16; Jan. 31, 1957, ORNL-2272, p 119-23; Apr. 31, 1957, ORNL-2331, p 124-28; July 31, 1957, ORNL-2379, p 122-26; Oct. 31, 1957, ORNL-2432, p 131-33; Jan. 31, 1958, ORNL-2493, p 141-43; Apr. 30 and July 31, 1958, ORNL-2561, p 245; Oct. 31, 1958, ORNL-2654, p 188; Jan. 31, 1960, ORNL-2920, p 128.

2. M. L. Picklesimer et al., Met. Div. Ann. Prog. Rep. Sept. 1959, ORNL-2839, p 113-14.

3. G. M. Adamson et al., HRP Quar. Prog. Rep. Apr. 30, 1959, ORNL-2743, p 180.

4. G. M. Adamson et al., Met. Div. Ann. Prog. Rep. Oct. 1959, ORNL-2839, p 131-35.

Part VII

ANALYTICAL CHEMISTRY

17. ANALYTICAL CHEMISTRY

O. Menis H. P. House

C. M. Boyd T. C. Rains
U. Koskela P. F. Thomason
H. E. Zittel

17.1 FLAME-PHOTOMETRIC DETERMINATION OF CALCIUM IN ThO_2

In the preparation of high-density ThO_2 for use in packed and fluidized beds of thermal-breeder reactors, calcium may be added intentionally or inadvertently and must be determined. To provide a simple, yet adequate, method for this determination, flame-photometric methods were investigated even though thorium is known to repress the radiant intensity of calcium. As a consequence, it was established that the extent to which thorium interferes is strongly influenced by the medium in which the ThO_2 is dissolved. In $HClO_4$ solutions, the suppressing effect of thorium on the radiant intensity of calcium at 423 mμ is strikingly less than in either an HNO_3 or HCl solution. When 0.01 N acidic solutions containing 10 μg of Ca and 10 mg of Th per ml were aspirated, the loss in radiant intensity of the calcium in HNO_3, HCl, and $HClO_4$ solutions was 60, 15, and 5%, respectively. For the flame-photometric determination of calcium in the presence of large amounts of thorium, therefore, $HClO_4$ solutions of the ThO_2 are utilized, and calibration curves are established with calcium standards which contain approximately the same amount of thorium as the unknown in an $HClO_4$ medium.

17.2 FLAME-PHOTOMETRIC DETERMINATION OF RARE-EARTH ELEMENTS IN SOLUTIONS OF THORIUM SALTS

Previous studies[1] have revealed that flame photometry can be applied to the estimation of a number of rare-earth elements in mixtures thereof. A further investigation was made to extend the use of flame photometry to the determination of rare-earth elements in solutions of thorium simulating those anticipated upon dissolution of ThO_2-UO_x slurries or solids, following their use in thermal-breeder reactors.

To avoid interference, large quantities of thorium must be removed prior to making the radiant-intensity measurements. Although the conventional reagent, thenoyltrifluoroacetone, is utilized in the extraction of thorium, a significant modification of the extraction procedure has been devised whereby gram quantities rather than a few milligrams of thorium can be removed rapidly in a single extraction. The acidic (nitric, hydrochloric, or perchloric) solution of thorium is adjusted to pH 1.5 with an ammonium acetate - acetic acid buffer of pH 4, after which the thorium is extracted with thenoyltrifluoroacetone in chloroform. As the pH decreases, due to the reaction of thorium with thenoyltrifluoroacetone, additional acetate buffer rather than NH_3 or NH_4OH is added continuously to restore the pH to 1.5. Completion of the extraction is indicated when no further decrease in pH is noted.

By this method, two extractions with 40-ml portions of the chelate solution suffice to remove 2 g of thorium from a nitrate solution. Furthermore, the operation requires only a few minutes, and no difficulty is encountered from precipitate formation. By comparison, about 3 hr was required to remove 1 g of thorium by a continuous extraction method, utilizing NH_3 gas to neutralize the acid formed, and precautions were necessary to avoid difficulty due to precipitate formation.[2]

After removal of the thorium, the ammonium acetate in the aqueous phase is destroyed by heating it with aqua regia. The solution is then adjusted to pH 5, and the rare-earth elements are extracted with 0.1 M thenoyltrifluoroacetone in hexone (4-methyl-2-pentanone), after which they are determined flame-photometrically in the organic extract.

17.3 DETERMINATION OF U(IV) IN ThO_2-UO_x BY DIRECT COULOMETRIC OXIDATION

In the evaluation of slurries of ThO_2 which contain oxides of uranium for use in thermal-breeder reactors, it is necessary to determine U(IV) and U(VI) and also changes in the U(IV)/U(VI) ratio under varying test conditions. This can be accomplished by the indirect coulometric method previously described,[1] if the sample does not contain a significant amount of easily reduced impurities.

To circumvent difficulties encountered in the application of this indirect method, especially in the analysis of impure samples, an investigation was made of a direct coulometric oxidation procedure for titrating the U(IV). As a consequence of this investigation, it was established that the U(IV) can be titrated coulometrically by oxidizing it to U(VI), utilizing a platinum anode at a potential of +1.4 v versus an Ag/AgCl electrode. For samples containing from 1 to 10 mg of U(IV) in 3 M H_3PO_4, the coefficient of variation is 1%. A correction must be applied for the decomposition of water, which occurs to some extent at the high potential utilized in this coulometric oxidation. Chromium(III) does not interfere since it is not oxidized at the potential used, but Fe(II) must be preoxidized at a potential of +0.4 v to prevent its interference.

17.4 DETERMINATION OF FREE ACID IN RADIOACTIVE HRP FUELS

A conductometric method for the titration of free acid in impure uranyl sulfate solutions[3] has been applied to the determination of free H_2SO_4 in radioactive HRP fuels at the High-Radiation-Level Analytical Facility. The free acid is titrated conductometrically in a methanol medium by remote control with NaOH as the titrant. For H_2SO_4 solutions of the order of 0.05 N, the relative standard deviation is less than 3%.

REFERENCES

1. O. Menis et al., HRP Prog. Rep. Oct. 31, 1959, ORNL-2879, p 248.

2. W. Meinke and R. E. Anderson, "Methods for Continuous Extraction with a Chelating Agent," Anal. Chem. 24, 708 (1952).

3. G. Goldstein, Determination of Free Acid in Uranyl Sulfate Solutions by Conductometric Titration, ORNL CF-59-12-32.

OAK RIDGE NATIONAL LABORATORY
HOMOGENEOUS REACTOR PROJECT

SEPT. 1, 1960

PROGRAM DIRECTOR
R. N. BRIGGS — D
A. L. GUNNELS, SEC. — REE

PROGRAM EDITOR
W. D. REEL — TI

DESIGN AND ENGINEERING
R. N. LYON, ASSOCIATE DIRECTOR — REE
P. A. HICKEY,* SEC. — REE

DESIGN
W. R. GALL,** SECTION CHIEF — REE
M. T. LUNDIN,** ASSISTANT SECTION CHIEF — REE
R. C. ROBERTSON** — REE
R. L. CAUBLE** — REE
T. E. HAYNES — REE
J. E. JONES — REE
W. ROBINSON — REE

REACTOR ANALYSIS
P. R. KASTEN,** SECTION CHIEF — REE

REACTOR PHYSICS
M. TOBIAS, GROUP LEADER — REE
D. R. VONDY — REE
H. A. MACCOLL — REE

ENGINEERING RESEARCH
H. W. HOFFMAN,** SECTION CHIEF — REE

AQUEOUS HOMOGENEOUS REACTOR SLURRY STUDIES
D. G. THOMAS — REE
P. N. HAYES** — REE
R. M. SUMMERS** — REE

ENGINEERING DEVELOPMENT SECTION
I. SPIEWAK, SECTION CHIEF — REE
P. N. PEEBLES, ASSISTANT SECTION CHIEF — REE

MAINTENANCE DEVELOPMENT
R. C. HISE, GROUP LEADER — REE
R. BLUMBERG — REE
P. P. HOLZ — REE
T. L. CASTLE — REE
C. JONES — REE

COMPONENT DEVELOPMENT
C. H. GABBARD, GROUP LEADER — REE
J. C. MOYERS — REE
H. R. PAYNE — REE
J. P. HURST — REE
G. A. WINDLE — REE

CORE AND BLANKET DEVELOPMENT
C. G. LAWSON, GROUP LEADER — REE
R. J. KEDL — REE
M. RICHARDSON — REE
R. P. WICHNER — REE
H. J. YOUNG — REE

SYSTEM DEVELOPMENT
L. F. PARSLY, GROUP LEADER — REE
P. H. HARLEY — REE
R. E. CARNES — REE

SLURRY LOOP PROGRAM
O. M. EISSENBERG, GROUP LEADER — REE
A. N. SMITH — REE
J. T. DICKEY — REE
C. A. GIFFORD — REE
H. G. MOORE — REE

INSTRUMENTATION AND CONTROLS
R. L. MOORE,** SECTION CHIEF — I&C

REACTOR I&C SYSTEM DESIGN
J. R. BROWN,** GROUP LEADER — I&C
R. W. BORGERS** — I&C

HRP SUPPORTING SERVICES
H. D. MILLS, GROUP LEADER — I&C
P. G. HERNDON — I&C
R. M. BURNETT — I&C

VALVE DEVELOPMENT AND SPECIFICATION
A. M. BILLINGS,** GROUP LEADER — I&C
B. J. JONES** — I&C

INSTRUMENT DEVELOPMENT AND EVALUATION
D. G. DAVIS,** GROUP LEADER — I&C
T. M. CATE** — I&C

REACTOR MATERIALS RESEARCH
E. G. BOHLMANN, ASSOCIATE DIRECTOR — REE
P. A. HICKEY,* SEC — REE

SOLUTIONS
J. C. ORIESS,** SECTION CHIEF — REE
J. L. ENGLISH** — REE
L. L. FAIRCHILD** — REE
P. D. NEUMANN** — REE
H. L. BARKER** — REE
W. H. HINDS** — REE
B. L. JOHNSON** — REE

BLANKET MATERIALS
E. L. COMPERE, SECTION CHIEF — REE

OUT-OF-PILE STUDIES
S. A. REED — REE
R. B. GALLAMER — REE
R. F. BENSON — REE
J. L. RUTHERFORD* — REE
G. G. WARNER — REE

IN-PILE EXPERIMENTS
A. J. SHOR — REE
L. F. WOO — REE
J. L. RUTHERFORD* — REE

MATERIALS EXPERIMENT ENGINEERING
H. C. SAVAGE, SECTION CHIEF — REE

OUT-OF-PILE OPERATIONS
S. E. BOLT* — REE
T. H. MAUNEY** — REE

100A LOOPS
J. F. WIESSETTE — REE
C. R. BENSON — REE
C. M. BURCHELL — REE

IN-PILE EXPERIMENT FABRICATION
S. E. BOLT* — REE
J. R. HART* — REE
R. W. RAY — REE

IN-PILE SLURRY LOOP
J. M. BAKER — REE
J. R. HART* — REE

REACTOR OPERATIONS
V. A. DECARLO — REE
E. M. GUNN — REE
J. W. MOSER — REE
J. W. MYERS — REE
D. G. PEACH* — REE
C. E. ROBERTS — REE
R. G. ROSS — REE
A. L. SUTTON — REE
W. E. TEICHERT — REE
R. M. WALLER* — REE

SOLUTION MATERIALS RADIATION
G. H. JENKS, SECTION CHIEF — REE

IN-PILE STUDIES
J. E. BAKER — REE
R. J. DAVIS — C
S. H. WHEELER — REE

SUPPORTING RESEARCH
A. L. BACARELLA — C

METALLURGY
A. TABOADA, SECTION CHIEF — M
R. W. COOKE — M
W. J. LEONARD — M
M. L. PICKLESIMER** — M
P. T. RITTENHOUSE** — M
C. H. HOLTKE — M
P. J. JONES** — M
G. C. NELSON** — M
C. M. SMITH — M

METALLOGRAPHY
T. M. KEGLEY,** LEADER — M
E. R. BOYD** — M
B. F. DAY** — M
T. J. HENSON** — M

CHEMICAL TECHNOLOGY
D. E. FERGUSON,** PROBLEM LEADER — CT
J. MAYES, SEC. — CT

CHEMICAL DEVELOPMENT
D. E. FERGUSON,** SECTION CHIEF — CT

OXIDE PREPARATION
O. C. DEAN,** GROUP LEADER — CT
A. T. KLEINSTEUBER** — CT
K. H. McCORKLE** — CT
C. E. SCHILLING** — CT
C. W. GREENE** — CT

THORIUM OXIDE STUDIES
J. P. McBRIDE, GROUP LEADER — CT
L. E. MORSE — CT
P. F. HAYDON — CT
W. L. PATTISON — CT
H. F. SCARD — CT

SURFACE CHEMISTRY
C. H. SECOY, GROUP LEADER — CT
H. F. HOLMES — CT
F. H. SWETTON — CT

DESIGN
W. E. UNGER,** ASSISTANT SECTION CHIEF — CT

TiO_2 DEVELOPMENT AND HRT-CP DESIGN SUPPORT
H. O. WEEREN** — CT

INSTRUMENTATION
C. S. LISSER** — CT

PILOT PLANT
J. C. BREESE,** SECTION CHIEF — CT

THORIUM OXIDE PREPARATION
W. H. E. FAIS,** GROUP LEADER — CT
R. H. WINGET, PROBLEM LEADER — CT

UNIT OPERATIONS
R. A. HAAS,** GROUP LEADER — CT

SLURRY PREPARATION DEVELOPMENT
C. C. HAAS, JR. — CT
K. O. JOHNSON — CT
V. L. FOWLER — CT

CHEMICAL RESEARCH
H. F. McDUFFIE,** ASSISTANT DIRECTOR — RC
T. F. KELLY, SEC. — RC

HETEROGENEOUS EQUILIBRIA IN AQUEOUS SYSTEMS
R. L. MARSHALL,** GROUP LEADER — RC
J. S. GILL** — RC
E. V. JONES** — CONSULTANT
R. SLUSHER** — RC
J. E. SAVOLAINEN** — RC

REACTIONS IN AQUEOUS SOLUTIONS
G. M. WATSON,** SUPERVISOR — RC
W. J. KELLY,** GROUP LEADER — RC
D. R. CUNEO** — RC
L. D. GILPATRICK** — RC
M. D. SILVERMAN** — RC
H. H. STONE** — RC

ANALYTICAL CHEMISTRY
MYRON T. KELLEY,** DIRECTOR — AC
C. D. SUSANO,** ASSOCIATE DIRECTOR — AC
K. A. COOK,** SEC. — AC
H. E. ZITTEL,* COORDINATOR, NRP ANALYTICAL CHEMISTRY — AC

CORROSION ANALYTICAL LABORATORY
D. MENIS, SECTION CHIEF — AC

RESEARCH
H. E. ZITTEL,** GROUP LEADER — AC
C. M. NOYD — AC
D. L. MANNING, GROUP LEADER — AC
G. GOLDSTEIN — AC

DEVELOPMENT AND SPECIAL ANALYSES
T. C. RAINS, GROUP LEADER — AC
W. R. FERGUSON — AC

SERVICE
C. K. TALBOTT, SUPERVISOR — AC
T. P. BACON — AC
W. D. CLIFF — AC
C. A. CLARK — AC
P. S. GOODWIN — AC
E. DAST — AC

SPECTROCHEMICAL SERVICES
C. FELDMAN,** SUPERVISOR — AC
W. R. MUNOZ** — AC
A. H. MARSHALL** — AC
J. A. NORRIS, GROUP LEADER — AC
J. J. MUNDZAK — AC

HRT AND IN-PILE LOOP ANALYSES
L. KOSKELA, SUPERVISOR — AC
C. F. BAKER — AC
S. R. DINSMORE — AC
R. E. HAGA — AC
F. K. HEATH — AC
W. S. McDONOUGH — AC
J. L. SHARP — AC
H. L. WERR — AC
A. D. WILSON — AC

RADIOCHEMICAL ANALYSIS
E. I. WYATT,** SUPERVISOR — AC

HRT DEVELOPMENT
P. F. THOMASON,** GROUP LEADER — AC
R. E. BROOKS** — AC
T. J. MILLER** — AC
S. A. REYNOLDS,** GROUP LEADER — AC
J. D. REDMOND** — AC
T. H. HANDLEY** — AC
A. S. OLSON** — AC

HIGH RADIATION LABORATORY
L. D. FERRARA,** SUPERVISOR — AC

NUCLEAR ANALYSIS LABORATORY
D. A. [illegible],** GROUP LEADER — AC
C. E. BATEY** — AC
R. A. HANSEN** — AC

OPTICAL AND ELECTRON MICROSCOPY
C. E. ALLEWELDT,** GROUP LEADER — AC

HOMOGENEOUS REACTOR TEST
S. E. BEALL, PROJECT ENGINEER — REE
B. EUBANK, SEC. — REE
D. SCOTT, JR., SPECIAL ASSIGNMENT — REE

J. W. HILL, JR., ASSISTANT SECTION CHIEF — REE
H. F. BAUMAN, SPECIAL ASSIGNMENT — CT
J. R. BUCHANAN, ASSISTANT FOR PLANNING — CT
R. H. GUYMON, CHIEF OF OPERATIONS — CT
J. D. JONES — REE
R. J. HARVEY, SHIFT SUPERVISOR — REE
R. SMITH, JR., CONTROL ROOM SUPERVISOR — REE
D. T. CODWIN — REE
T. G. HILL — REE
A. L. JOHNSON — REE
H. C. ROLLER, SHIFT SUPERVISOR — REE
E. W. BROWN, CONTROL ROOM SUPERVISOR — CT
E. D. BOLLING — REE
W. T. BOSTIC — CT
F. L. ROUSER — REE
D. F. FRECH, SHIFT SUPERVISOR — REE
R. J. SHANNON, CONTROL ROOM SUPERVISOR — CT
J. E. EVE — REE
L. J. SHERSKY — CT
J. E. WOLFE — REE
N. C. BRADLEY, SHIFT SUPERVISOR — CT
J. L. STEPP, CONTROL ROOM SUPERVISOR — REE
J. D. BARNES — REE
H. D. CURTIS — REE
T. W. HODGE — REE

MAINTENANCE PLANNING
W. TERRY, SUPERVISOR — REE
G. H. JOHNSTONE — REE
L. P. PINH — REE

INSTRUMENTATION
J. L. REDFORD, GROUP LEADER — I&C

P. N. HAUBENREICH,* ASSISTANT SECTION CHIEF — REE

REACTOR ANALYSIS
P. N. HAUBENREICH,* GROUP LEADER — REE
S. K. BURTON — REE
J. O. KOLB — REE
H. B. PIPER — REE
P. VIGNET — FRENCH ATOMIC ENERGY COMMISSION
J. A. WATTS — REE

REACTOR CHEMISTRY
D. M. RICHARDSON, GROUP LEADER — REE
D. G. PEACH* — REE
R. M. WALLER* — REE

CHEMICAL PLANT
R. D. BURCH, GROUP LEADER — CT
D. O. YARBRO — CT

NON-CITIZEN ASSIGNEE

P. VIGNET
COMMISSARIAT A L'ENERGIE ATOMIQUE
CENTRE D'ETUDES NUCLEAIRES DE SACLAY FRANCE

AC ANALYTICAL CHEMISTRY DIVISION
C CHEMISTRY DIVISION
CT CHEMICAL TECHNOLOGY DIVISION
D DIRECTOR'S DIVISION
I&C INSTRUMENTATION AND CONTROLS DIVISION
M METALLURGY DIVISION
RC REACTOR CHEMISTRY DIVISION
REE REACTOR EXPERIMENTAL ENGINEERING DIVISION
TI TECHNICAL INFORMATION DIVISION
* DUAL CAPACITY
** PART TIME ON HRP

PERSONNEL SUMMARY

	FULL TIME	PART TIME	NON-CITIZEN ASSIGNEE	TOTAL
ADMINISTRATION	5	4	0	9
ANALYTICAL CHEMISTRY	24	16	0	40
CHEMICAL RESEARCH	0	11	0	11
CHEMICAL TECHNOLOGY	12	11	0	23
DESIGN AND ENGINEERING	25	13	0	38
HOMOGENEOUS REACTOR TEST	38	0	1	39
REACTOR MATERIALS RESEARCH	36	16	1	52
TOTAL	130	72	2	224

ORNL-2947
Reactors-Power
TID-4500 (15th ed.)

INTERNAL DISTRIBUTION

1. C. E. Center
2. Biology Library
3. Health Physics Library
4. Metallurgy Library
5-6. Reactor Experimental Engineering Library
7-9. Central Research Library
10-14. Laboratory Records Department
15. Laboratory Records, ORNL R. C.
16. G. M. Adamson
17. A. L. Bacarella
18. J. E. Baker
19. S. J. Ball
20. J. C. Banter
21. S. E. Beall
22. L. L. Bennett
23. A. M. Billings
24. D. S. Billington
25. E. P. Blizard
26. R. Blumberg
27. E. G. Bohlmann
28. S. E. Bolt
29. C. J. Borkowski
30. G. E. Boyd
31. J. C. Bresee
32. F. R. Bruce
33. J. R. Buchanan
34. W. D. Burch
35. C. A. Burchsted
36. S. R. Buxton
37. A. D. Callihan
38. W. L. Carter
39. G. H. Cartledge
40. R. H. Chapman
41. R. A. Charpie
42. R. D. Cheverton
43. C. J. Claffey
44. H. C. Claiborne
45. T. E. Cole
46. C. W. Collins
47. E. L. Compere
48. F. L. Culler
49. D. G. Davis
50. R. J. Davis
51. V. A. DeCarlo
52. W. K. Eister
53. L. B. Emlet (K-25)
54. J. L. English
55. D. E. Ferguson
56. D. F. Frech
57. J. H. Frye, Jr.
58. C. H. Gabbard
59. J. L. Gabbard
60. W. R. Gall
61. R. B. Gallaher
62. E. H. Gift
63. H. E. Goeller
64. A. T. Gresky
65. J. C. Griess
66. W. R. Grimes
67. E. Guth
68. R. H. Guymon
69. L. A. Haack
70. P. A. Haas
71. J. Halperin
72. P. H. Harley
73. R. J. Harvey
74. P. N. Haubenreich
75. D. N. Hess
76. J. W. Hill
77. E. C. Hise
78. A. Hollaender
79. P. P. Holz
80. H. P. House
81. A. S. Householder
82. S. Jaye
83. G. H. Jenks
84. D. T. Jones
85. E. V. Jones
86. J. E. Jones Jr.
87. W. H. Jordan
88. P. R. Kasten
89. C. P. Keim
90. M. T. Kelley
91. F. Kertesz
92. J. O. Kolb
93. U. Koskela
94. K. A. Kraus
95. N. A. Krohn
96. J. A. Lane
97. C. G. Lawson
98. S. C. Lind
99. R. S. Livingston
100. R. A. Lorenz
101. M. I. Lundin
102. R. N. Lyon
103. J. L. Marsh (C&CC, South Charleston)
104. W. L. Marshall

105. J. P. McBride
106. H. F. McDuffie
107. H. A. McLain
108. J. R. McWherter
109. E. C. Miller
110. R. L. Moore
111. C. S. Morgan
112. K. Z. Morgan
113. L. E. Morse
114. J. P. Murray (Y-12)
115. M. L. Nelson
116. P. D. Neumann
117. A. R. Olsen
118. L. F. Parsly
119. F. N. Peebles
120. M. L. Picklesimer
121. H. B. Piper
122. B. E. Prince
123. L. R. Quarles
124. S. A. Reed
125. W. D. Reel
126. P. M. Reyling
127. S. A. Reynolds
128. L. Rice
129. D. M. Richardson
130. R. C. Robertson
131. W. Robinson
132. H. C. Roller
133. M. W. Rosenthal
134. H. C. Savage
135. C. E. Schilling
136. H. E. Seagren
137. C. H. Secoy
138. C. L. Segaser
139. E. D. Shipley
140. M. D. Silverman
141. M. J. Skinner
142. A. N. Smith
143. A. H. Snell
144. I. Spiewak
145. H. H. Stone
146. R. W. Stoughton
147. C. D. Susano
148. J. A. Swartout
149. A. Taboada
150. E. H. Taylor
151. W. Terry
152. D. G. Thomas
153. P. F. Thomason
154. M. Tobias
155. W. E. Unger
156. W. C. Ulrich
157. R. Van Winkle
158. D. W. Vroom
159. R. E. Wacker
160. H. O. Weeren
161. A. M. Weinberg
162. S. H. Wheeler
163. E. P. Wigner (Consultant)
164. H. D. Wills
165. G. C. Williams
166. J. C. Wilson
167. R. H. Winget
168. C. E. Winters
169. C. H. Wodtke
170. L. F. Woo
171. F. C. Zapp
172. H. E. Zittel
173. ORNL - Y-12 Technical Library, Document Reference Section
174. HRP Director's Office, Y-12

EXTERNAL DISTRIBUTION

175. Division of Research and Development, AEC, ORO
176-752. Given distribution as shown in TID-4500 (15th ed.) under Reactors-Power Category (75 copies - OTS)

Reports previously issued in this series are as follows:

ORNL-527	Date Issued, December 28, 1949
ORNL-630	Period Ending February 28, 1950
ORNL-730	Feasibility Report - Date Issued, July 6, 1950
ORNL-826	Period Ending August 31, 1950
ORNL-925	Period Ending November 30, 1950
ORNL-990	Period Ending February 28, 1951
ORNL-1057	Period Ending May 15, 1951
ORNL-1121	Period Ending August 15, 1951
ORNL-1221	Period Ending November 15, 1951
ORNL-1280	Period Ending March 15, 1952
ORNL-1318	Period Ending July 1, 1952
ORNL-1424	Period Ending October 1, 1952
ORNL-1478	Period Ending January 1, 1953
ORNL-1554	Period Ending March 31, 1953
ORNL-1605	Period Ending July 31, 1953
ORNL-1658	Period Ending October 31, 1953
ORNL-1678	Period Ending January 31, 1954
ORNL-1753	Period Ending April 30, 1954
ORNL-1772	Period Ending July 31, 1954
ORNL-1813	Period Ending October 31, 1954
ORNL-1853	Period Ending January 31, 1955
ORNL-1895	Period Ending April 30, 1955
ORNL-1943	Period Ending July 31, 1955
ORNL-2004	Period Ending October 31, 1955
ORNL-2057	Period Ending January 31, 1956
ORNL-2096	Period Ending April 30, 1956
ORNL-2148	Period Ending July 31, 1956
ORNL-2222	Period Ending October 31, 1956
ORNL-2272	Period Ending January 31, 1957
ORNL-2331	Period Ending April 30, 1957
ORNL-2379	Period Ending July 31, 1957
ORNL-2432	Period Ending October 31, 1957
ORNL-2493	Period Ending January 31, 1958
ORNL-2561	Periods Ending April 30 and July 31, 1958
ORNL-2654	Period Ending October 31, 1958
ORNL-2696	Period Ending January 31, 1959
ORNL-2743	Period Ending April 30, 1959
ORNL-2879	Period May 1 Through October 31, 1959
ORNL-2920	Period Ending January 31, 1960